

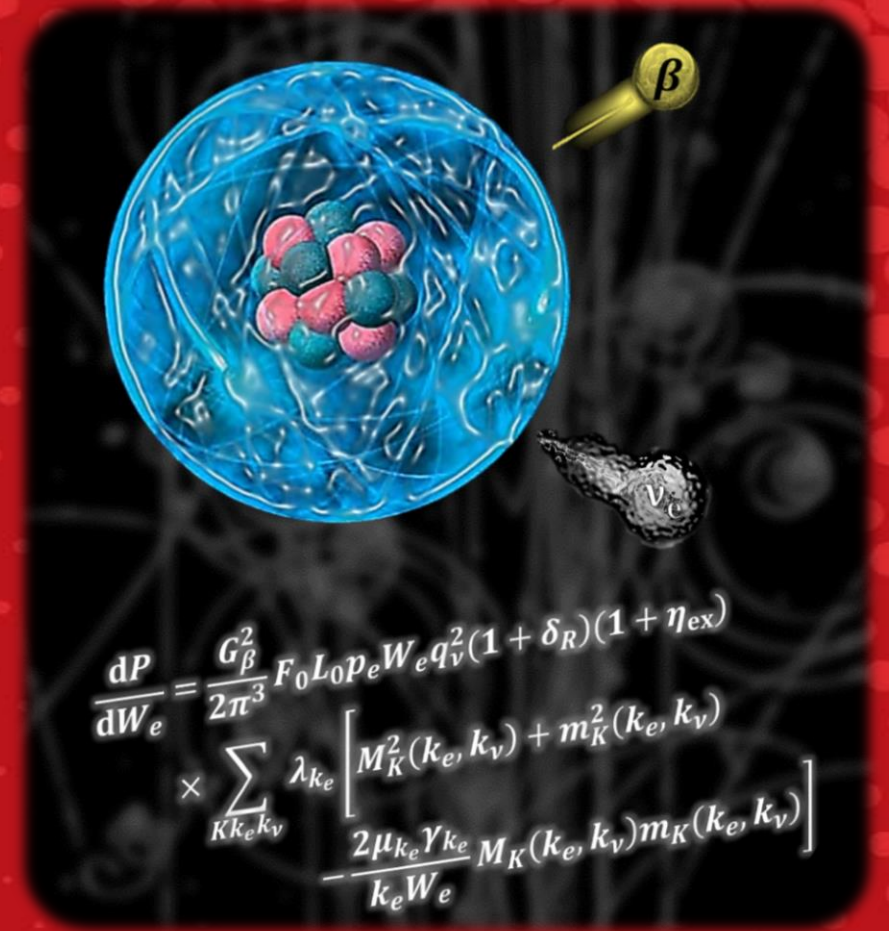


DE LA RECHERCHE  
À L'INDUSTRIE

# Beta decays

*Experiments, Theory and the BetaShape code*

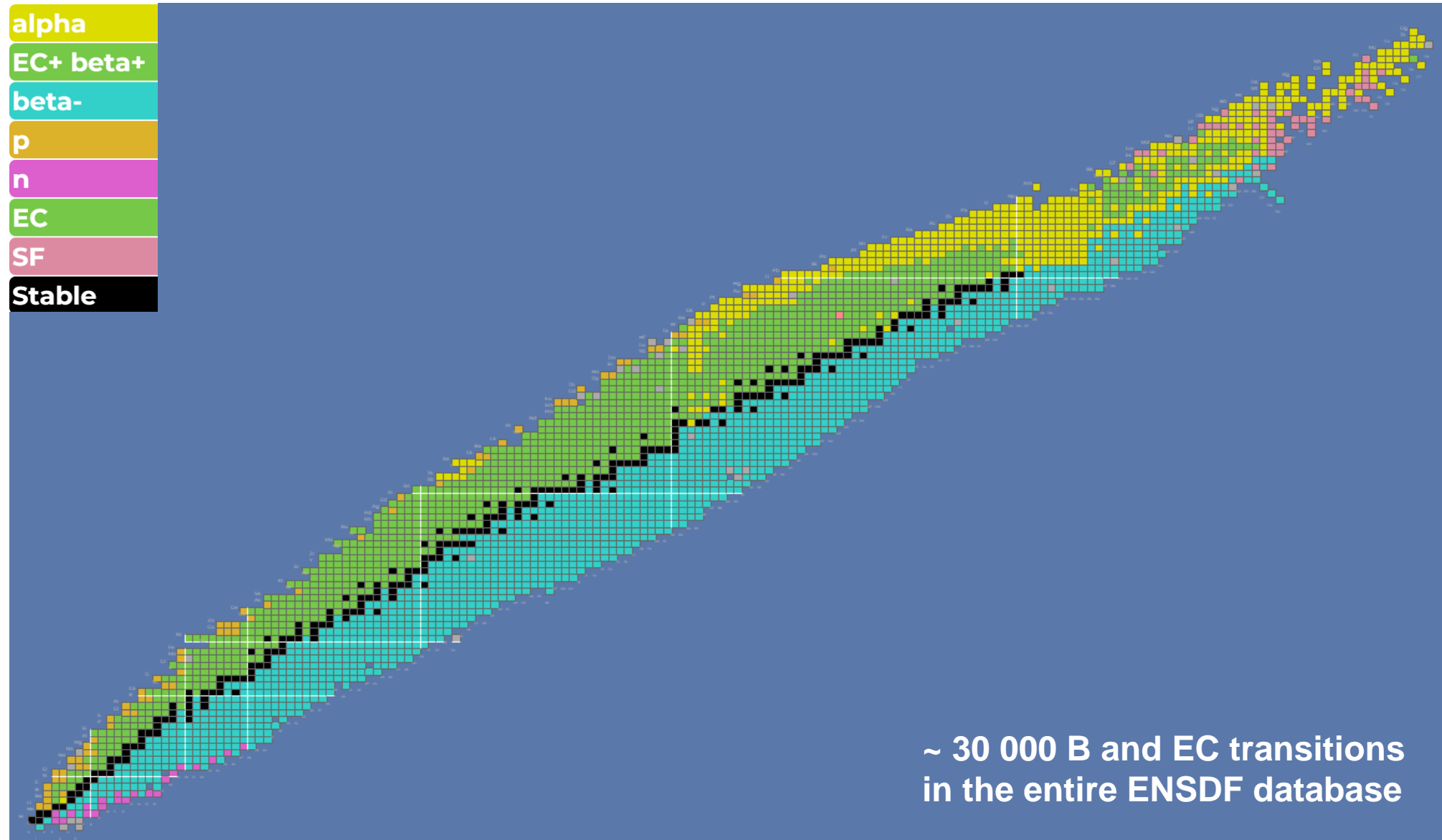
X. Mougeot, CEA-LNHB (France)



**Joint ICTP-IAEA Workshop on Nuclear Structure and Decay Data: Experiment, Theory and Evaluation**  
**October 3 – 14, 2022**

Commissariat à l'énergie atomique et  
aux énergies alternatives - [www.cea.fr](http://www.cea.fr)





Weak interaction is not so weak:  $\alpha_W \sim 1/30$  while  $\alpha_{EM} \sim 1/137$ . It only appears weak at low energy due to a massive propagator.

Interaction was built in analogy with electromagnetism.

Invariances and symmetries  $\rightarrow$  only 5 possible types of interaction:

scalar (S), vector (V), axial-vector (A), tensor (T), pseudo-scalar (P)

Experiments (helicity, maximum violation of charge conjugation symmetry, possibility of parity violation) demonstrate **the (V-A) nature of the weak interaction**.

Each interaction has its own coupling constant:

$\rightarrow$  Gauge invariance leads to  $f_V = 1$ .

$\rightarrow$  Axial-vector current sensitive to strong force and renormalized within nucleus:  $f_A \sim 1.27$ .

Within the Standard Model, additional currents can appear. For example, considering extended nucleons induces the so-called weak magnetism term.

Beyond the Standard Model, other additional currents can appear with an effect on beta decay. For example, assuming left- and right- handed leptons.

- Interest of beta decays
- Physics of beta decays
- High-precision study of atomic effects
- Study of beta spectra at medium energies
- Forbidden non-unique beta transitions
- The BetaShape code

## Interest of beta decays

## Metrology

### Activity measurements

(Liquid scintillation,  
ionization chambers)



Better knowledge → **Improvement of accuracy  
and uncertainties**

## Fundamental research

- Nuclear astrophysics (r-process)
- Neutrino physics (reactor anomaly, reactor monitoring, non-proliferation)
- Standard Model (CKM matrix unitarity, weak magnetism)
- New physics (Fierz interference, sterile neutrino, dark matter)



## Atomic and nuclear decay data

- **DDEP**, decay data in **JEFF** database
- **ENSDF** nuclear decay data  
**Properties calculated** with the LogFT code  
(Gove and Martin, 1971)  
**No beta spectrum**



### Medical uses

Micro-dosimetry, internal radiotherapy, contamination



### Nuclear fuel cycle

Decay heat, nuclear waste



### Developments

Beta-voltaic batteries, new detectors (e.g.  $\text{LaBr}_3$ )



LNHB (National Laboratory Henri Becquerel) is the French Designated Institute for primary standards in ionizing radiation metrology.

- **Definition of activity (Bq) and dose (Sv, Gy)** through international intercomparisons and transfer to users through standards. International and national traceability is ensured by BIPM referencing and COFRAC certification.



**Instrumentation + Methods = Primary standards**, reference uncertainty  
**Instrumentation + Calibration = Secondary standards**, transfer

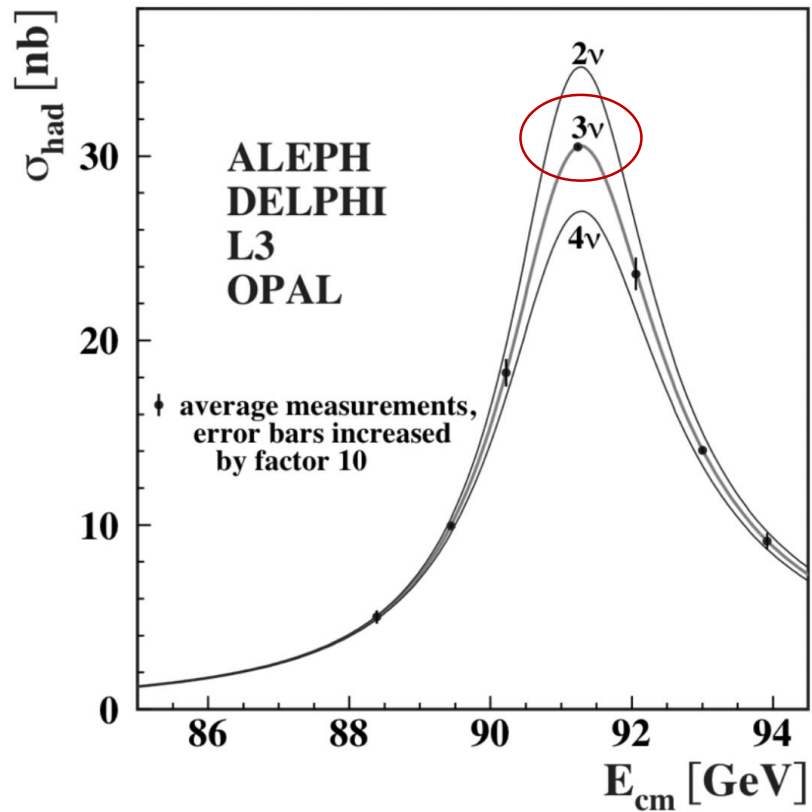


**The diversity of radioactive processes makes necessary a certain knowledge: decay schemes, atomic and nuclear data.**

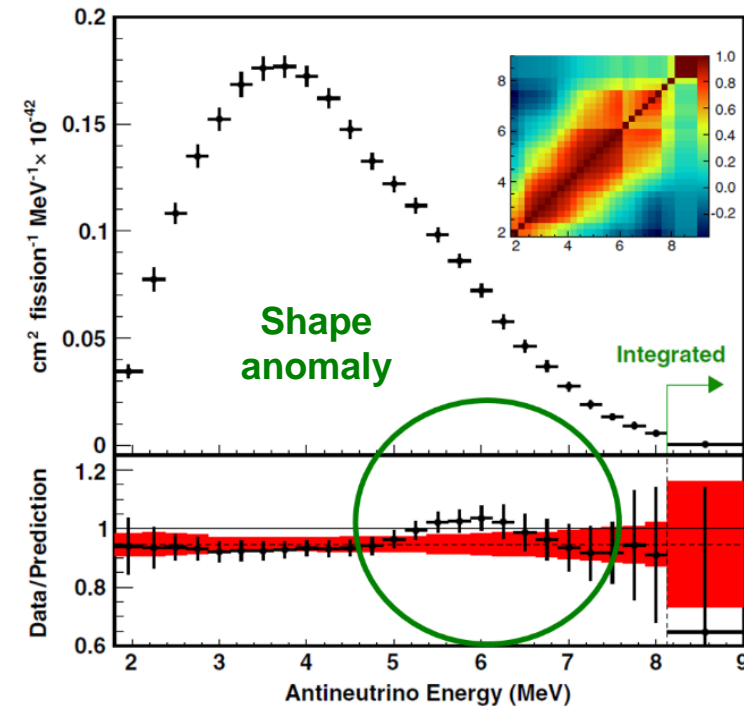
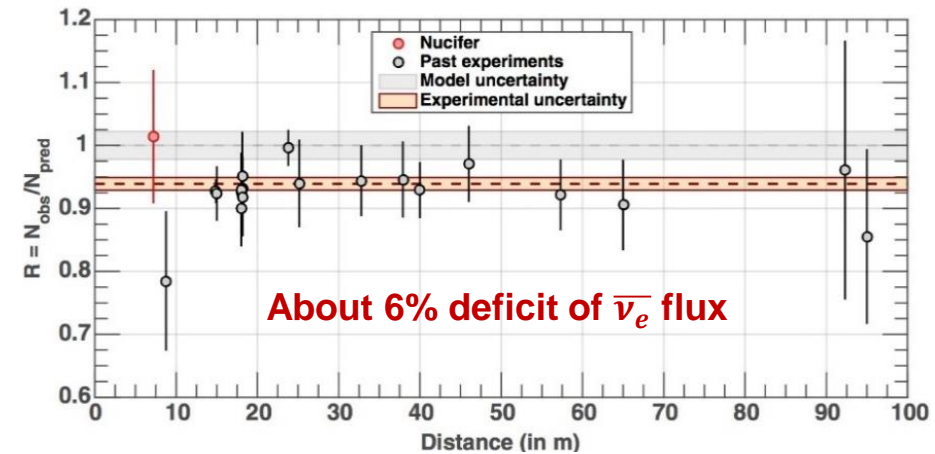
LNHB is highly involved in the evaluation of atomic and nuclear decay data and associated decay schemes, for metrology.

- **Coordination of the DDEP (Decay Data Evaluation Project) international collaboration.** Links with IAEA and ENSDF community.
- **Decay data recommended by the BIPM.**



Production cross section of  $Z^0$  boson

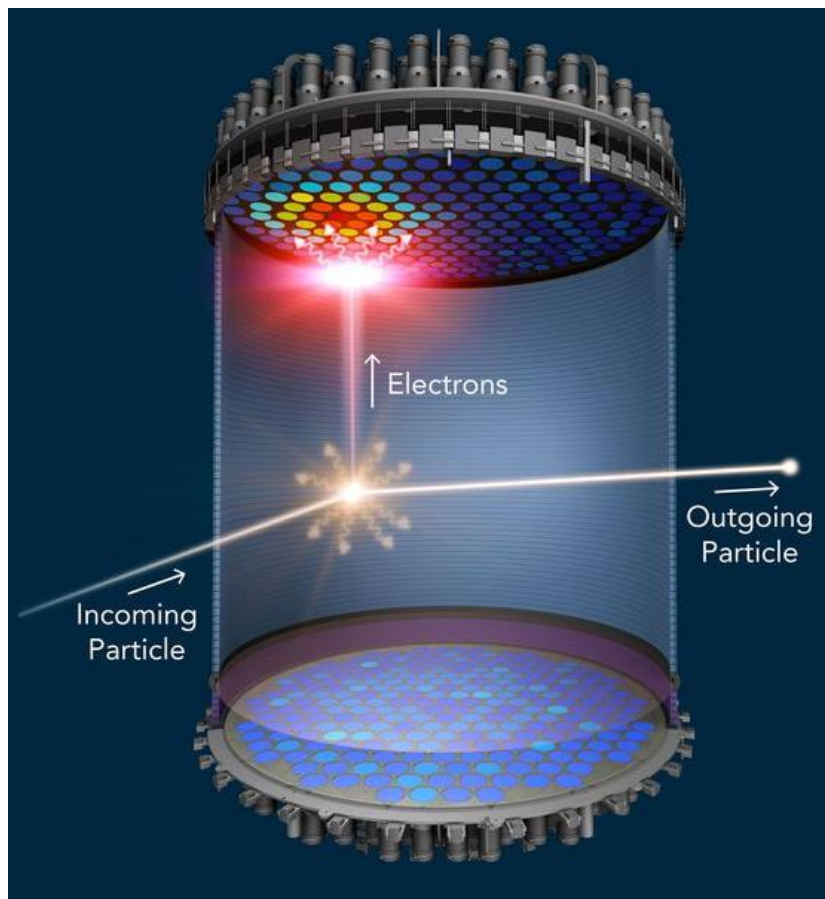
G. Mention et al., Phys. Rev. D 83, 073006 (2011)  
 F.P. An et al., Phys. Rev. Lett. 118, 251801 (2017)  
 G. Bak et al., Phys. Rev. Lett. 122, 232501 (2019)



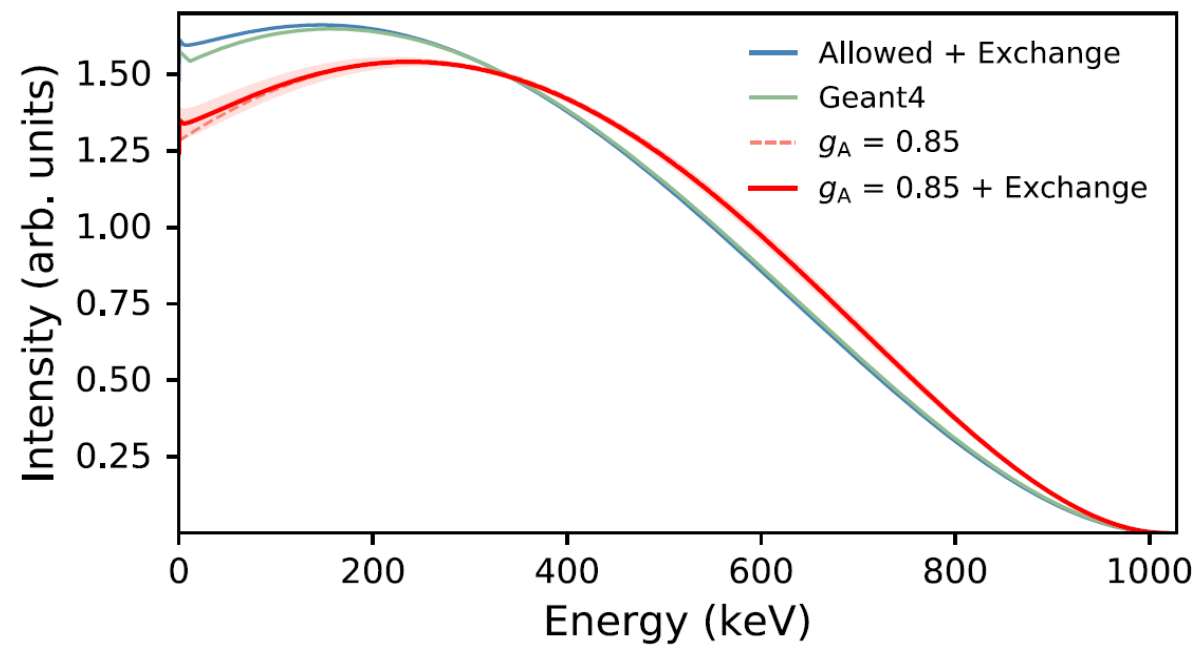
## XENON Collaboration

Accurate description of low energy radioactive background is essential.

Excess of electron events as a mono-energetic peak at low energy ( $\sim 2$  keV).



$^{214}\text{Pb}$  gs to gs decay: influence of nuclear structure



E. Aprile et al., Phys. Rev. D 102, 072004 (2020)

S.J. Haselschwardt et al., Phys. Rev. C 102, 065501 (2020)

$$\frac{dP}{dW} \propto pWq^2 \times \left[ 1 \pm \frac{4W}{3M} b_{\text{wm}} + \frac{\gamma m_e}{W} \cdot b_{\text{Fierz}} \right]$$

### Weak magnetism

Point-like nucleons → Finite size nucleons with internal structure.

L. Hayen et al.,  
Rev. Mod. Phys.  
90, 015018 (2018)

### Fierz interference

Additional interactions induced by exotic currents beyond the Standard Model.

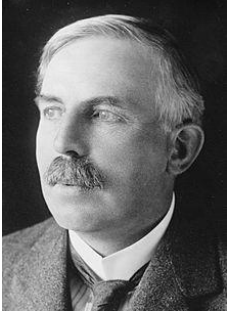
→ Their energy dependency allows an almost independent treatment through the analysis of both low and high energy transitions.

**French project bSTILED:** PI O. Naviliat-Cuncic (LPC Caen).

High-precision measurement of  ${}^6\text{He}$  beta spectrum at GANIL.

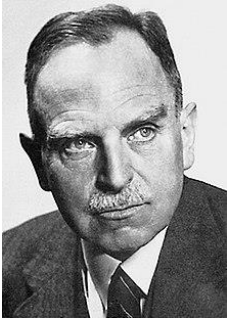
Accepted in PRC: new high-precision half-life measurement  $T_{1/2} = (807.25 \pm 0.16_{\text{stat}} \pm 0.11_{\text{sys}}) \text{ ms}$

# Physics of beta decays



**1898:** E. Rutherford distinguishes  $\alpha$  and  $\beta$  rays.

**1910:** O. Hahn and L. Meitner build the first  $\beta$  spectrometer and observe some rays.  
→ Two-body disintegration is claimed. Unknown radiochemical substances are identified.



**1914:** J. Chadwick uses proportional counter from H. Geiger and observes continuous spectra.

→ With a two-body disintegration, energy is not conserved.

**1922-1923:** Discovery of Compton effect. For L. Meitner, continuity of beta spectra is due to a secondary phenomenon.

**1927-1929:** With a fine calorimetry measurement, C. Ellis demonstrates that beta spectra are continuous.

→ End of 15 years controversy, but still a mystery!





**1924:** For H. Kramers, J. Slater and N. Bohr, energy conservation could be only statistical.

**1925:** First coincidence measurement from H. Geiger et W. Bothe.  
→ Energy is conserved event-by-event in beta decay.

**1930:** W. Pauli invents the neutrino to save energy conservation.

“Today, I did what a theorist should never do in his life. I have indeed tried to explain something we cannot understand by something we cannot observe”.

**1933:** E. Fermi establishes his theory of beta decay. Electron and neutrino are created at the moment of the decay. His quantitative calculations reproduce very well Sargent’s rule (empirical relationship between  $E_{\max}$  and  $T_{1/2}$ ).

→ Article rejected by Nature editors: his theory was considered as “speculations too far from reality”!

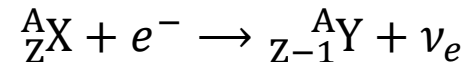
$$\beta^-: n \rightarrow p + e^- + \bar{\nu}_e$$



$$\beta^+: p \rightarrow n + e^+ + \nu_e$$



$$\text{Electron capture: } p + e^- \rightarrow n + \nu_e$$



$$E_{\max} = Q + E_{\text{nuc}}^{\text{initial}} - E_{\text{nuc}}^{\text{final}}$$

$$E_{\max} = Q + E_{\text{nuc}}^{\text{initial}} - E_{\text{nuc}}^{\text{final}} - 2m_e$$

$$E_{\max} = Q + E_{\text{nuc}}^{\text{initial}} - E_{\text{nuc}}^{\text{final}}$$

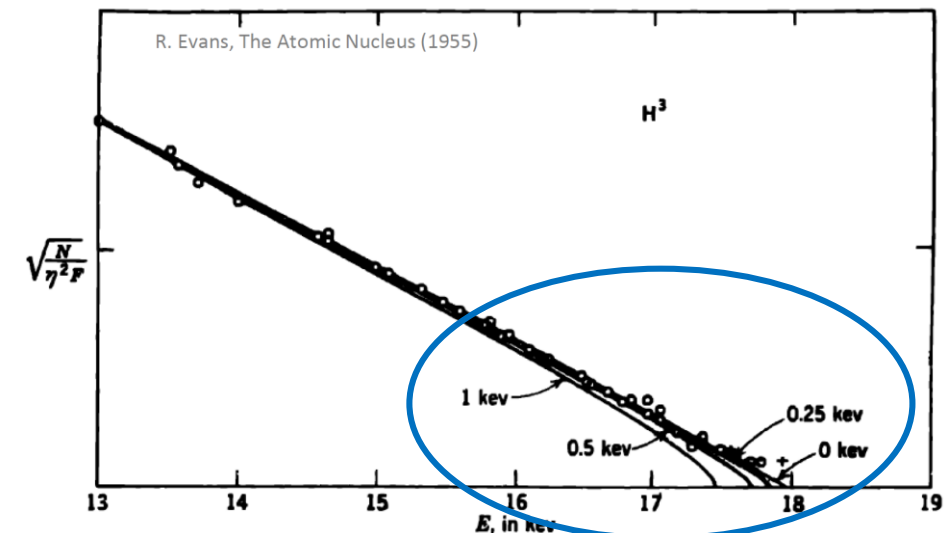
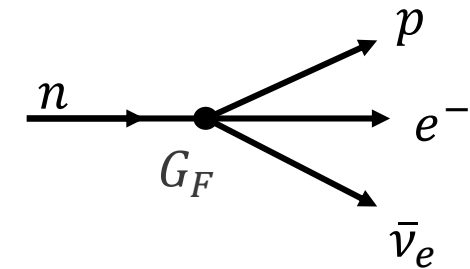
### Fermi theory is a low-energy effective theory

- Weak interaction mediated by  $W^\pm$  bosons.
- However,  $m_W \approx 80 \text{ GeV} \gg E_{\max}(\text{decay}) \leq 30 \text{ MeV}$ .
- Instantaneous contact interaction of 4 fermions.
- Fermi coupling constant:  $G_F/(\hbar c)^3 = 1.1163787(6) \cdot 10^{-5} \text{ GeV}^{-2}$ .

It is common to assume a **massless neutrino** and an **infinitely massive nucleus** (max. recoil energy in  ${}^7\text{Be}$  decay: 57 eV).

**Fermi's golden rule:** weak perturbation → transition probability

$$\Gamma = \frac{2\pi}{\hbar} \underbrace{|\langle \Psi_{\text{final}} | H' | \Psi_{\text{initial}} \rangle|^2}_{\text{matrix element}} \underbrace{\rho(E_{\text{final}})}_{\text{density of final states}}$$



Similarly we obtain for the space components

$$\langle p | \mathbf{V} + \mathbf{A} | n \rangle = i u_p^\dagger \gamma_4 \gamma_\mu (1 + \lambda \gamma_5) u_n = \sqrt{\frac{W_n + M_n}{2W_n}} \sqrt{\frac{W_p + M_p}{2W_p}} \begin{pmatrix} 0 & \mathbf{i}\boldsymbol{\sigma} \\ \mathbf{i}\boldsymbol{\sigma} & 0 \end{pmatrix} \lambda \begin{pmatrix} 0 & 1 \\ 1 & 0 \end{pmatrix} \times \left\{ \left( \frac{\boldsymbol{\sigma} \mathbf{p}}{W_p + M_p} \chi_p^m \right)^\dagger \boldsymbol{\sigma} \chi_n^m + (\chi_p^m)^\dagger \boldsymbol{\sigma} \frac{\boldsymbol{\sigma} \mathbf{p}}{W_n + M_n} \chi_n^m - \lambda (\chi_p^m)^\dagger \boldsymbol{\sigma} \chi_n^m - \lambda \left[ \left( \frac{\boldsymbol{\sigma} \mathbf{p}}{W_p + M_p} \chi_p^m \right)^\dagger \boldsymbol{\sigma} \frac{\boldsymbol{\sigma} \mathbf{p}}{W_n + M_n} \chi_n^m \right] \right\}. \quad (6.38)$$

This equals to

$$\langle p | \mathbf{V} + \mathbf{A} | n \rangle = \sqrt{\frac{W_n + M_n}{2W_n}} \sqrt{\frac{W_p + M_p}{2W_p}} \left\{ (\chi_p^m)^\dagger \frac{\boldsymbol{\sigma} \mathbf{p}_p}{W_p + M_p} \boldsymbol{\sigma} \chi_n^m + (\chi_p^m)^\dagger \boldsymbol{\sigma} \frac{\boldsymbol{\sigma} \mathbf{p}_n}{W_n + M_n} \chi_n^m - \lambda (\chi_p^m)^\dagger \boldsymbol{\sigma} \chi_n^m + \lambda \left[ \left( \frac{\boldsymbol{\sigma} \mathbf{p}_p}{W_p + M_p} \boldsymbol{\sigma} \frac{\boldsymbol{\sigma} \mathbf{p}_n}{W_n + M_n} \chi_n^m \right)^\dagger \boldsymbol{\sigma} \chi_n^m - \frac{(\mathbf{p}_p \mathbf{p}_n) \boldsymbol{\sigma} + (\boldsymbol{\sigma} \mathbf{p}_p) \mathbf{p}_n + \mathbf{p}_p (\boldsymbol{\sigma} \mathbf{p}_n) - i(\mathbf{p}_p \times \mathbf{p}_n)}{(W_p + M_p)(W_n + M_n)} \right] \right\}. \quad (6.39)$$

Finally we obtain for the space components

$$\langle p | \mathbf{V}(0) + \mathbf{A}(0) | n \rangle = \sqrt{\frac{W_n + M_n}{2W_n}} \sqrt{\frac{W_p + M_p}{2W_p}} \times \left\{ \left[ \frac{\mathbf{p}_p}{W_p + M_p} + \frac{\mathbf{p}_n}{W_n + M_n} \right] (\chi_p^m)^\dagger \chi_n^m + (\chi_p^m)^\dagger \times \left[ \frac{i(\boldsymbol{\sigma} \times \mathbf{p}_p)}{W_p + M_p} - \frac{i(\boldsymbol{\sigma} \times \mathbf{p}_n)}{W_n + M_n} \right] \chi_p^m - \lambda (\chi_p^m)^\dagger \boldsymbol{\sigma} \chi_n^m + \lambda \frac{\mathbf{p}_p \mathbf{p}_n}{(W_p + M_p)(W_n + M_n)} \{ (\chi_p^m)^\dagger \boldsymbol{\sigma} \chi_n^m \} + \lambda \frac{i(\mathbf{p}_p \times \mathbf{p}_n)}{(W_p + M_p)(W_n + M_n)} \times \left\{ (\chi_p^m)^\dagger \chi_n^m - \lambda \left[ \left( \frac{\boldsymbol{\sigma} \mathbf{p}_p}{W_p + M_p} \boldsymbol{\sigma} \frac{\boldsymbol{\sigma} \mathbf{p}_n}{W_n + M_n} \chi_n^m \right)^\dagger \boldsymbol{\sigma} \chi_n^m \right] \right\}. \quad (6.40)$$

$$-\frac{i}{2M_A} F_M(q^2) (\mathbf{P} \times \mathbf{q}) \boldsymbol{\sigma} - F_S(q^2) q_0 + \frac{1}{4(2M_A)^2} F_S(q^2) q_0 (\mathbf{P}^2 - \mathbf{q}^2) - \frac{i}{2(2M_A)^2} F_S(q^2) q_0 (\mathbf{P} \times \mathbf{q}) \boldsymbol{\sigma} \chi^M, \quad (9.15)$$

$$\langle \phi_f(p_f) | A_0(0) | \phi_i(p_i) \rangle = N(\chi^M)^\dagger \left\{ -\frac{1}{2M_A} F_A(q^2) (\mathbf{P} \boldsymbol{\sigma}) - \frac{q_0}{2M_A} F_P(q^2) (\mathbf{q} \boldsymbol{\sigma}) - F_T(q^2) (\mathbf{q} \boldsymbol{\sigma}) + \frac{1}{4(2M_A)^2} F_T(q^2) \times [(\mathbf{P} \mathbf{q})(\boldsymbol{\sigma} \mathbf{P} + \boldsymbol{\sigma} \mathbf{q}) - (\boldsymbol{\sigma} \mathbf{q})(\mathbf{P}^2 + \mathbf{q}^2)] \right\} \chi^M. \quad (9.16)$$

$$\langle \phi_f(p_f) | \mathbf{V}(0) | \phi_i(p_i) \rangle = N(\chi^M)^\dagger \left\{ \frac{1}{2M_A} F_V(q^2) \mathbf{P} + \frac{i}{2M_A} F_V(q^2) (\boldsymbol{\sigma} \times \mathbf{q}) + i F_M(q^2) (\boldsymbol{\sigma} \times \mathbf{q}) - \frac{1}{2M_A} F_M(q^2) q_0 \mathbf{q} - \frac{i}{4M_A} F_M(q^2) q_0 (\boldsymbol{\sigma} \times \mathbf{P}) - F_S(q^2) \mathbf{q} + \frac{1}{4(2M_A)^2} F_S(q^2) \mathbf{q} (\mathbf{P}^2 - \mathbf{q}^2) - \frac{i}{2(2M_A)^2} F_S(q^2) \mathbf{q} \times ((\mathbf{P} \times \mathbf{q}) \boldsymbol{\sigma}) - \frac{i}{2(2M_A)^2} F_M(q^2) \mathbf{P} ((\mathbf{P} \times \mathbf{q}) \boldsymbol{\sigma}) - \frac{i}{4(2M_A)^2} \times F_M(q^2) (\mathbf{P}^2 + \mathbf{q}^2) (\boldsymbol{\sigma} \times \mathbf{q}) + \frac{i}{2(2M_A)^2} F_M(q^2) (\mathbf{P} \mathbf{q})(\boldsymbol{\sigma} \times \mathbf{P}) \right\} \chi^M. \quad (9.17)$$

$$\langle \phi_f(p_f) | \mathbf{A}(0) | \phi_i(p_i) \rangle = N(\chi^M)^\dagger \left\{ -F_A(q^2) \boldsymbol{\sigma} + \frac{1}{2(2M_A)^2} \times F_A(q^2) \mathbf{P}^2 \boldsymbol{\sigma} - \frac{1}{4(2M_A)^2} F_A(q^2) (\mathbf{P}^2 + \mathbf{q}^2) \boldsymbol{\sigma} - \frac{i}{2(2M_A)^2} \times F_A(q^2) (\mathbf{P} \times \mathbf{q}) - \frac{1}{2(2M_A)^2} F_A(q^2) [(\boldsymbol{\sigma} \mathbf{P}) \mathbf{P} - (\boldsymbol{\sigma} \mathbf{q}) \mathbf{q}] + \frac{1}{2M_A} F_T(q^2) [(\mathbf{P} \mathbf{p}) \boldsymbol{\sigma} - \mathbf{q} (\boldsymbol{\sigma} \mathbf{P})] - F_T(q^2) q_0 \boldsymbol{\sigma} + \frac{1}{2(2M_A)^2} F_T(q^2) q_0 \mathbf{P}^2 \boldsymbol{\sigma} - \frac{1}{4(2M_A)^2} F_T(q^2) q_0 (\mathbf{P}^2 + \mathbf{q}^2) \boldsymbol{\sigma} - \frac{i}{2(2M_A)^2} F_T(q^2) q_0 (\mathbf{P} \times \mathbf{q}) - \frac{1}{2(2M_A)^2} F_T(q^2) q_0 [(\boldsymbol{\sigma} \mathbf{P}) \mathbf{P} - (\boldsymbol{\sigma} \mathbf{q}) \mathbf{q}] - \frac{1}{2M_A} F_P(q^2) (\boldsymbol{\sigma} \mathbf{q}) \mathbf{q} \right\} \chi^M. \quad (9.18)$$

340 FORM FACTORS AND NUCLEAR MATRIX ELEMENTS

$${}^{\wedge} F_{KK0}(q^2) = \lambda {}^{\wedge} \mathfrak{M}_{KK0}(q^2) + \frac{f_T}{R} \left[ \sqrt{\{K(2K+1)\}} {}^{\mathcal{D}} \mathfrak{M}_{KK-11}(q^2) - \sqrt{\left\{ \frac{K+1}{(2K+3)^2(2K+1)} \right\}} (qR)^2 {}^{\mathcal{D}} \mathfrak{M}_{KK+11}(q^2) - \frac{f_P}{R} \{W_0 R \pm \frac{1}{2} \alpha Z\} {}^{\mathcal{D}} \mathfrak{M}_{KK0}(q^2) \right] \quad (8.263b)$$

$${}^{\vee} F_{KK1}(q^2) = {}^{\vee} \mathfrak{M}_{KK1}(q^2) + \frac{f_M}{R} \left[ \sqrt{\{(K+1)(2K+1)\}} {}^{\mathcal{D}} \mathfrak{M}_{KK-11}(q^2) + \sqrt{\left\{ \frac{K}{(2K+3)^2(2K+1)} \right\}} (qR)^2 {}^{\mathcal{D}} \mathfrak{M}_{KK+11}(q^2) + (W_0 R \pm \frac{1}{2} \alpha Z) {}^{\mathcal{C}} \mathfrak{M}_{KK1}(q^2) \right] \quad (8.263c)$$

$${}^{\wedge} F_{KK1}(q^2) = \lambda {}^{\wedge} \mathfrak{M}_{KK1}(q^2) + \frac{f_T}{R} \left[ \sqrt{\{(K+1)(2K+1)\}} {}^{\mathcal{C}} \mathfrak{M}_{KK-11}(q^2) + \sqrt{\left\{ \frac{K}{(2K+3)^2(2K+1)} \right\}} (qR)^2 {}^{\mathcal{C}} \mathfrak{M}_{KK+11}(q^2) + (W_0 R \pm \frac{1}{2} \alpha Z) {}^{\mathcal{D}} \mathfrak{M}_{KK1}(q^2) \right] \quad (8.263d)$$

$$-{}^{\vee} F_{KK-11}(q^2) = {}^{\vee} \mathfrak{M}_{KK-11}(q^2) + \frac{f_M}{R} \left[ \sqrt{\left\{ \frac{K+1}{(2K+1)^3} \right\}} (qR)^2 {}^{\mathcal{D}} \mathfrak{M}_{KK1}(q^2) + (W_0 R \pm \frac{1}{2} \alpha Z) {}^{\mathcal{C}} \mathfrak{M}_{KK-11}(q^2) - \frac{f_S}{R} \sqrt{\left\{ \frac{K}{(2K+1)^3} \right\}} \times (qR)^2 {}^{\mathcal{C}} \mathfrak{M}_{KK0}(q^2) \right] \quad (8.263e)$$

$$-{}^{\wedge} F_{KK-11}(q^2) = \lambda {}^{\wedge} \mathfrak{M}_{KK-11}(q^2) + \frac{f_T}{R} \left[ \sqrt{\left\{ \frac{K+1}{(2K+1)^3} \right\}} (qR)^2 {}^{\mathcal{C}} \mathfrak{M}_{KK1}(q^2) + (W_0 R \pm \frac{1}{2} \alpha Z) {}^{\mathcal{D}} \mathfrak{M}_{KK-11}(q^2) - \frac{f_P}{R} \sqrt{\left\{ \frac{K}{(2K+1)^3} \right\}} \times (qR)^2 {}^{\mathcal{D}} \mathfrak{M}_{KK0}(q^2) \right] \quad (8.263f)$$

$$-{}^{\vee} F_{KK+11}(q^2) = {}^{\vee} \mathfrak{M}_{KK+11}(q^2) + \frac{f_M}{R} \left[ \sqrt{\left\{ \frac{K(2K+3)^2}{2K+1} \right\}} {}^{\mathcal{D}} \mathfrak{M}_{KK1}(q^2) + (W_0 R \pm \frac{1}{2} \alpha Z) {}^{\mathcal{C}} \mathfrak{M}_{KK+11}(q^2) + \frac{f_S}{R} \sqrt{\left\{ \frac{(K+1)(2K+3)^2}{2K+1} \right\}} {}^{\mathcal{C}} \mathfrak{M}_{KK0}(q^2) \right] \quad (8.263g)$$

$$-{}^{\wedge} F_{KK+11}(q^2) = \lambda {}^{\wedge} \mathfrak{M}_{KK+11}(q^2) + \frac{f_T}{R} \left[ \sqrt{\left\{ \frac{K(2K+3)^2}{2K+1} \right\}} {}^{\mathcal{C}} \mathfrak{M}_{KK1}(q^2) + (W_0 R \pm \frac{1}{2} \alpha Z) {}^{\mathcal{D}} \mathfrak{M}_{KK+11}(q^2) + \frac{f_P}{R} \sqrt{\left\{ \frac{(K+1)(2K+3)^2}{2K+1} \right\}} {}^{\mathcal{D}} \mathfrak{M}_{KK0}(q^2) \right] \quad (8.263h)$$

454

SPECIAL FORMULAE

$$+ \sqrt{\frac{2}{3}} \left\{ \int \left( \frac{r}{R} \right) r I'(r) \beta \gamma_5 T_{121} \right\} \mp \frac{f_P}{R} (W_0 R \pm \frac{1}{2} \alpha Z) {}^{\mathcal{D}} \mathfrak{M}_{110}^{(0)}(1, 1, 1, 1) \quad (14.101)$$

$${}^{\wedge} F_{121}^{(0)} = \mp \lambda {}^{\wedge} \mathfrak{M}_{121}^{(0)} - \frac{f_T}{R} \left[ \frac{5}{\sqrt{3}} {}^{\mathcal{C}} \mathfrak{M}_{111}^{(0)} - (W_0 R \pm \frac{1}{2} \alpha Z) {}^{\wedge} \mathfrak{M}_{121}^{(0)} \right] \mp \frac{f_P}{R} 5\sqrt{\frac{2}{3}} {}^{\mathcal{D}} \mathfrak{M}_{110}^{(0)} \quad (14.102)$$

$${}^{\wedge} F_{121}^{(0)}(1, 1, 1, 1) = \mp \lambda {}^{\wedge} \mathfrak{M}_{121}^{(0)}(1, 1, 1, 1) - \frac{f_T}{R} \left\{ \sqrt{\frac{2}{3}} \left[ \int \left( \frac{r}{R} \right) [5I(r) + r I'(r)] \beta T_{111} \right] - (W_0 R \pm \frac{1}{2} \alpha Z) {}^{\wedge} \mathfrak{M}_{121}^{(0)}(1, 1, 1, 1) \right\} \mp \frac{f_P}{R} \sqrt{\frac{2}{3}} \left[ \int \left( \frac{r}{R} \right) [5I(r) + r I'(r)] \beta \gamma_5 T_{110} \right] \quad (14.103)$$

$${}^{\vee} F_{211}^{(0)} = -{}^{\vee} \mathfrak{M}_{211}^{(0)} - \frac{f_M}{R} (W_0 R \pm \frac{1}{2} \alpha Z) {}^{\mathcal{C}} \mathfrak{M}_{211}^{(0)} \quad (14.104)$$

$${}^{\vee} F_{220}^{(0)} = {}^{\vee} \mathfrak{M}_{220}^{(0)} + \frac{f_M}{R} \sqrt{10} {}^{\mathcal{C}} \mathfrak{M}_{211}^{(0)} \pm \frac{f_S}{R} (W_0 R \pm \frac{1}{2} \alpha Z) {}^{\vee} \mathfrak{M}_{220}^{(0)} \quad (14.105)$$

$${}^{\vee} F_{220}^{(0)}(1, 1, 1, 1) = {}^{\vee} \mathfrak{M}_{220}^{(0)}(1, 1, 1, 1) + \frac{f_M}{R} \left\{ \sqrt{\frac{2}{3}} \left[ \int \left( \frac{r}{R} \right) [5I(r) + r I'(r)] \beta T_{211} \right] + \sqrt{\frac{2}{3}} \left[ \int \left( \frac{r}{R} \right) r I'(r) \beta T_{231} \right] \right\} \pm \frac{f_S}{R} (W_0 R \pm \frac{1}{2} \alpha Z) {}^{\vee} \mathfrak{M}_{220}^{(0)}(1, 1, 1, 1) \quad (14.106)$$

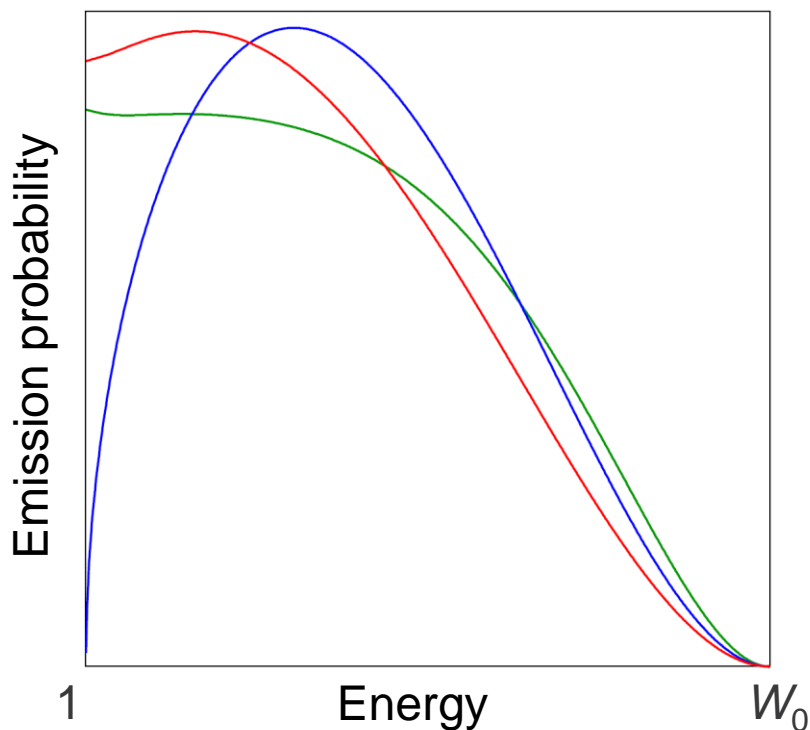
$${}^{\wedge} F_{221}^{(0)} = \pm \lambda {}^{\wedge} \mathfrak{M}_{221}^{(0)} + \frac{f_T}{R} \left[ \sqrt{15} {}^{\mathcal{C}} \mathfrak{M}_{211}^{(0)} - (W_0 R \pm \frac{1}{2} \alpha Z) {}^{\wedge} \mathfrak{M}_{221}^{(0)} \right] \quad (14.107)$$

$${}^{\wedge} F_{221}^{(0)}(1, 1, 1, 1) = \pm \lambda {}^{\wedge} \mathfrak{M}_{221}^{(0)}(1, 1, 1, 1) + \frac{f_T}{R} \left\{ \sqrt{\frac{2}{3}} \left[ \int \left( \frac{r}{R} \right) [5I(r) + r I'(r)] \beta T_{211} \right] - \sqrt{\frac{2}{3}} \left[ \int \left( \frac{r}{R} \right) r I'(r) \beta T_{231} \right] - (W_0 R \pm \frac{1}{2} \alpha Z) {}^{\wedge} \mathfrak{M}_{221}^{(0)}(1, 1, 1, 1) \right\} \quad (14.108)$$

H. Behrens and W. Bühring, *Electron Radial Wave functions and Nuclear Beta Decay*, Oxford Science Publications (1982)

More than 600 p.!

$$\frac{dP}{dW} \propto \underbrace{pWq^2}_{\text{Phase space}} \cdot \underbrace{F(Z, W)}_{\text{Fermi function}} \cdot \underbrace{C(W)}_{\text{Shape factor}}$$

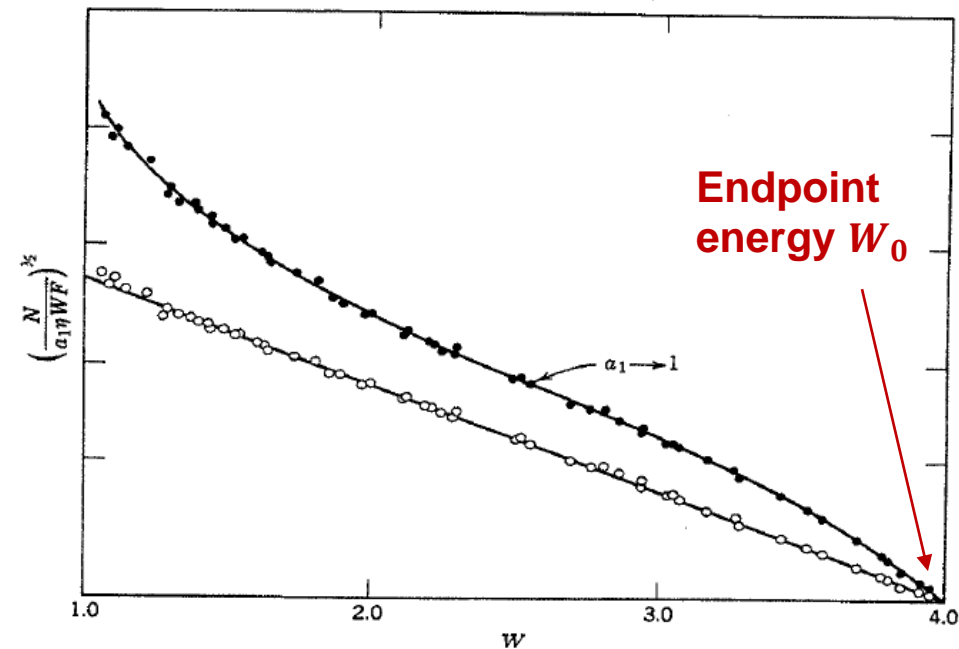


$$W = 1 + E_{\text{kin}}/m_e \quad \text{electron energy}$$

$$W_0 = 1 + E_{\text{max}}/m_e \quad \text{transition energy}$$

$$\text{Kurie plot: } \sqrt{N_{\text{exp}}/pWF(Z, W)} = (W_0 - W)$$

- Straight line for allowed transitions.
- Shape factor needed otherwise, in fit or Kurie plot.



$$p = \sqrt{W^2 - 1} \quad \text{electron momentum}$$

$$q = W_0 - W \quad \text{neutrino momentum}$$

Allowed:

$$C(W) = 1$$

First forbidden unique:

$$C(W) = q^2 + \lambda_2 p^2$$

Second forbidden unique:

$$C(W) = q^4 + \lambda_2 q^2 p^2 + \lambda_3 p^4$$

Third forbidden unique:

$$C(W) = q^6 + \lambda_2 q^4 p^2 + \lambda_3 q^2 p^4 + \lambda_4 p^6$$

Etc.

Much more complicated for forbidden non-unique transitions (see later).

In Behrens and Bühring formalism:

$$F(Z, W) = \frac{\alpha_{-1}^2 + \alpha_{+1}^2}{2p^2} \quad \lambda_k = \frac{\alpha_{-k}^2 + \alpha_{+k}^2}{\alpha_{-1}^2 + \alpha_{+1}^2}$$

Coulomb amplitudes of the relativistic electron wave functions, determined by normalization conditions.

Tabulated unscreened parameters and screened-to-unscreened ratios can be found in

Behrens, Jänecke, Landolt-Börnstein, New Series, Group I, vol. 4, Springer Verlag, Berlin (1969)

## Dirac equation

Contrary to Schrödinger equation,  $L^2$  does not commute with Hamiltonian.

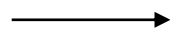
→ Appropriate operator is  $K = \beta(\vec{\sigma} \cdot \vec{L}) + 1$

→ System of coupled differential equations

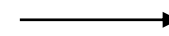
$$\begin{cases} \frac{df_\kappa}{dr} = \frac{(\kappa - 1)}{r} f_\kappa - [W - 1 - V(r)] g_\kappa \\ \frac{dg_\kappa}{dr} = [W + 1 - V(r)] f_\kappa - \frac{(\kappa + 1)}{r} g_\kappa \end{cases}$$

## Power series expansion (exact solutions)

Regular singular  $r = 0$



Ordinary  $r = r_0$



Irregular singular  $r = \infty$

$$\begin{Bmatrix} f(r) \\ g(r) \end{Bmatrix} = \frac{(pr)^{k-1}}{(2k-1)!!} \sum_{n=0}^{\infty} \begin{Bmatrix} a_n \\ b_n \end{Bmatrix} r^n$$

$$\begin{Bmatrix} rf(r) \\ rg(r) \end{Bmatrix} = \sum_{n=0}^{\infty} \begin{Bmatrix} a_n \\ b_n \end{Bmatrix} (r - r_0)^n$$

$$\begin{Bmatrix} f_{\infty j}(r) \\ g_{\infty j}(r) \end{Bmatrix} = \frac{r^{-1+yt_0/p}}{W(W+1)} e^{t_0 r} \sum_{n=0}^{\infty} \begin{Bmatrix} a_n \\ b_n \end{Bmatrix} r^{-n}$$

## Electron wave function

→ Spherical symmetry

$$\Psi(\vec{r}) = \begin{pmatrix} S_\kappa f_\kappa(r) \chi_{-\kappa}^\mu \\ g_\kappa(r) \chi_\kappa^\mu \end{pmatrix}$$

Radial  
component

Spin-angular functions  
→ spherical harmonics  
expansion

Beta decay half-lives span several order of magnitudes. Direct comparison is not practical.

Partial half-life  $t = T_{1/2}/P_{\text{trans}}$

**Comparative half-lives  $ft$  defined by**

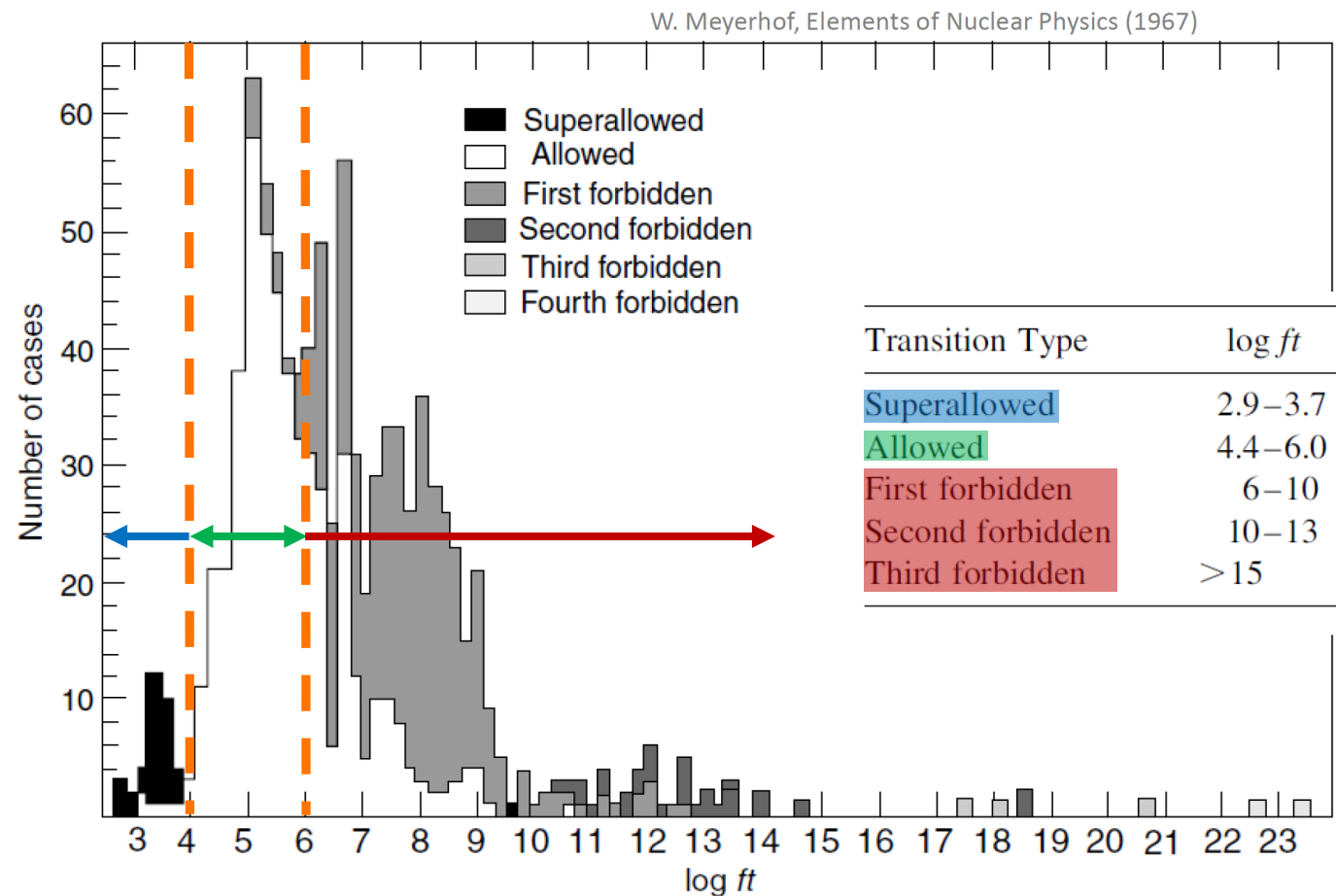
$$f = \int_1^{W_0} pWq^2 F(Z, W) dW$$

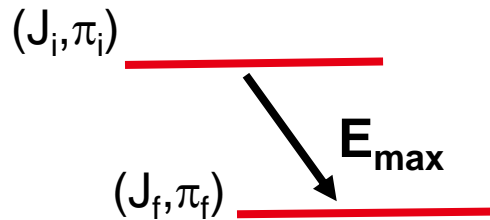
$$ft = \frac{2\pi^3 \ln 2}{G_F^2 C(W)}$$

(in relativistic units,  $\hbar = m_e = c = 1$ )

$\log_{10} ft$  values are usually compared.

N.B. Gove, M.J. Martin, *Log-f tables for beta decay*, Nuclear Data Tables 10, 205-317 (1971).





$$J_i = J_f + L_\beta + S_\beta$$

$$\Delta J = L_\beta + S_\beta$$

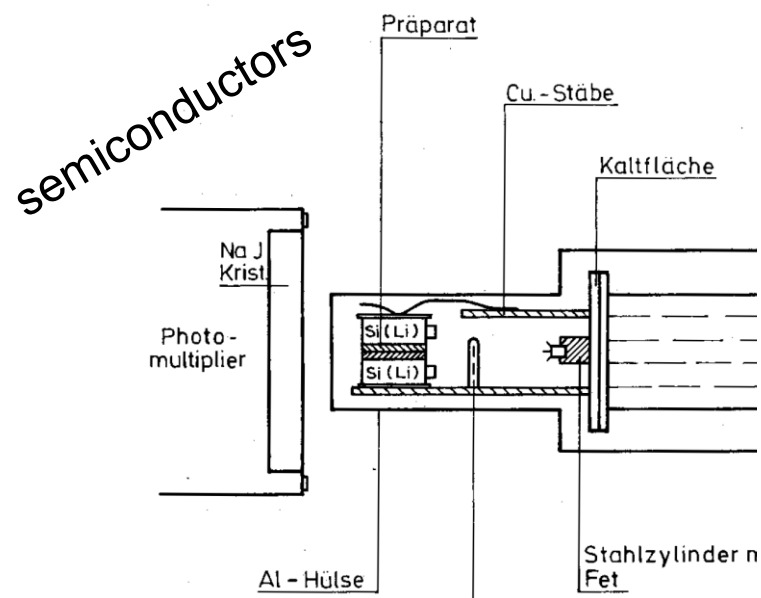
$$\pi_i \pi_f = (-1)^{L_\beta}$$

Independent of nuclear structure in first, but good approximation

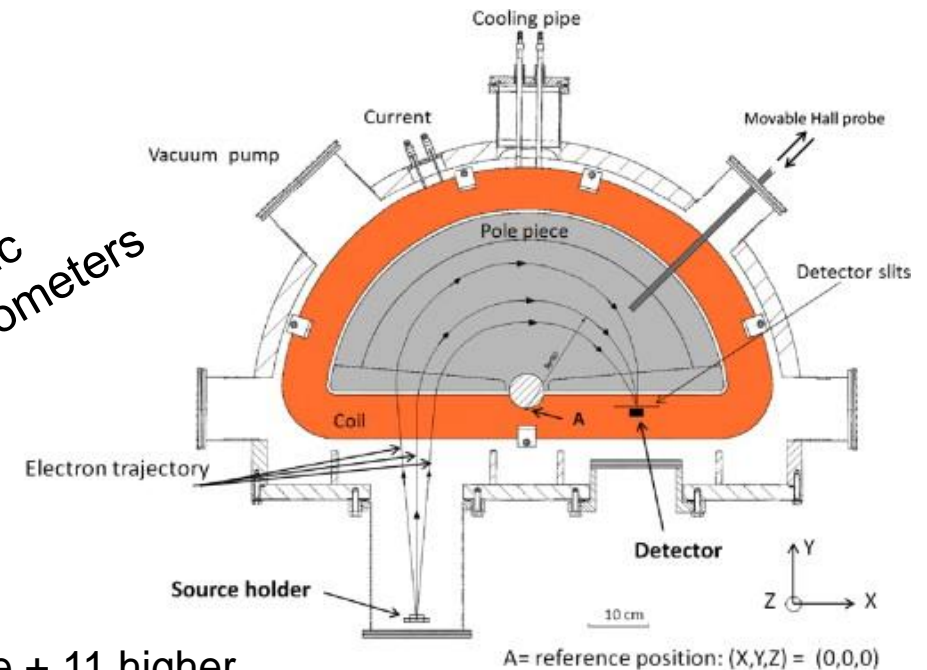
Sensitive to nuclear structure

Type of transition	Order of forbiddenness ( $L_\beta$ )	$\Delta J$	$\pi_i \pi_f$
Allowed		$0, \pm 1$	$+1$
Forbidden unique	1 <sup>st</sup>	$\pm 2$	$-1$
	2 <sup>nd</sup>	$\pm 3$	$+1$
	$(\Delta J - 1)$ th	$> 1$	$(-1)^{(\Delta J - 1)}$
Forbidden non-unique	1 <sup>st</sup>	$0, \pm 1$	$-1$
	2 <sup>nd</sup>	$\pm 2$	$+1$
	3 <sup>rd</sup>	$\pm 3$	$-1$
	$(\Delta J)$ th	$> 1$	$(-1)^{(\Delta J)}$

- 1976 review: H. Behrens, L. Szybisz, Physik Daten Vol. 6-1, Zent. Atomker.-Dok. (1976).
- 2015 update + detailed calculations of beta and neutrino spectra: X. Mougeot, Phys. Rev. C 91, 055504 (2015).
- Created database of 130 experimental shape factors, essentially from



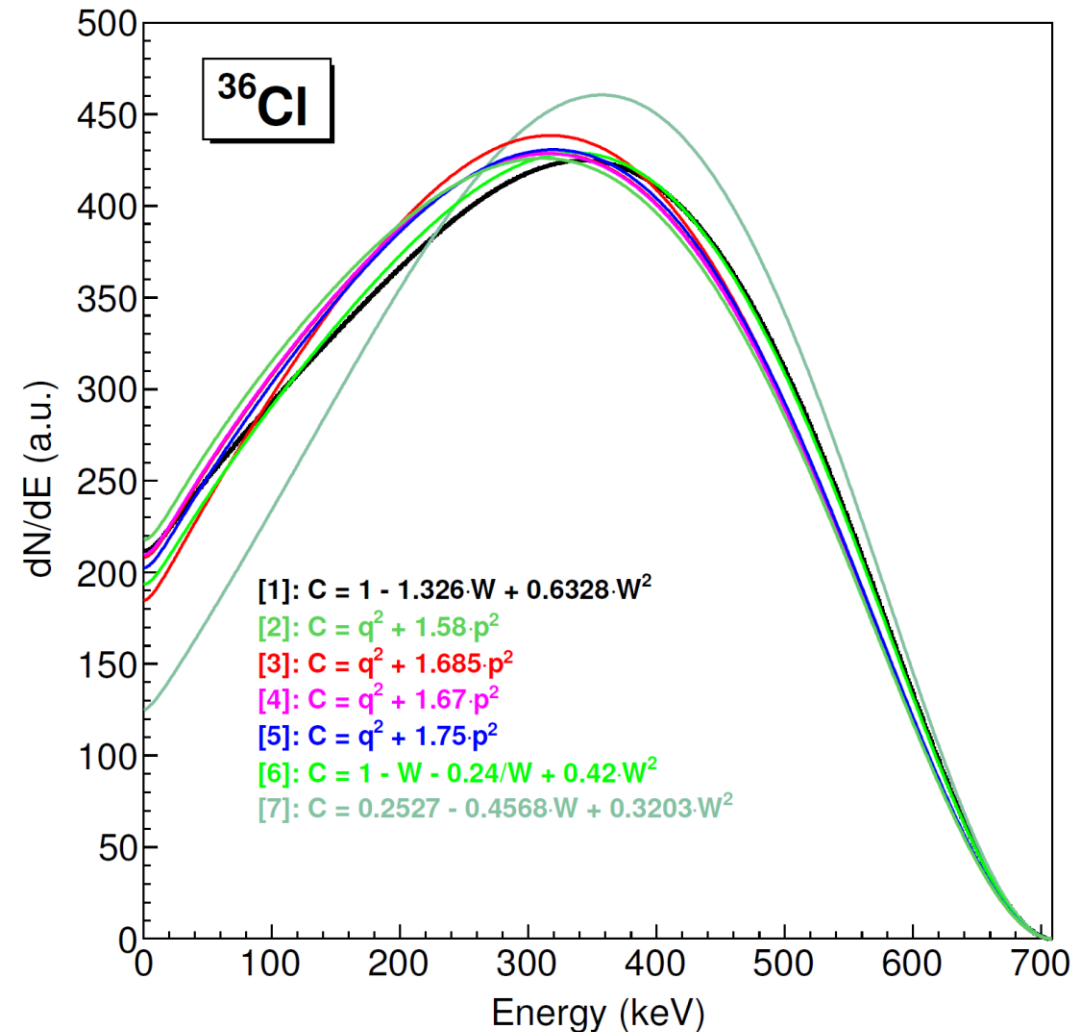
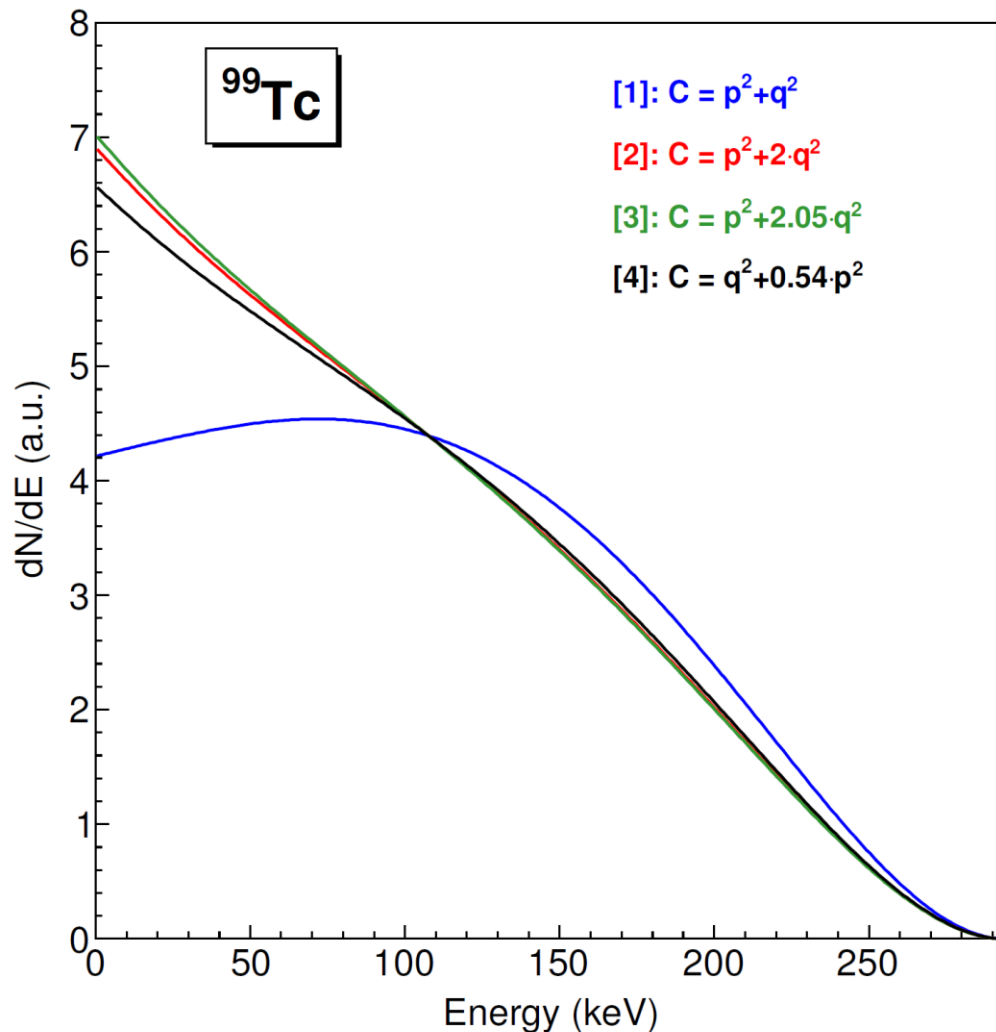
magnetic spectrometers



- Transitions: 36 allowed, 25 1<sup>st</sup> unique + 5 higher, 53 1<sup>st</sup> non-unique + 11 higher.
- Very few (6) measurements below 20 keV.
- Very few high order forbidden transitions.
- 11 published shape factors since 1976!

New precise measurements are needed to test the theoretical predictions.

Comparison of published experimental spectra for two second forbidden non-unique decays.



Electrons scatter very easily in matter:

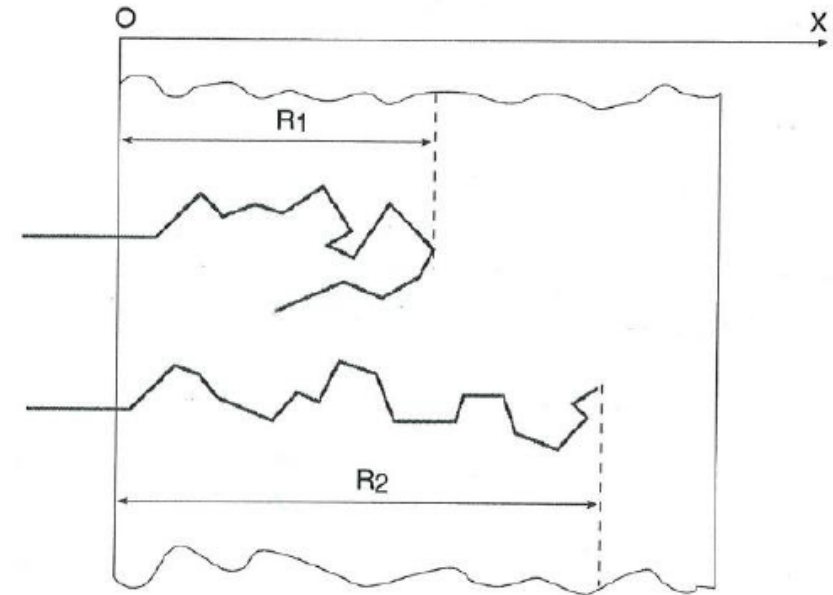
- Chaotic path, high angular straggling.
- Elastic collisions.
- Cherenkov effect.
- Inelastic collisions, excitation and ionisation of material atoms.
- Bremsstrahlung in material.

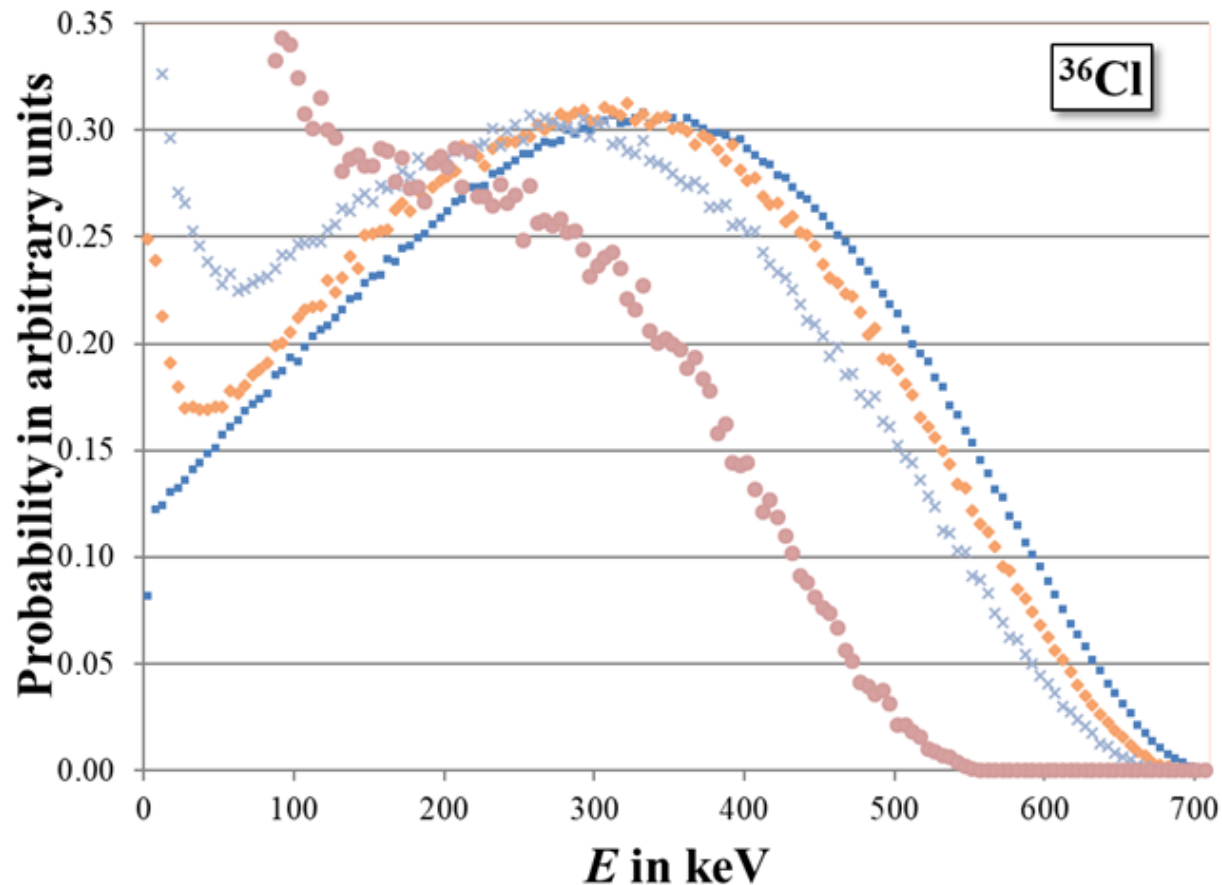
Some formulas to estimate electron range:

$$R \text{ (in cm)} \approx \frac{0.35 \times E_{\text{MeV}}}{\rho \text{ (in g} \cdot \text{cm}^{-3}\text{)}}$$

$$R \text{ (in mg} \cdot \text{cm}^{-2}\text{)} \approx 412 \times E_{\text{MeV}}^{(1.265 - 0.0964 \times \ln E)} \quad \text{from 10 keV to 2.5 MeV.}$$

$$R \text{ (in mg} \cdot \text{cm}^{-2}\text{)} \approx (530 \times E_{\text{MeV}}) - 106 \quad \text{beyond 2.5 MeV.}$$





- Self-absorption effect study for a  $^{36}\text{Cl}$  radioactive source.
- NaCl crystals as sphere of various sizes.
- Monte Carlo simulation of deposited energy within a  $4\pi$  absorber.

- MC input spectrum from
- ◆ MC, NaCl sphere,  $r = 0.05$  mm
- × MC, NaCl sphere,  $r = 0.1$  mm
- MC, NaCl sphere,  $r = 0.5$  mm

Rotzinger *et al.*, J. Low Temp. Phys. 151, 1087-1093 (2008)

Unpublished study performed by M. Paulsen, K. Kossert and J. Beyer (PTB Germany) within the **MetroBeta** project.

## Bound state decays

- Only bound electron in the final state, no beta particle emitted.
- Antineutrino carries away all the excess decay energy.

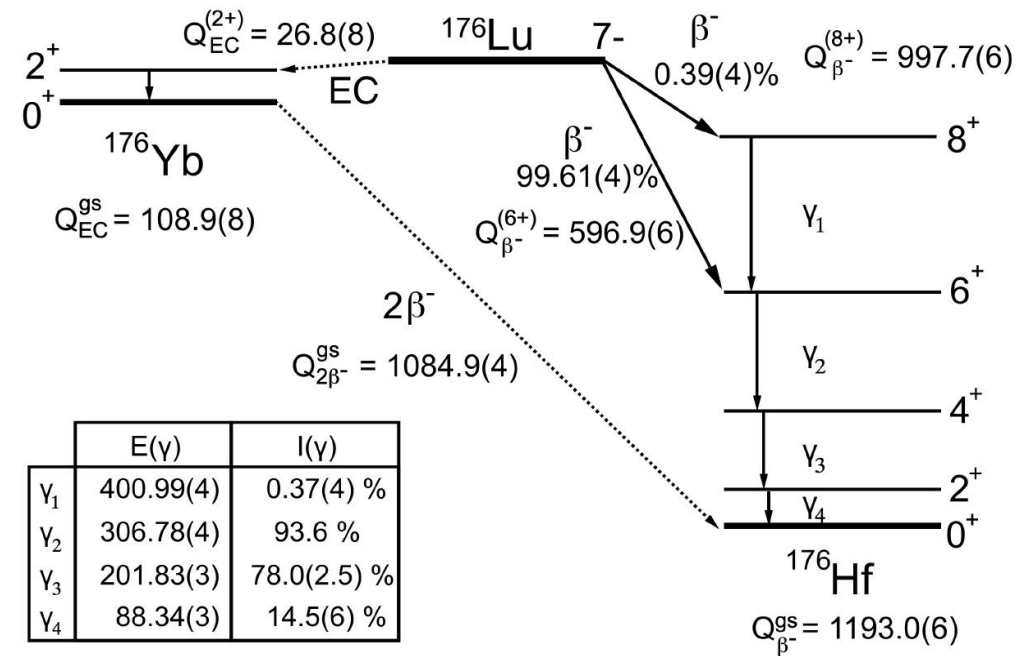
## Beta delayed decays

- Nuclei far from stability can populate unbound states and lead to direct nucleon emission.
- Typically, beta delayed neutron emission.

## Double beta decays

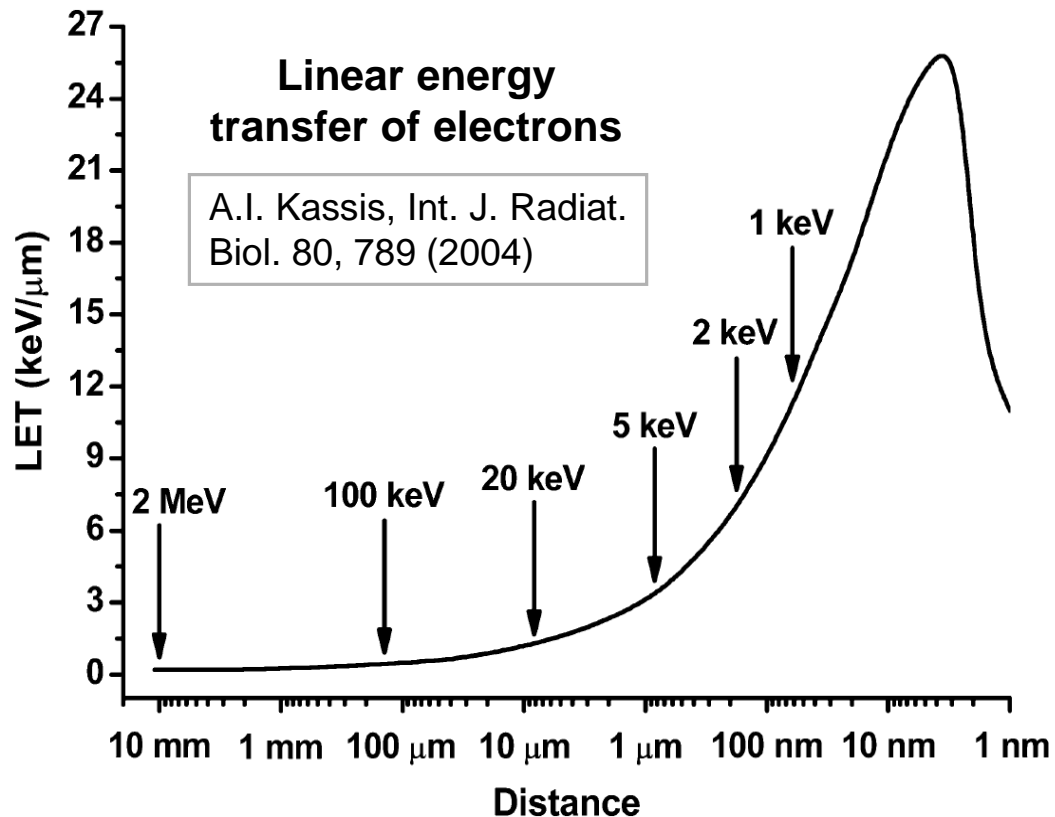
- Standard Model  $\rightarrow$  with neutrino emission ( $2\nu\beta\beta$ ).
- Beyond Standard Model  $\rightarrow$  no neutrino emission ( $0\nu\beta\beta$ ).
- Can be combined with electron capture: ( $2\nu ECEC$ ), ( $0\nu ECEC$ ), ( $2\nu\beta EC$ ), ( $0\nu\beta EC$ ).

These processes are of interest in themselves but are not treated in this presentation.



## High-precision study of atomic effects

- Measurements and calculations of  $^{63}\text{Ni}$  and  $^{241}\text{Pu}$  decays
- Impact in metrology: primary standardization of beta pure emitters



## Metrology

Primary activity measurements by liquid scintillation counting.

R. Broda, P. Cassette, K. Kossert, Metrologia 44, S36-S52 (2007)

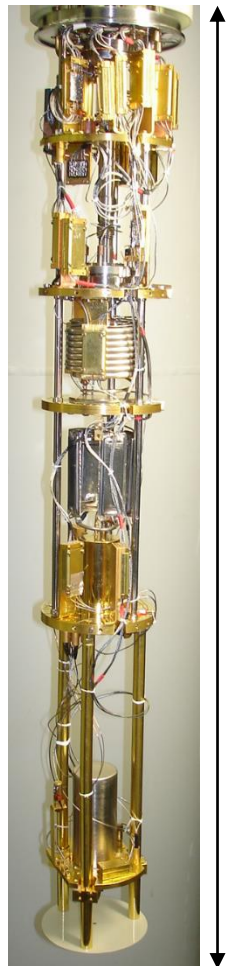
## Nuclear Medicine

Estimate of **deposited dose** in patient's cells. Impact at DNA level.

M. Bardiès, J.-F. Chatal, Phys. Med. Biol. 39, 961-981 (1994)

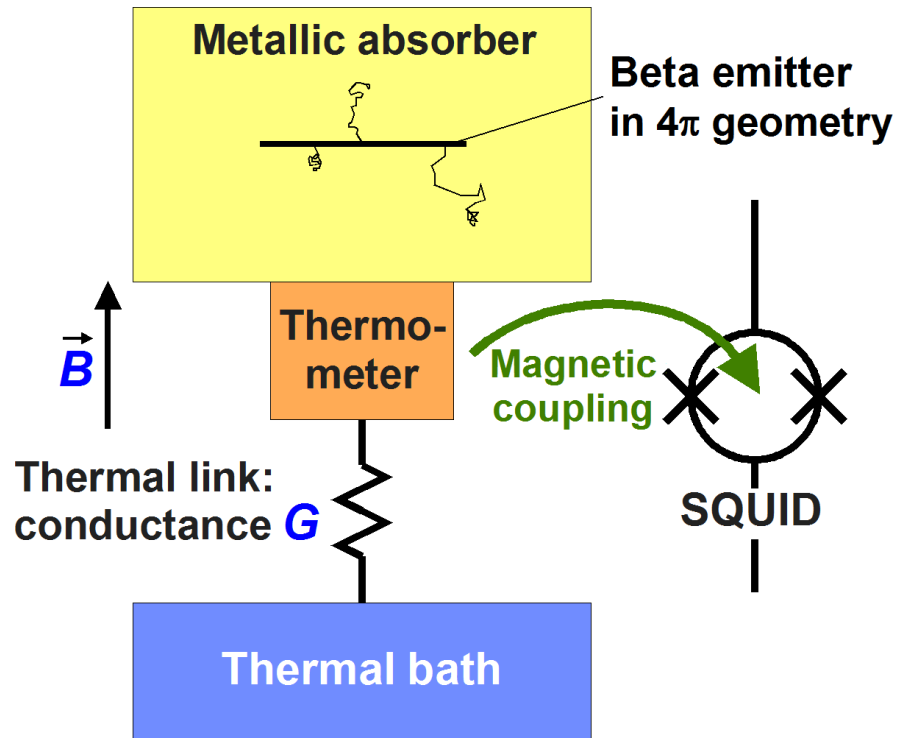
Precise knowledge of energy distribution is necessary for:

- electrons/positrons (beta decay)
- Auger electrons (subsequent to electron capture or ionization)

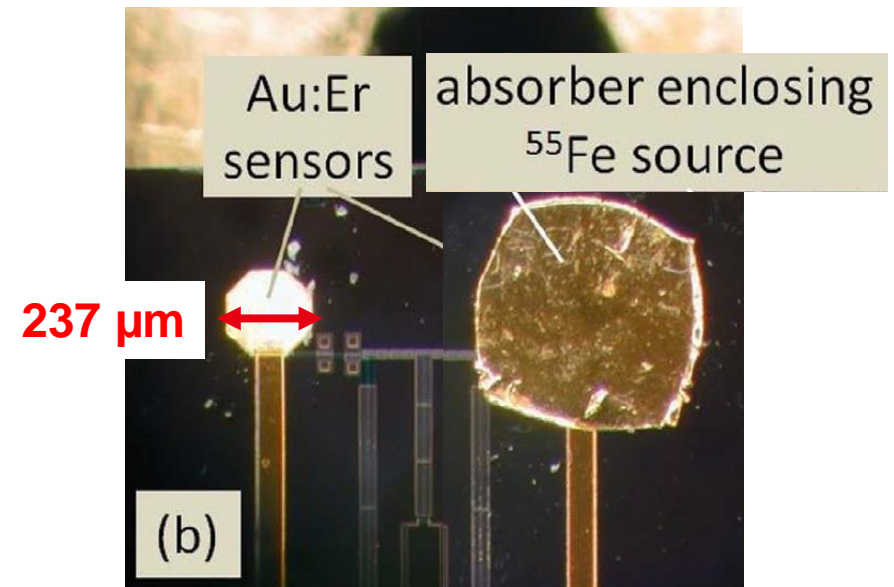
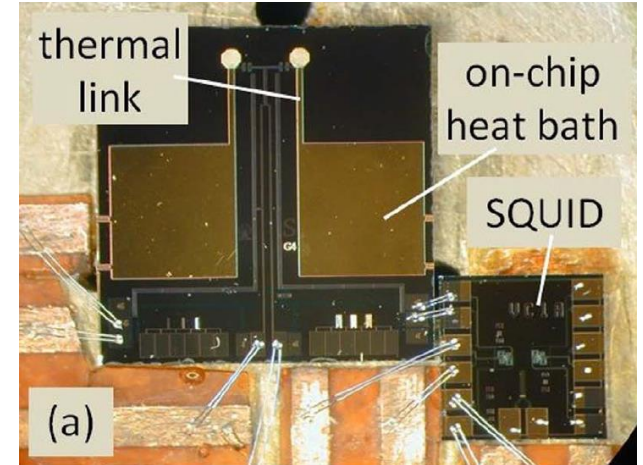


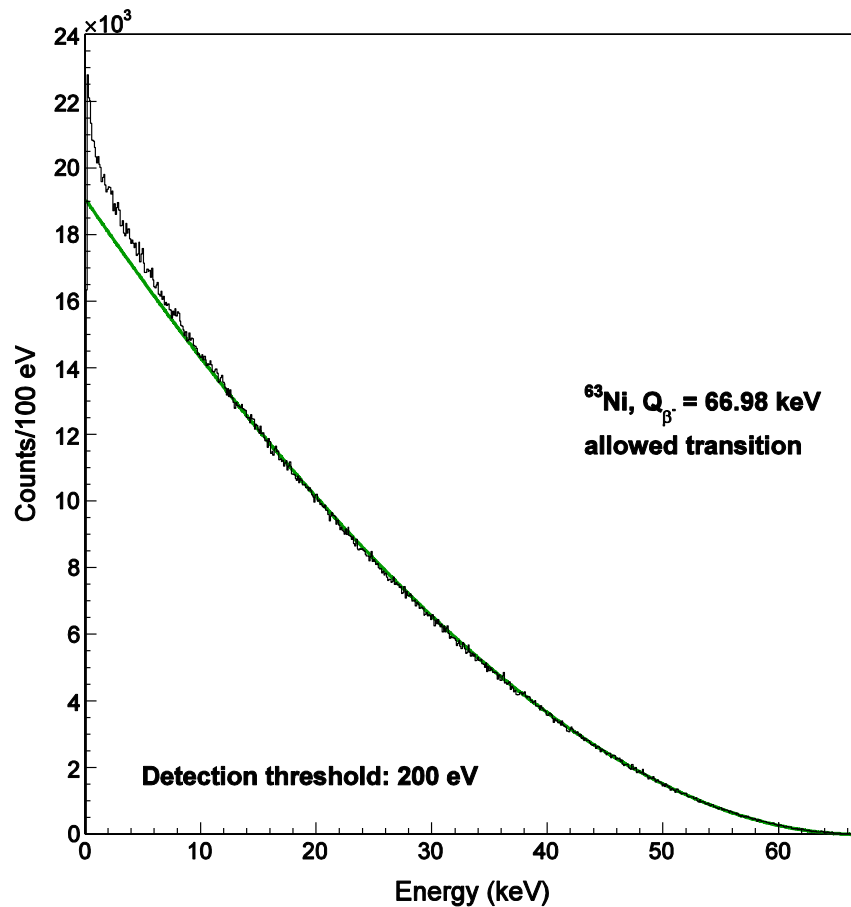
Dilution refrigerator  
(10 mK)

80 cm

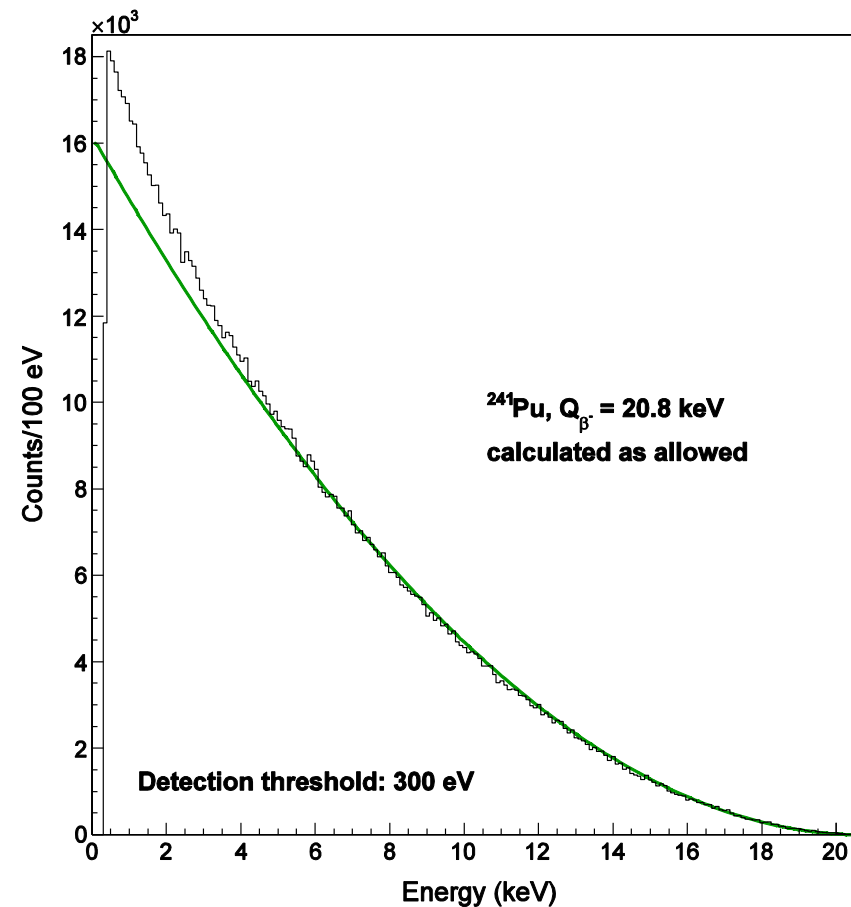


M. Loidl *et al.*, *App. Radiat. Isot.* 134, 395 (2018)





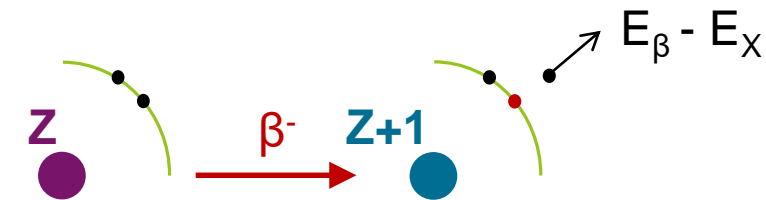
Usual beta decay calculations fail to reproduce these “simple” spectra.



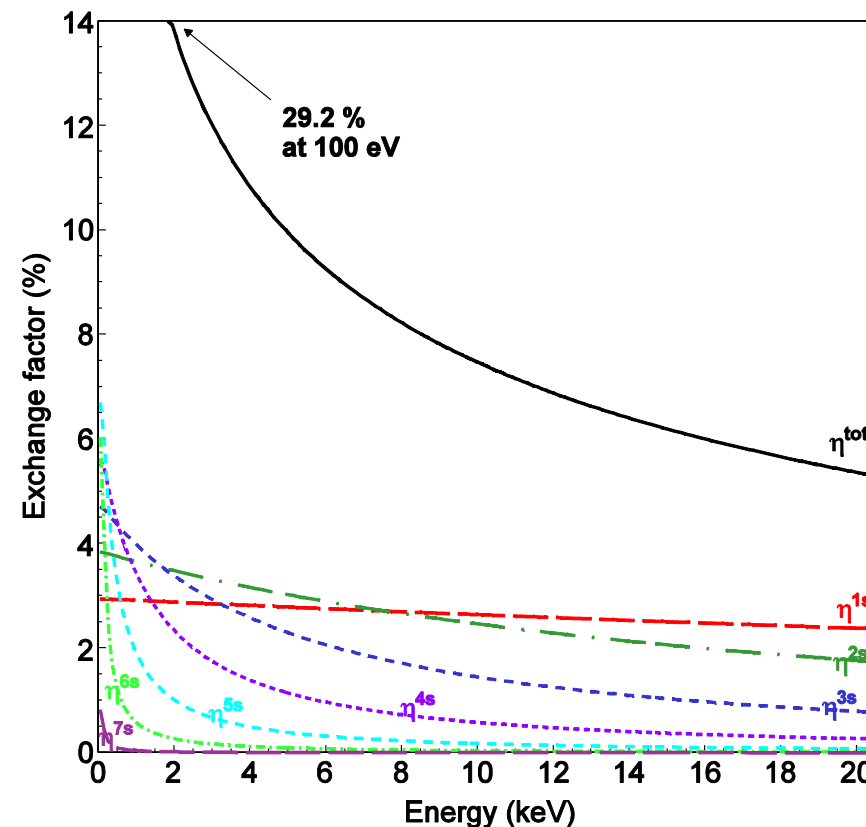
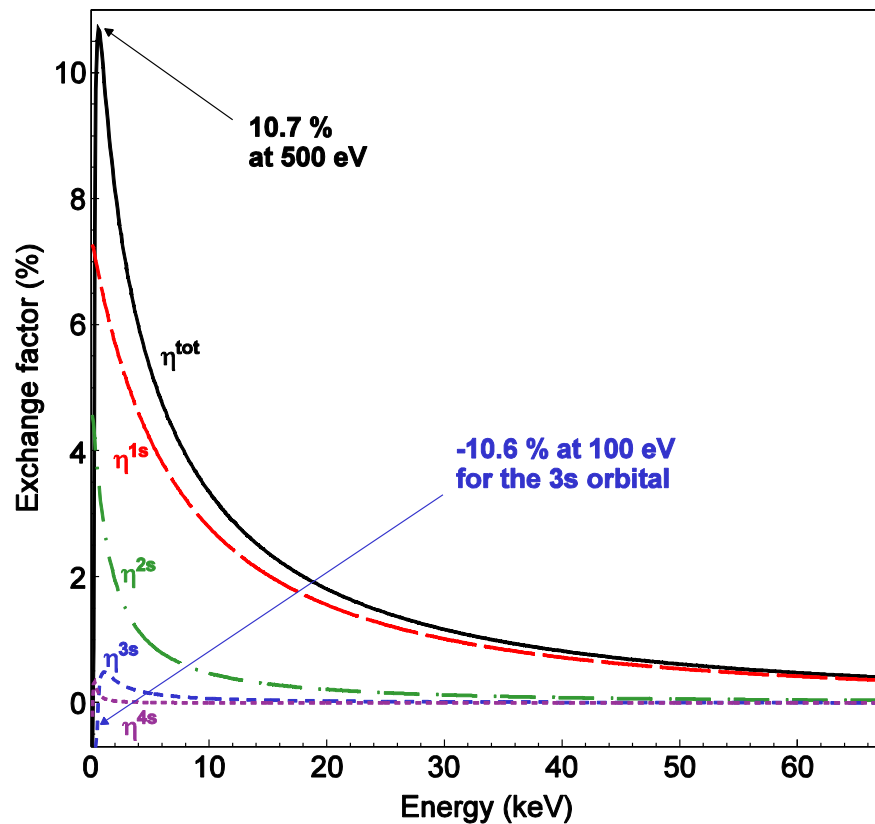
**1<sup>st</sup> forbidden non-unique transition**  
calculated as **allowed**

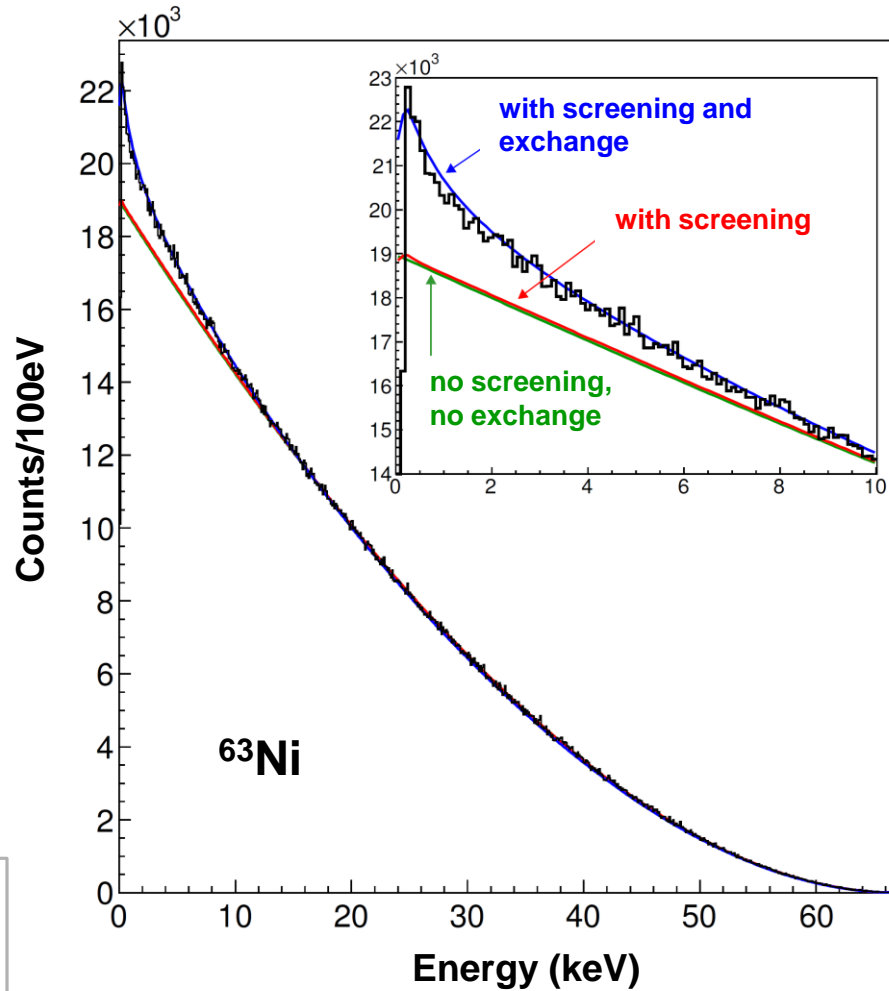
$$2\xi = \alpha Z/R \gg E_0 = 20.8 \text{ keV} \ll 19.8 \text{ MeV}$$

- Indistinguishable from the direct decay to a final continuum state.
- Depends on the **overlap of the continuum and bound electron wave functions**.
- **Allowed transitions:  $s_{1/2}$  and  $p_{1/2}$  orbitals only.**



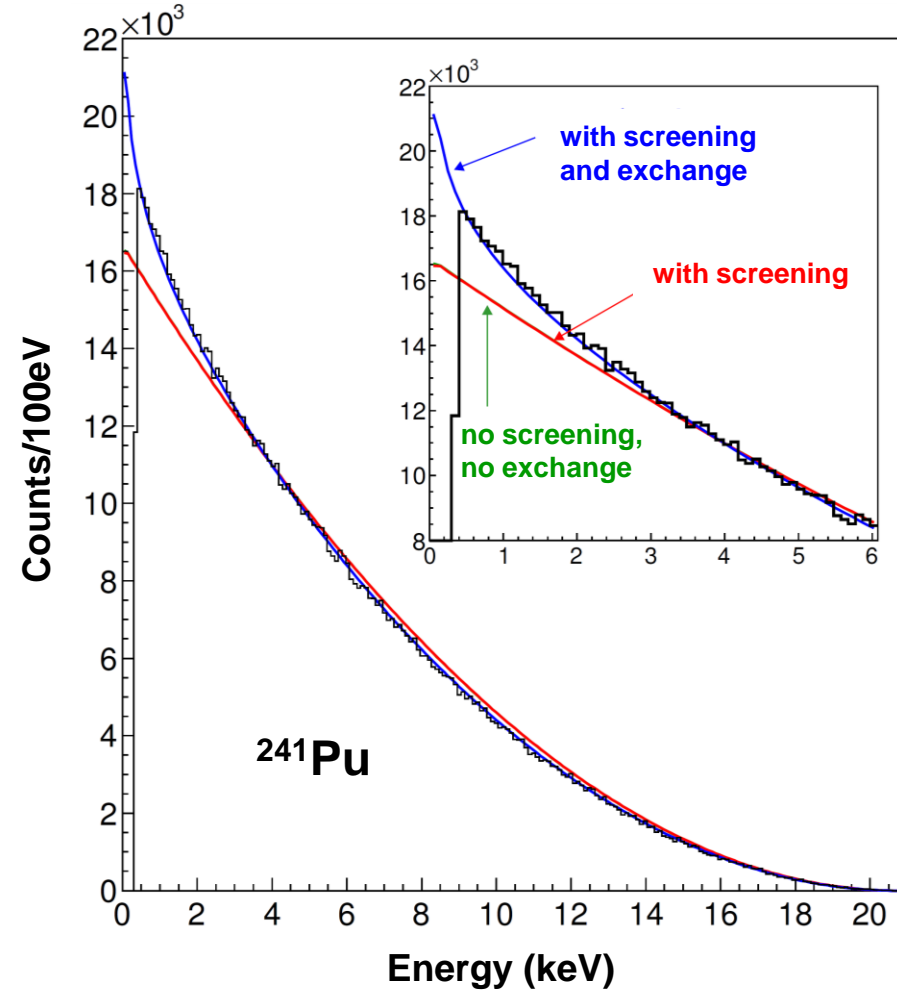
N.C. Pyper, M.R. Harston, Proc. Roy. Soc. Lond. A 420, 277 (1988)





Usual calculation:  $E_{\text{mean}} = 17.45 \text{ keV}$

Full calculation:  $E_{\text{mean}} = 17.06 \text{ keV}$



Usual calculation:  $E_{\text{mean}} = 5.24 \text{ keV}$

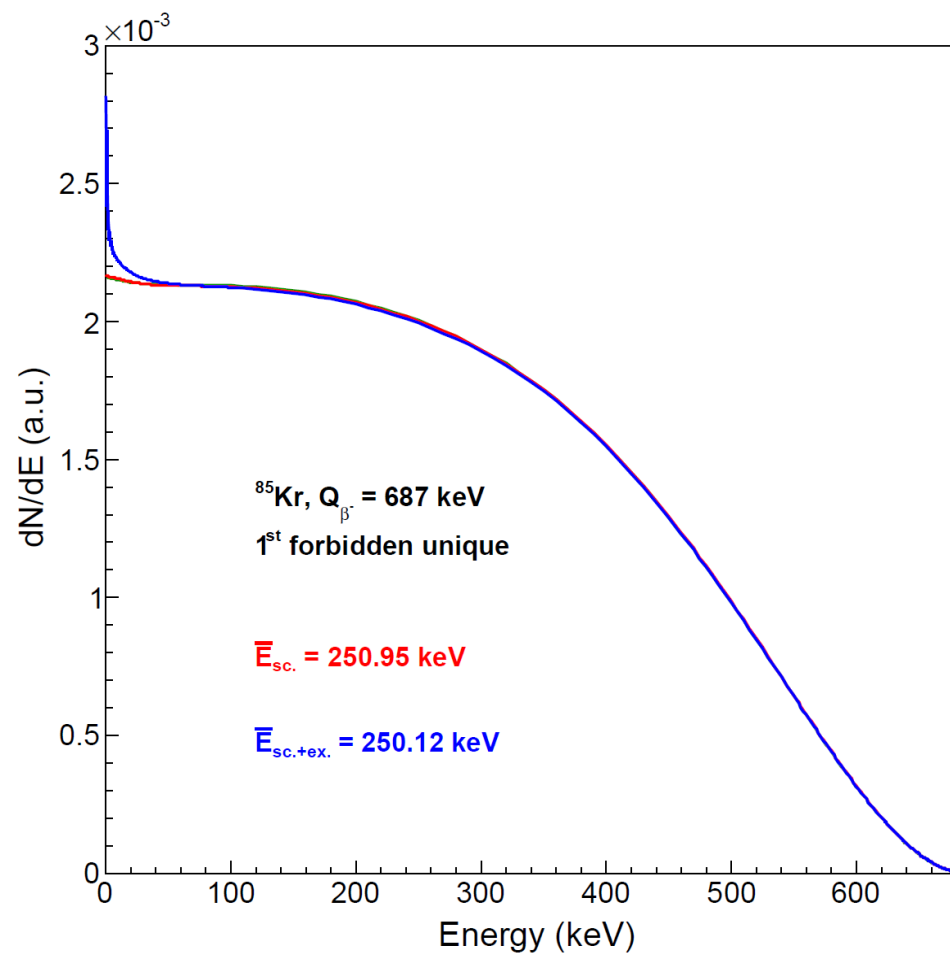
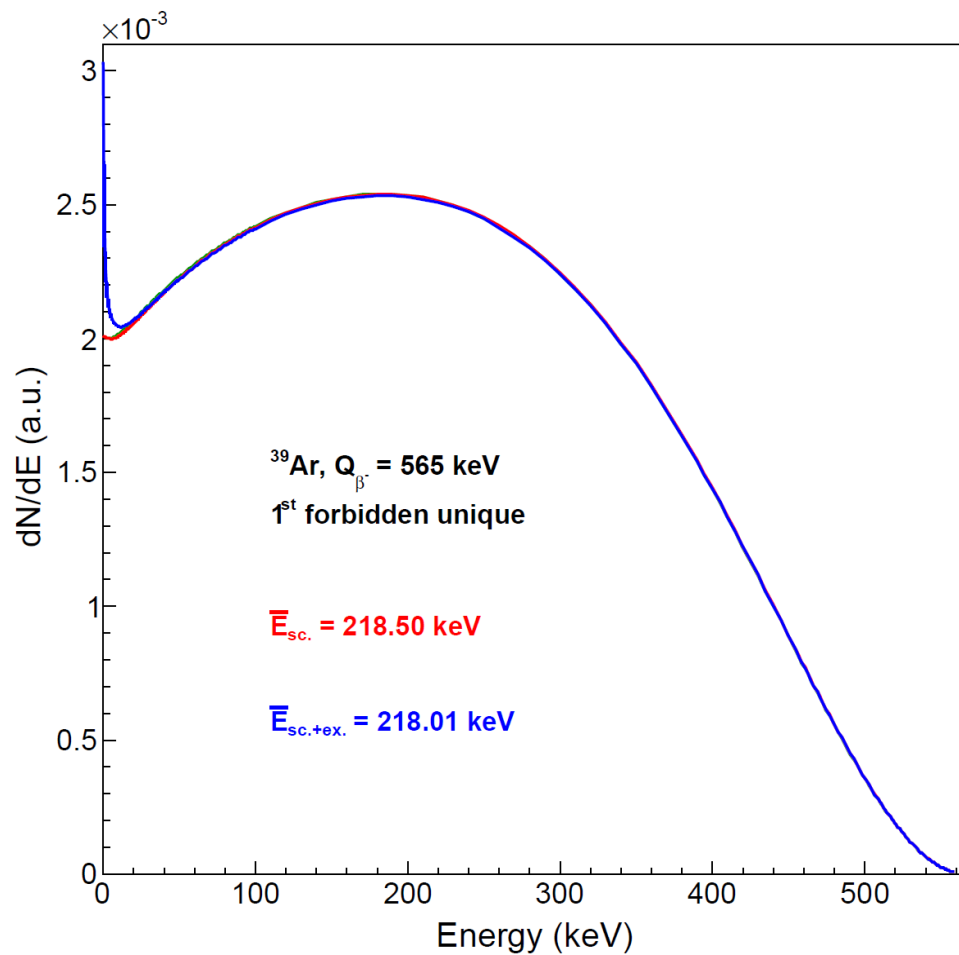
Full calculation:  $E_{\text{mean}} = 5.04 \text{ keV}$

M. Loidl *et al.*, App.  
Radiat. Isot. 68,  
1454 (2010)

X. Mougeot, C.  
Bisch, Phys. Rev. A  
90, 012501 (2014)

Recent extension of atomic exchange effect to forbidden unique transitions

→ **Contribution of additional atomic orbitals**



**Extension of SIR to pure beta emitters (and captures)**

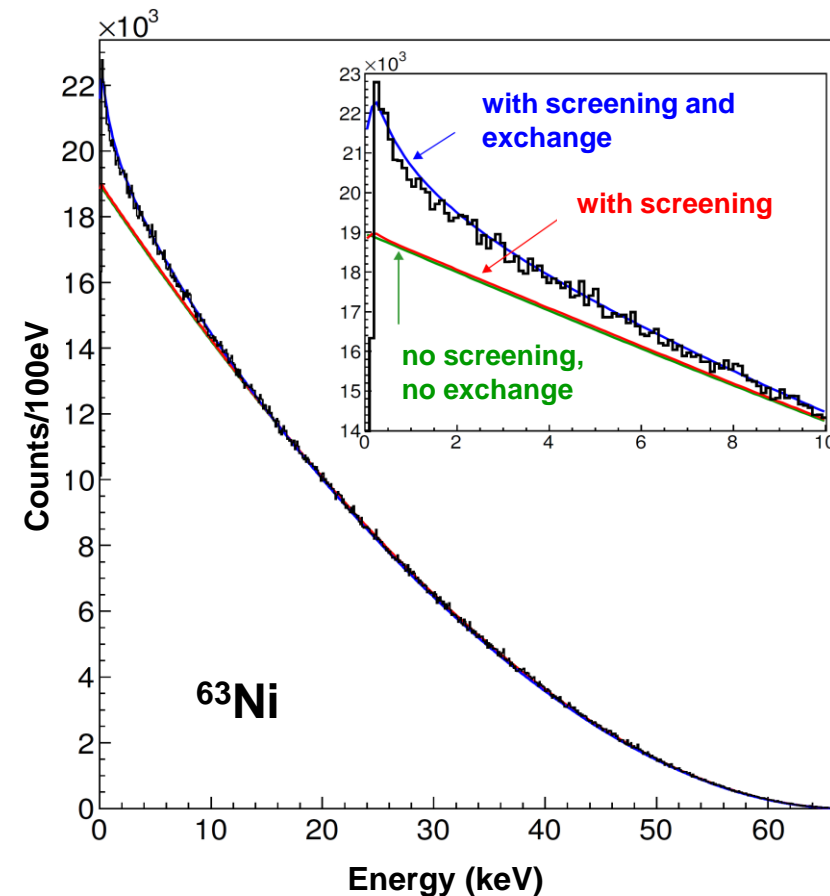
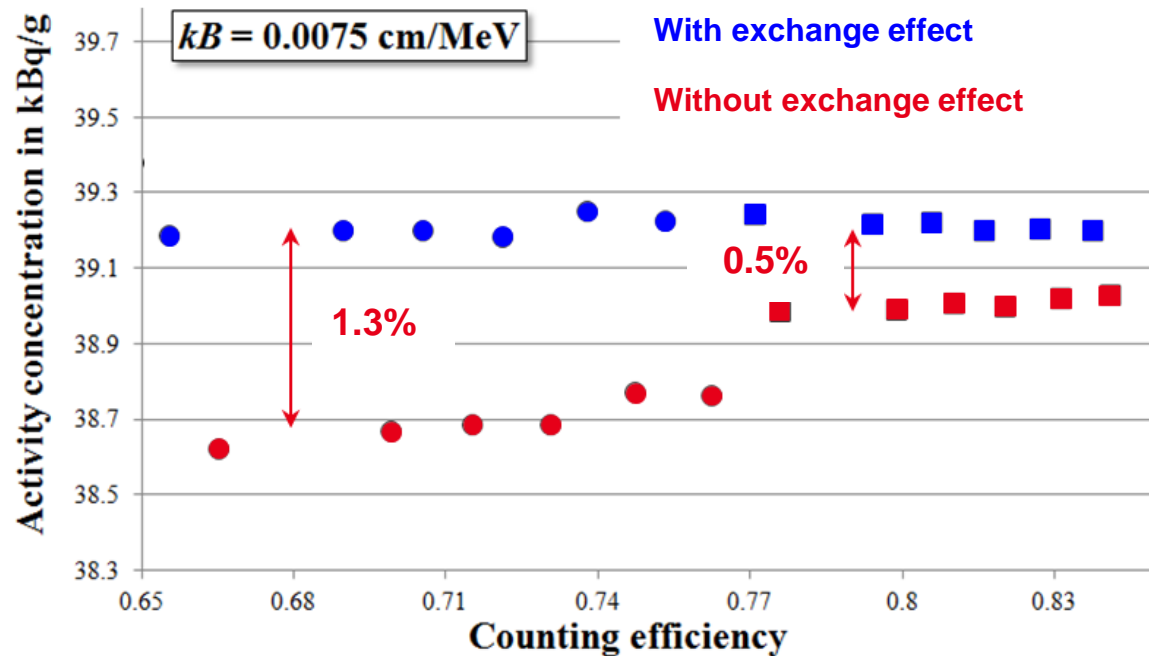
- Counting efficiency directly depends on beta spectrum
- Strong non-linearity at low energy
- **Typical uncertainty: 0.5%**

BIPM **ESIR** systemR. Coulon et al., Metrologia  
57, 035009 (2020)**CIEMAT/NIST** (2 PMTs, traceur)

$$\varepsilon = \int_0^{E_{\max}} S(E) (1 - e^{-\eta})^2 dE \quad \eta = \frac{\nu}{n} \int_0^E \frac{AdE}{1 + kB \frac{dE}{dx}}$$

**TDCCR** (3 PMTs, Triple to Double Coincidence Ratio)

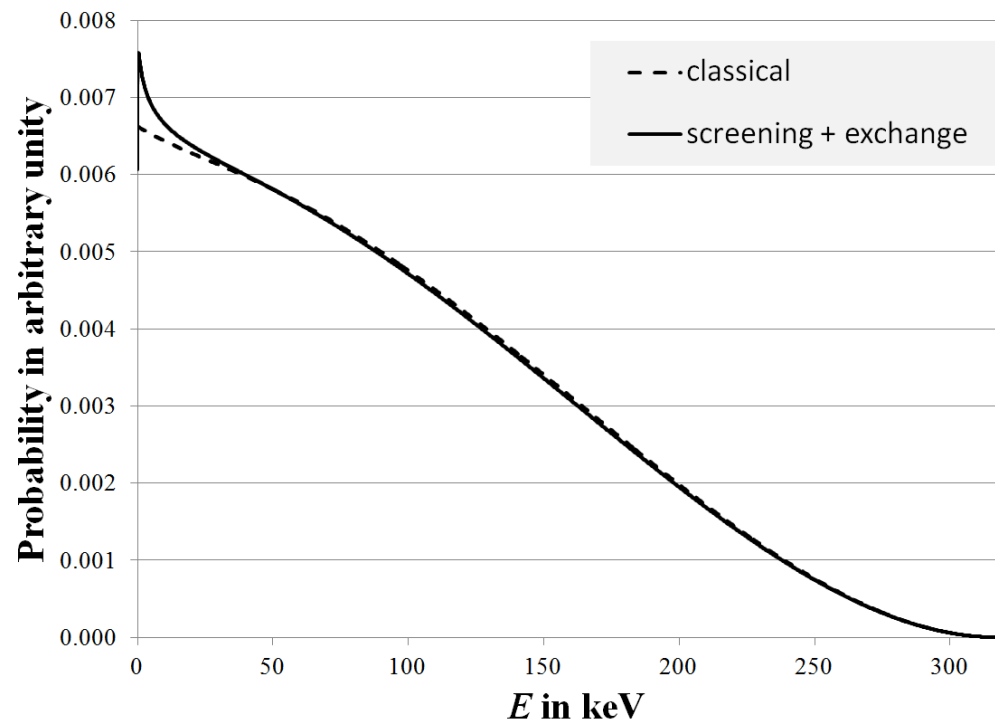
$$\frac{R_T}{R_D} = \frac{\int_0^{E_{\max}} S(E) (1 - e^{-\eta})^3 dE}{\int_0^{E_{\max}} S(E) [3(1 - e^{-\eta})^2 - 2(1 - e^{-\eta})^3] dE}$$



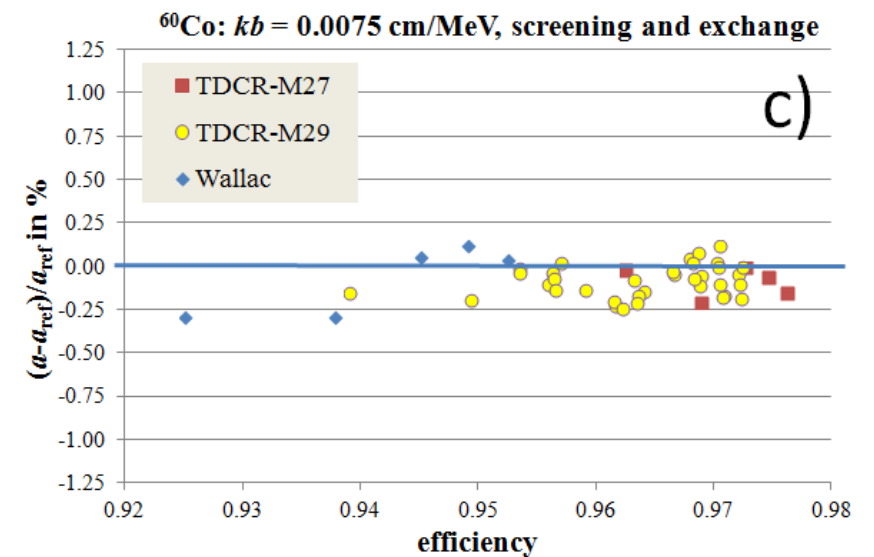
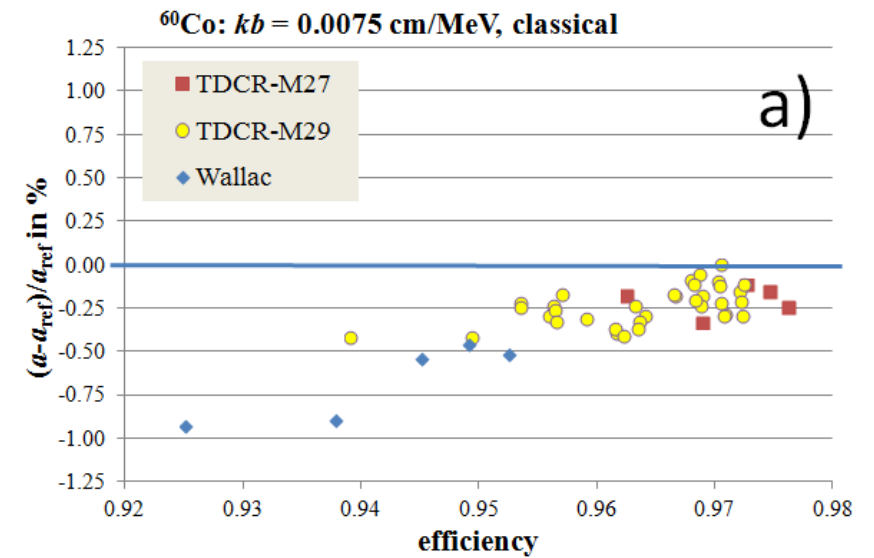
Excellent agreement between RCTD and CIEMAT/NIST

- $^{63}\text{Ni}$ : K. Kossert, X. Mougeot, Appl. Radiat. Isot. 101, 40 (2015)
- $^{60}\text{Co}$ : K. Kossert et al., Appl. Radiat. Isot. 134, 212 (2018)
- $^{90}\text{Sr}/^{90}\text{Y}$ : K. Kossert, X. Mougeot, Appl. Radiat. Isot. 168, 109478 (2021)

Reference activity with  $4\pi\beta\text{-}\gamma$  coincidence counting, independent of the beta spectrum



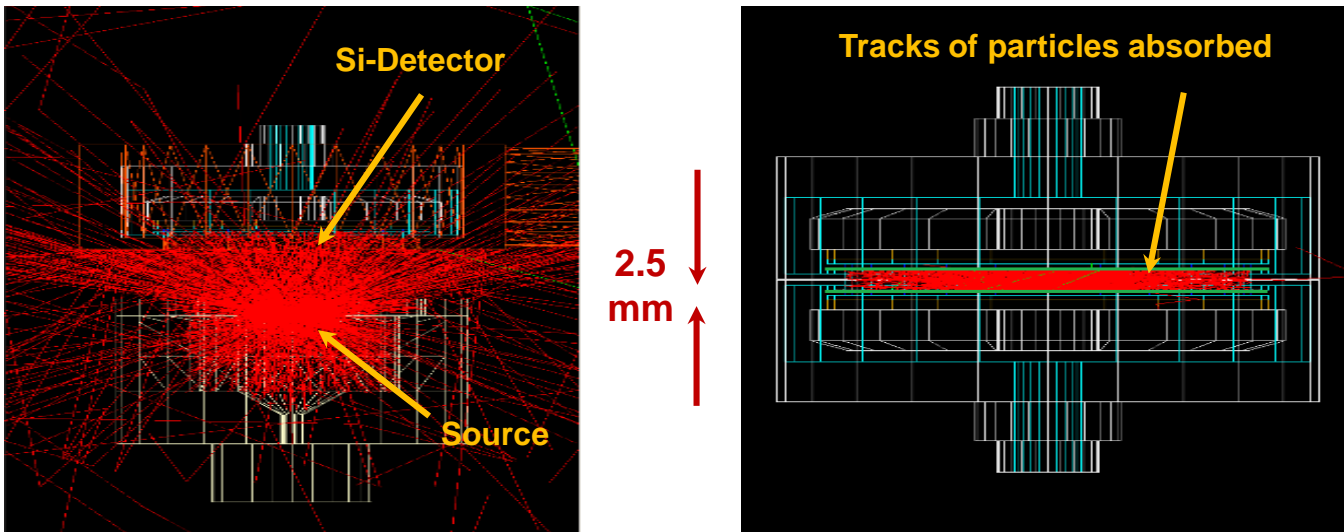
K. Kossert et al., Appl. Radiat. Isot. 134, 212 (2018)



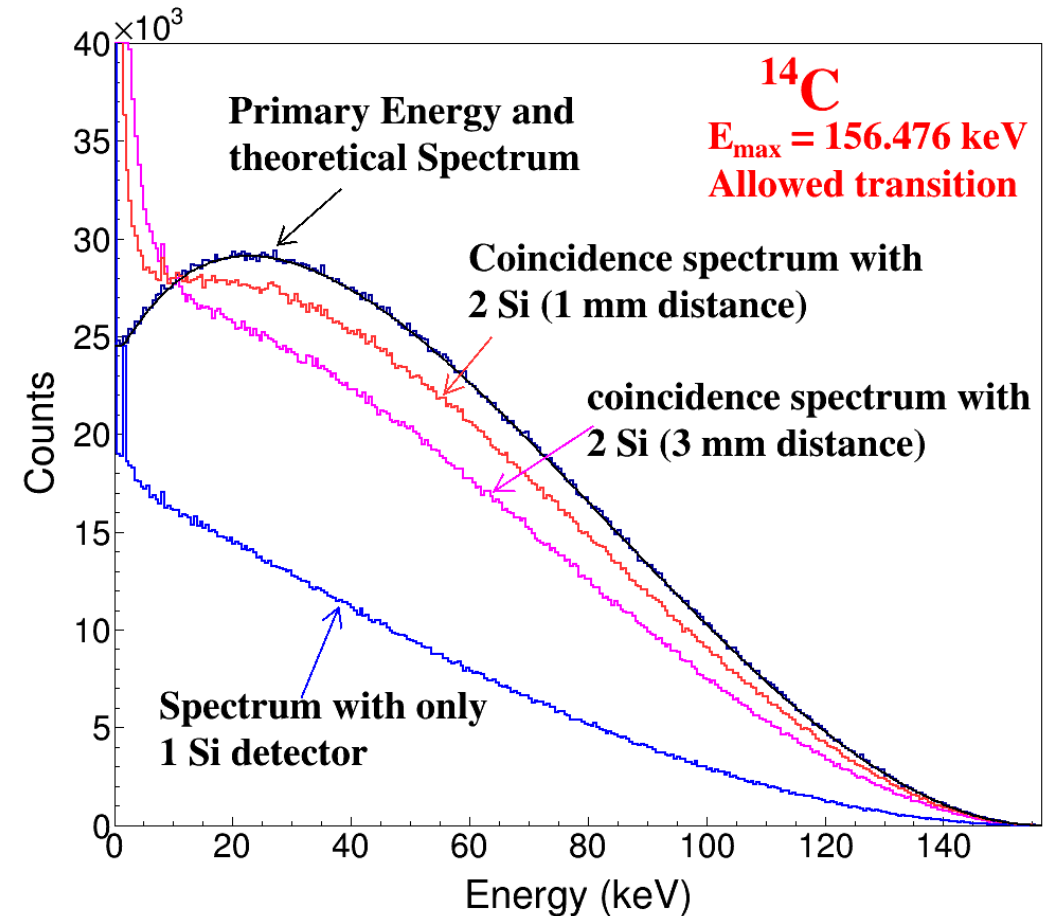
## Study of beta spectra at medium energies

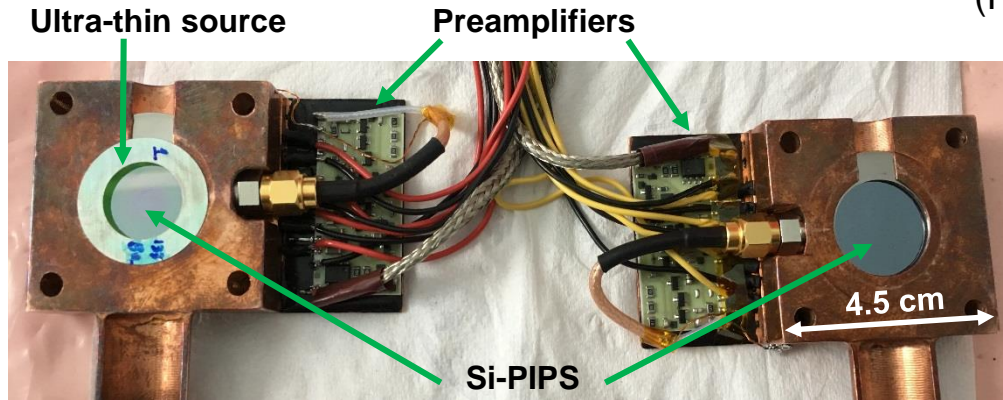
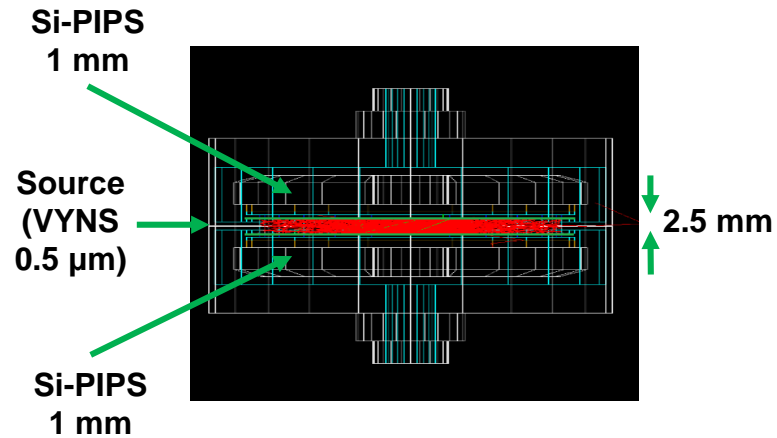
- An silicon-based apparatus
- $^{14}\text{C}$ ,  $^{204}\text{Tl}$  and  $^{99}\text{Tc}$  decays

Monte Carlo simulated tracks of particles in  $2\pi$  and  $4\pi$  geometries

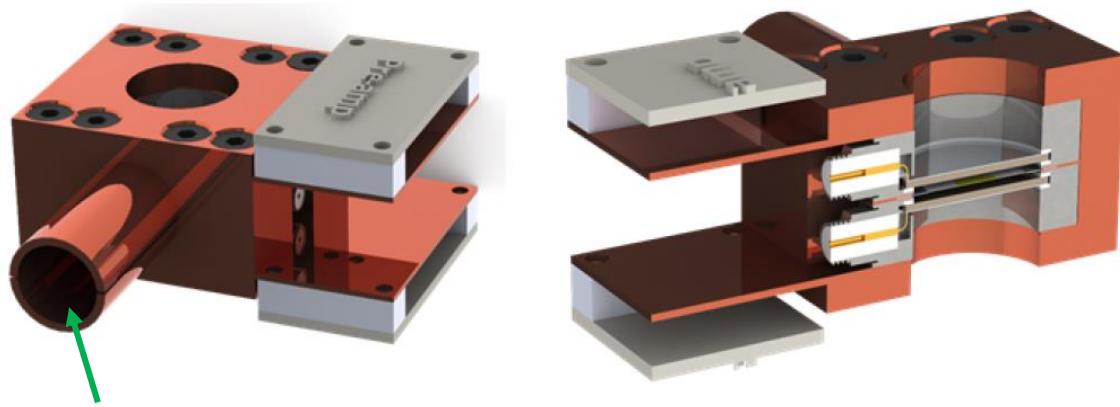


Monte Carlo Simulations  
with PENELOPE 2016



Abhilasha Singh  
(PhD 2017-2020)

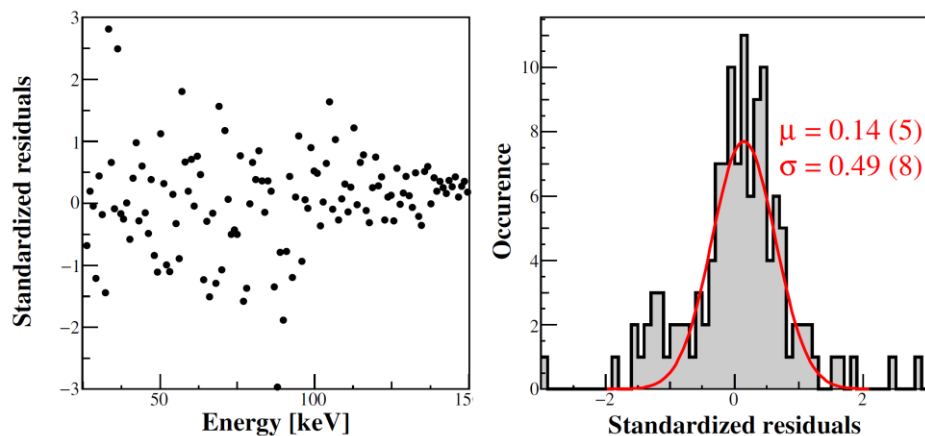
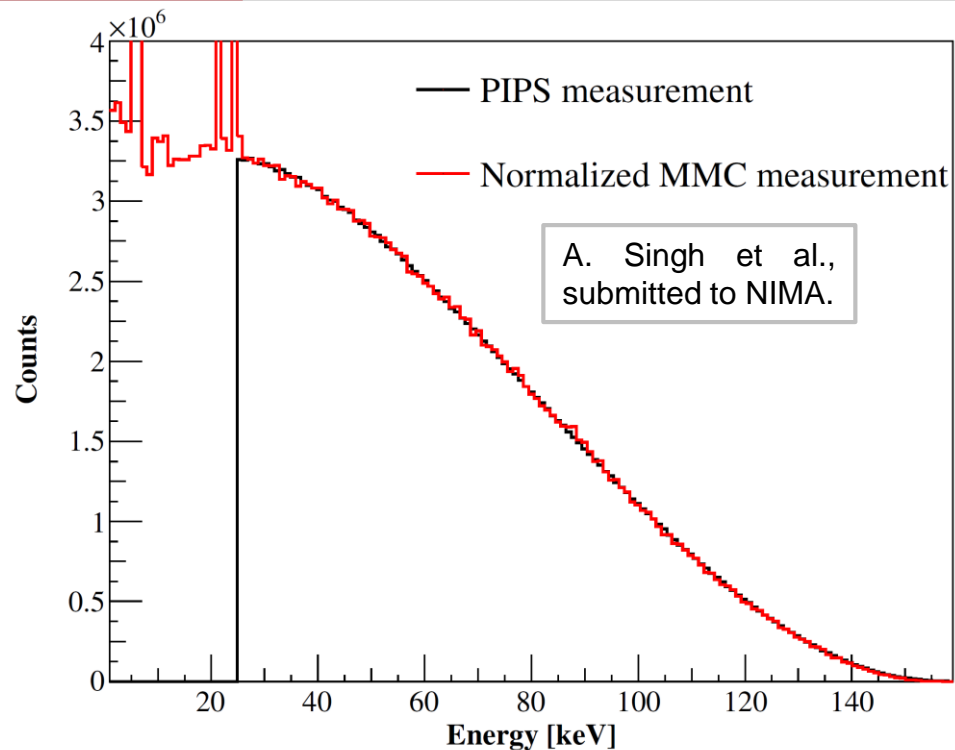
Configuration for measurement



Specific source preparation technique

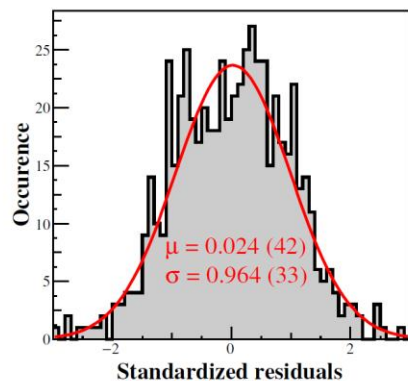
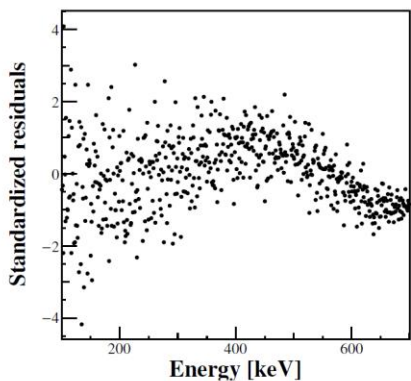
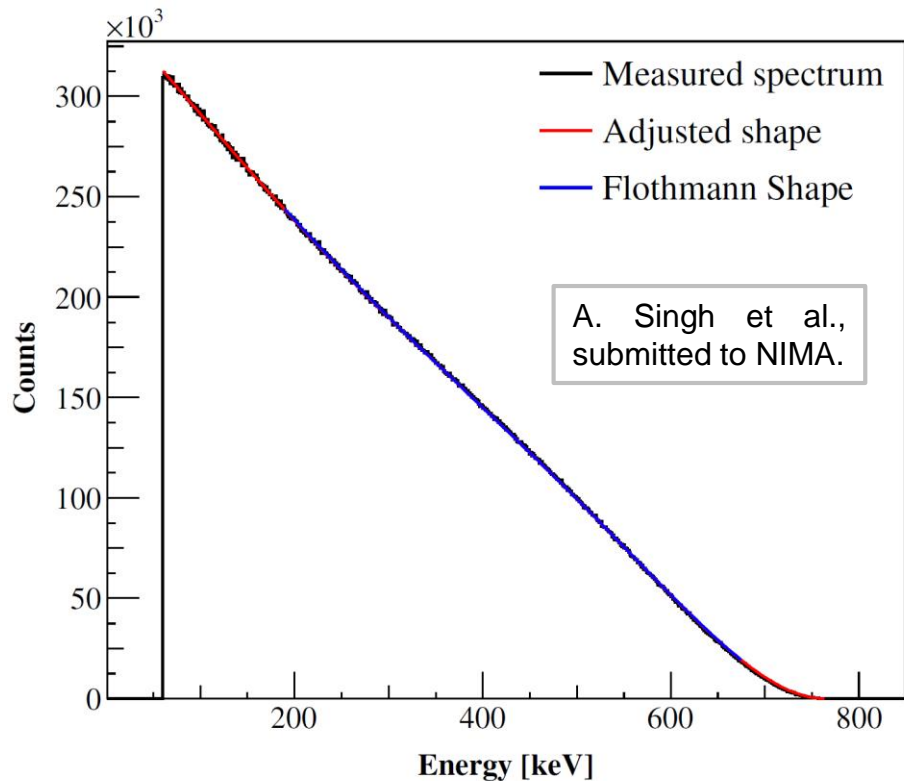


Unsealed sources: 0.5 to  $0.7 \mu\text{m}$  thick  
 Sealed sources: 1 to  $1.5 \mu\text{m}$  thick  
 Typical activity:  $\sim 1 \text{ kBq}$



- Distortion remains in the measured spectrum: particle escape, dead layers, source.
  - Unfolding process based on precise mono-energetic Monte Carlo simulations.
- Comparison with a high-precision measurement with a Metallic Magnetic Calorimeter (MMC) is possible.
- ✓ Excellent agreement of the spectra in the common energy range.
- ✓ Extracted Q-value = 156.49 (43) keV fully consistent with AME2020 value of 156.476 (4) keV.
- ✓ Controversy on the spectrum shape: weak magnetism term confirmed.

Study	$a$ in $\text{MeV}^{-1}$	Comment
[44]	-0.386	CVC from exp. not certain
[45]	-0.37 (4)	SM, $\times 2$ difference with CVC
[36]	-0.43	SM, consistent with CVC
[41]	-0.45 (4)	$^{14}\text{C}$ -doped Ge detector
[8]	-1.038 (28)	Wall-less prop. counter
This work	-0.430 (23)	Si detector, with $F_0 L_0$

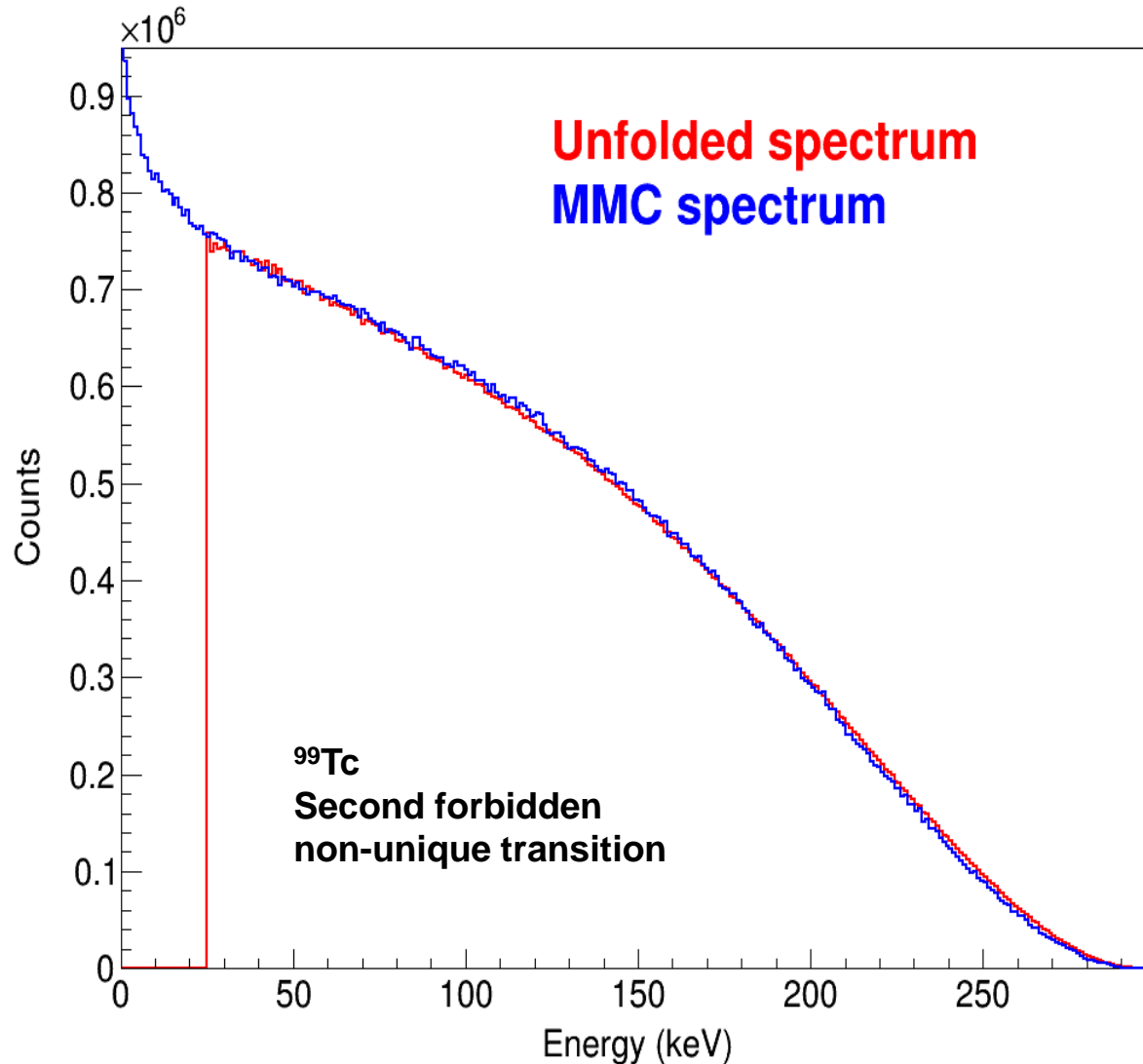


- Distortion remains in the measured spectrum: particle escape, dead layers, source.  
→ Unfolding process based on precise mono-energetic Monte Carlo simulations.
- Comparison with the reference spectrum in the literature from Flothmann et al., Z. Phys. A 225, 164 (1969).
- ✓ Excellent agreement of the spectra in the common energy range.

$$C(W) = dq^2 + \lambda_2 p^2$$

The shape parameter is identical if Fermi functions are too:  
Flothmann et al.  $d = 1.097$  (8) vs  $d = 1.095$  (7) here.

- ✓ Extracted Q-value = 763.7 (22) keV fully consistent with AME2020 value of 763.75 (18) keV.
- ✓ Extended knowledge of the spectrum from 60 keV to endpoint energy.  
With numerical Fermi function,  $d = 1.075$  (7).



- Distortion remains in the measured spectrum: particle escape, dead layers, source.  
→ Unfolding process based on precise mono-energetic Monte Carlo simulations.
- Comparison with a high-precision measurement with a Metallic Magnetic Calorimeter (MMC) is possible.
- ✓ Very good agreement of the spectra in the common energy range.
- Both measurements not consistent below 100 keV with the reference measurement in the literature from Reich and Schüpferling, Z. Phys. 271, 107 (1974).
- Analysis is detailed later in this presentation.

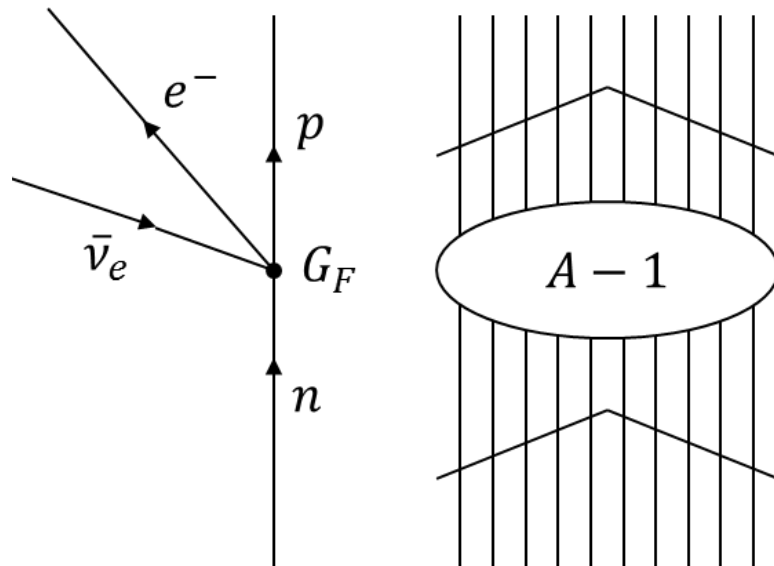
## Forbidden non-unique beta transitions

- Modelling with nuclear structure
- $^{36}\text{Cl}$ ,  $^{87}\text{Rb}$ ,  $^{151}\text{Sm}$ ,  $^{99}\text{Tc}$  and  $^{176}\text{Lu}$  decays

$$C(W_e) = \sum_{Kk_e k_\nu} \lambda_{k_e} \left[ M_K^2(k_e, k_\nu) + m_K^2(k_e, k_\nu) - \frac{2\mu_{k_e} \gamma_{k_e}}{k_e W_e} M_K(k_e, k_\nu) m_K(k_e, k_\nu) \right]$$

**Multipole expansion** of nuclear and lepton currents. Calculation of shape factors, half-lives, branching ratios, log  $ft$  values.

H. Behrens, W. Bühring,  
*Electron Radial Wave  
functions and Nuclear Beta  
Decay*, Oxford Science  
Publications (1982)



### Fermi theory

- Vertex of the weak interaction is assumed to be point-like. No propagation of  $W^\pm$  boson.
- Effective coupling constant  $G_F$ .

### Impulse approximation

- The nucleon is assumed to feel only the weak interaction.
- Other nucleons are spectators.

$${}^V \mathcal{M}_{KK0}(q^2) = \frac{\sqrt{2}}{\sqrt{2J_i + 1}} \cdot \frac{(2K + 1)!!}{(qR)^K}$$

Components of the relativistic bound wave function of the nucleon

$$\begin{aligned} & \times \left[ G_{KK0}(\kappa_f, \kappa_i) \int_0^\infty g_f(r, \kappa_f) j_K(qr) g_i(r, \kappa_i) r^2 dr \right. \\ & \left. + S_{\kappa_f} S_{\kappa_i} G_{KK0}(-\kappa_f, -\kappa_i) \int_0^\infty f_f(r, \kappa_f) j_K(qr) f_i(r, \kappa_i) r^2 dr \right] \end{aligned}$$

Geometrical coefficients

Some 3-6-9-j symbols

Transition described as the transformation of a single nucleon

→ Single particle matrix elements in spherical symmetry

→ **Relativistic wave functions are necessary**

Nuclear state described as a **superposition of nucleon states**

$$\langle \xi_f J_f || T_\lambda || \xi_i J_i \rangle = \hat{\lambda}^{-1} \sum_{a,b} \langle a || T_\lambda || b \rangle \langle \xi_f J_f || [c_a^\dagger \tilde{c}_b]_\lambda || \xi_i J_i \rangle$$

transition matrix element      tensor rank      single particle matrix element      one-body transition density

**One-body transition densities** must be given by a nuclear structure model.

→ **NushellX@MSU**: spherical shell model, effective Hamiltonians fitted on nuclear data, can be used by non-experts.

### **Nuclear structure models are non-relativistic**

The small component of the nucleon wave function can be estimated from the large (non-relativistic) component.

→ Such an approximation has been demonstrated for decades not to be sufficiently accurate for beta transitions.

$$M_K(k_e, k_\nu) = C_K (pR)^{k_e-1} (qR)^{k_\nu-1} \left\{ \underbrace{-\sqrt{\frac{2K+1}{K}} V F_{K,K-1,1}^{(0)}}_{\text{Relativistic matrix element}} - \frac{\alpha Z}{2k_e+1} \underbrace{V F_{K,K,0}^{(0)}(k_e, 1, 1, 1)}_{\text{Non-relativistic matrix elements}} \right. \\ \left. - \left[ \frac{WR}{2k_e+1} + \frac{qR}{2k_\nu+1} \right] \underbrace{V F_{K,K,0}^{(0)}}_{\text{Non-relativistic matrix elements}} - \frac{\alpha Z}{2k_e+1} \sqrt{\frac{K+1}{K}} \underbrace{A F_{K,K,1}^{(0)}(k_e, 1, 1, 1)}_{\text{Non-relativistic matrix elements}} - \left[ \frac{WR}{2k_e+1} - \frac{qR}{2k_\nu+1} \right] \sqrt{\frac{K+1}{K}} \underbrace{A F_{K,K,1}^{(0)}}_{\text{Non-relativistic matrix elements}} \right\}$$

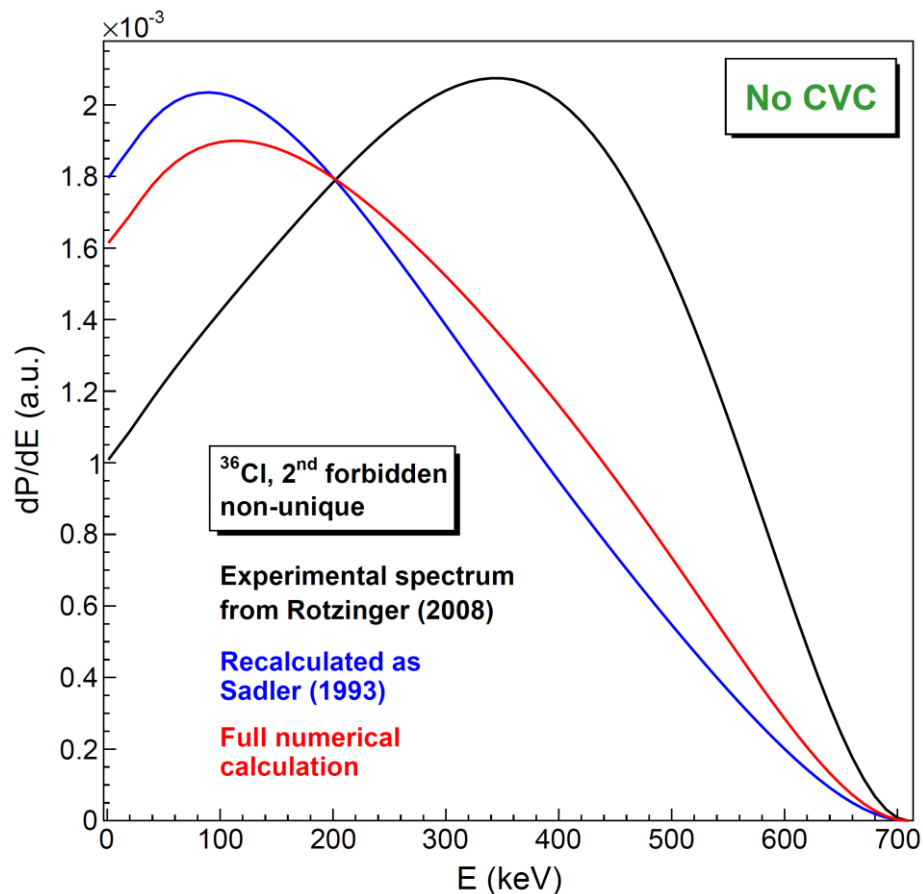
- Form factor coefficients  $V/A F_{K,L,S}^{(N)}$  are directly related to single-particle matrix elements.
- Here, lepton current has been simplified and developed, keeping only the dominant terms. One can also use a complete, full numerical lepton current.

### Conserved Vector Current (CVC) hypothesis

- Comes from gauge invariance of the weak interaction.
- Relationships between non-relativistic and relativistic vector matrix elements. Depends on Coulomb displacement energy  $\Delta E_C$ .

## Precise measurement from cryogenic detector

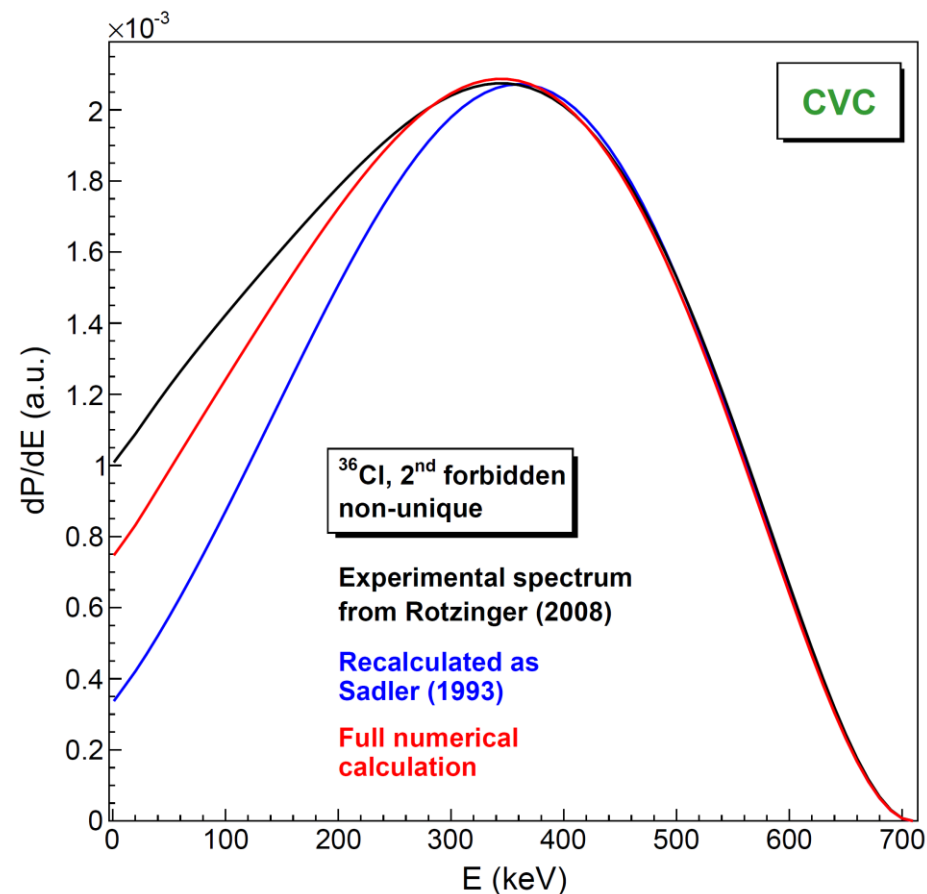
Rotzinger et al., J. Low Temp. Phys. 151, 1087 (2008)



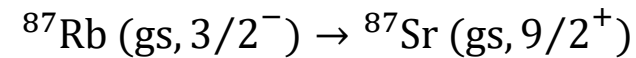
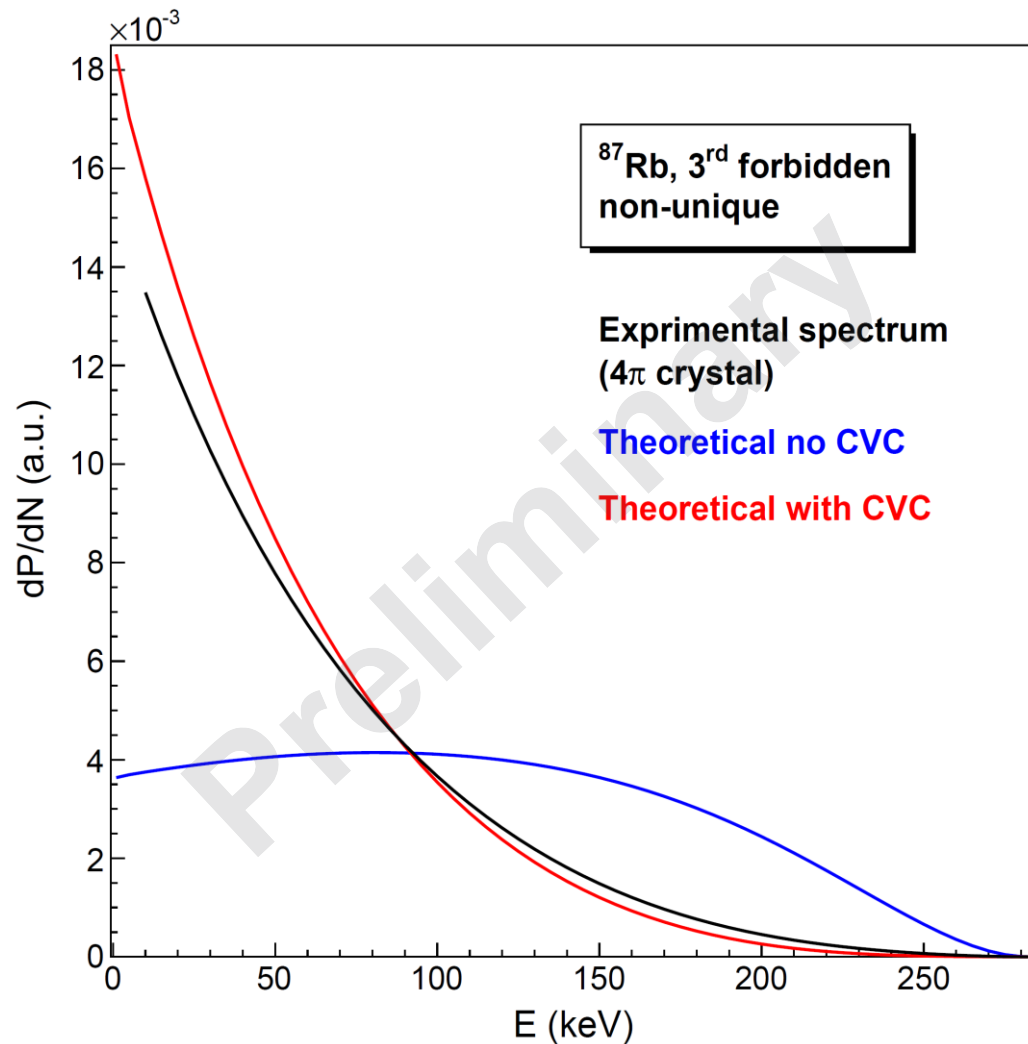
## Detailed theoretical study (with approximations)

→ Matrix elements are correctly recalculated

Sadler, Behrens, Z. Phys. A 346, 25 (1993)

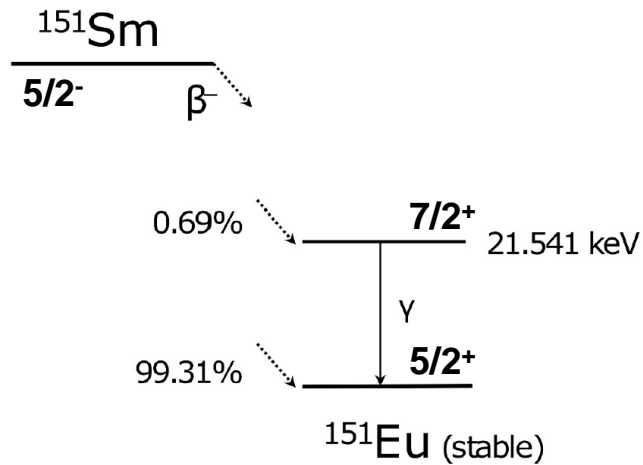


→ CVC hypothesis mandatory + Influence of lepton current treatment



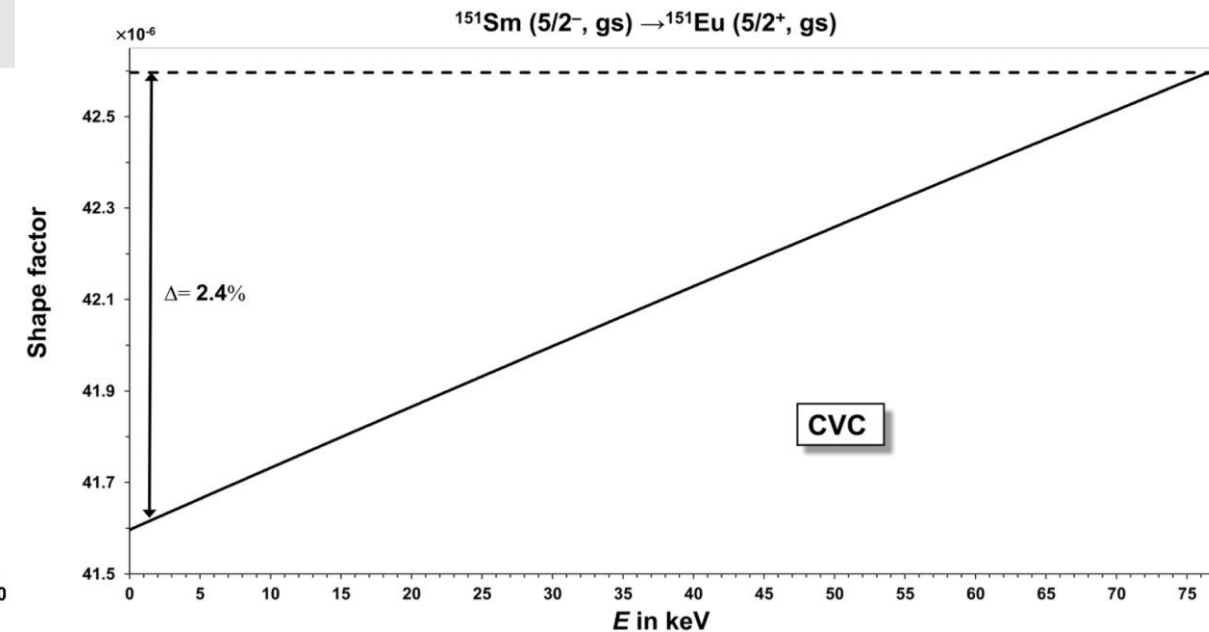
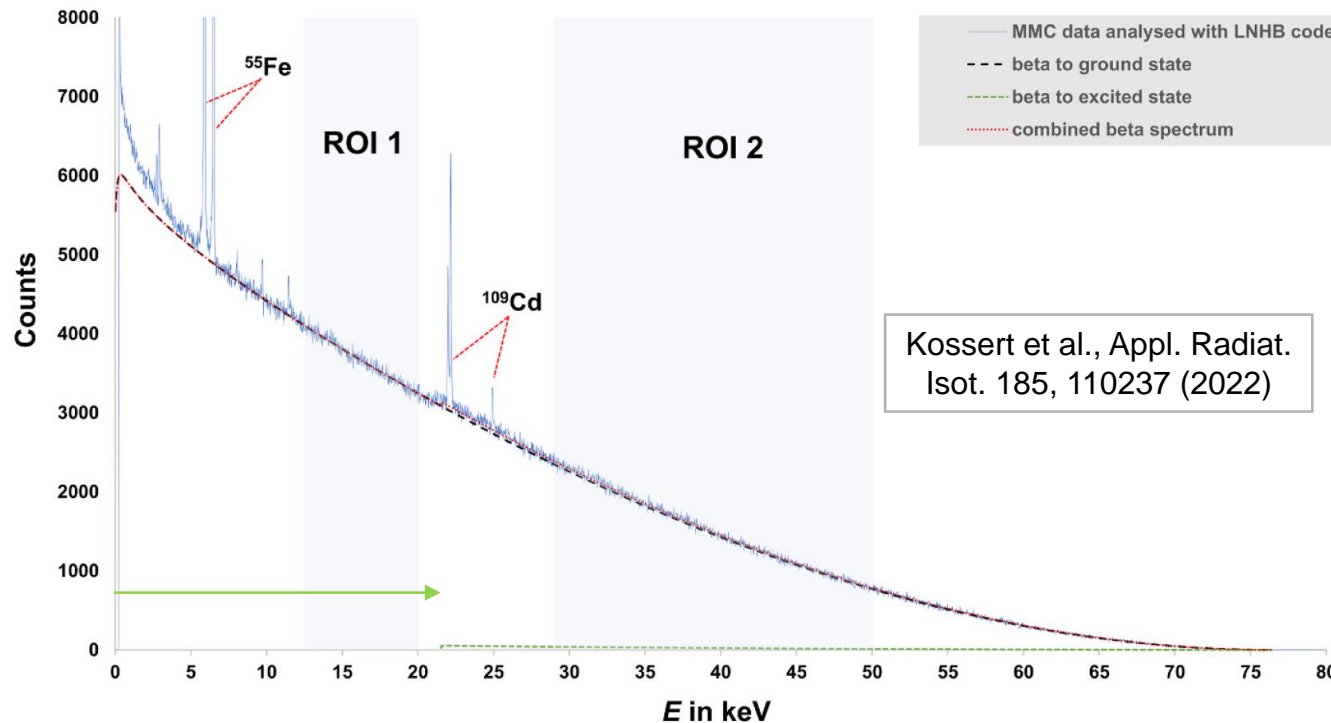
- Third forbidden non-unique transition
- NushellX  $^{56}\text{Ni}$  doubly magic core, jj44 model space, jj44b interaction
- Preliminary measurement from the European MetroBeta project (4 $\pi$  RbGd<sub>2</sub>Br<sub>7</sub> crystal)

→ **CVC hypothesis mandatory for an accurate description of the spectrum**



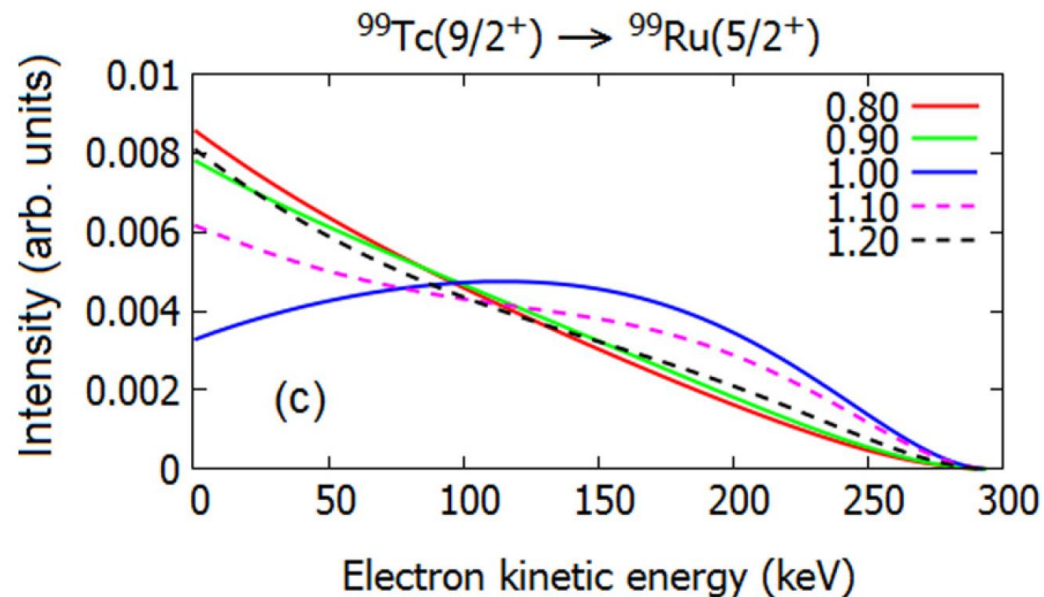
### First forbidden non-unique transitions

- ✓ High-precision measurement of  $^{151}\text{Sm}$  spectrum with Metallic Magnetic Calorimeters (MMC) at LNHB.
- ✓ Detailed calculations: accuracy of the  $\xi$ -approximation.
- ✓ New Q-value = 76.430 (68) keV more precise than AME2020 value of 76.5 (5) keV.
- ✓ New determination of branching ratios: 99.31 (11)% and 0.69 (11)%.



J. Kostensalo, J. Suhonen, PRC 96, 024317 (2017)

**$g_A$ -driven shapes of electron spectra of forbidden beta decays in the nuclear shell model**

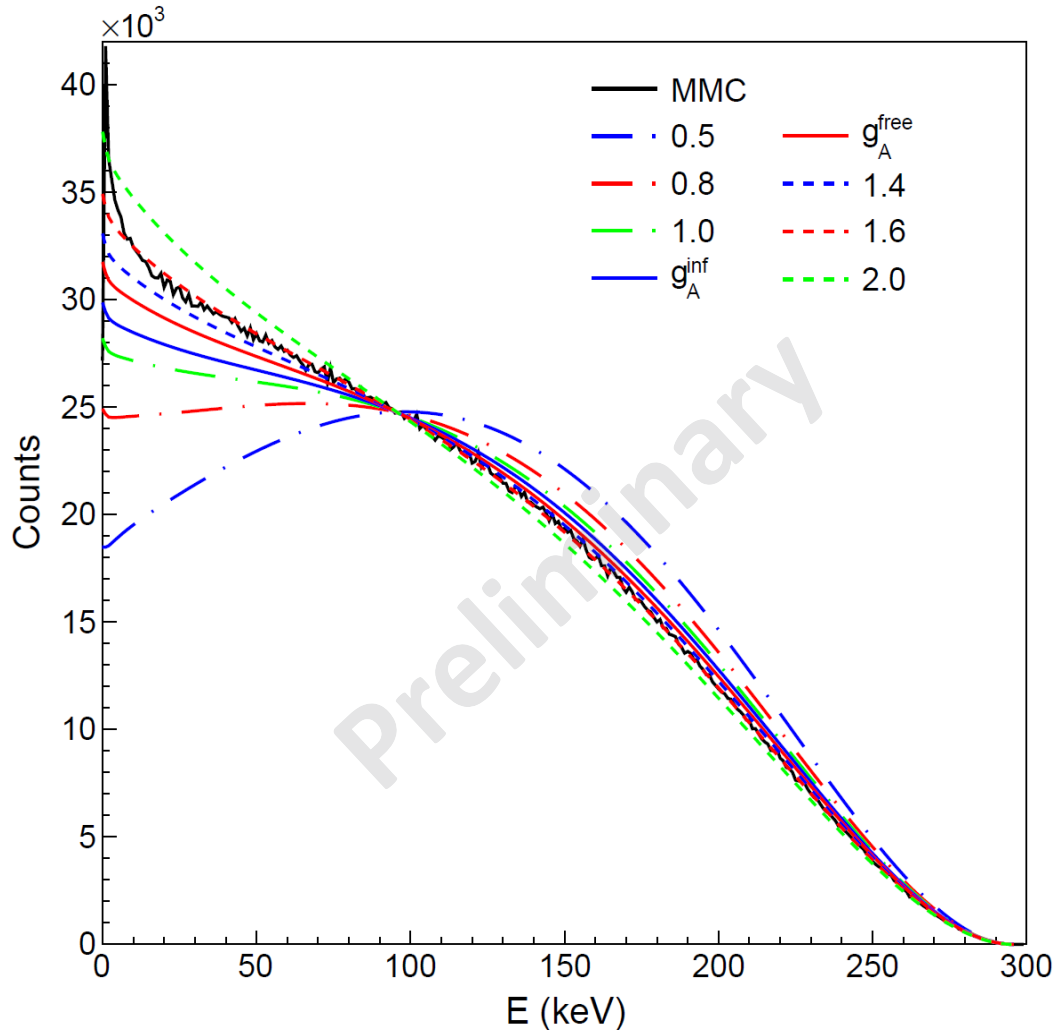


The value of  $g_A$  can be affected by several nuclear effects due to the necessary assumptions in nuclear models to deal with the many-body problem.

→  $^{99}\text{Tc}$  beta spectrum, second forbidden non-unique, has been predicted to be very sensitive to  $g_A$ .

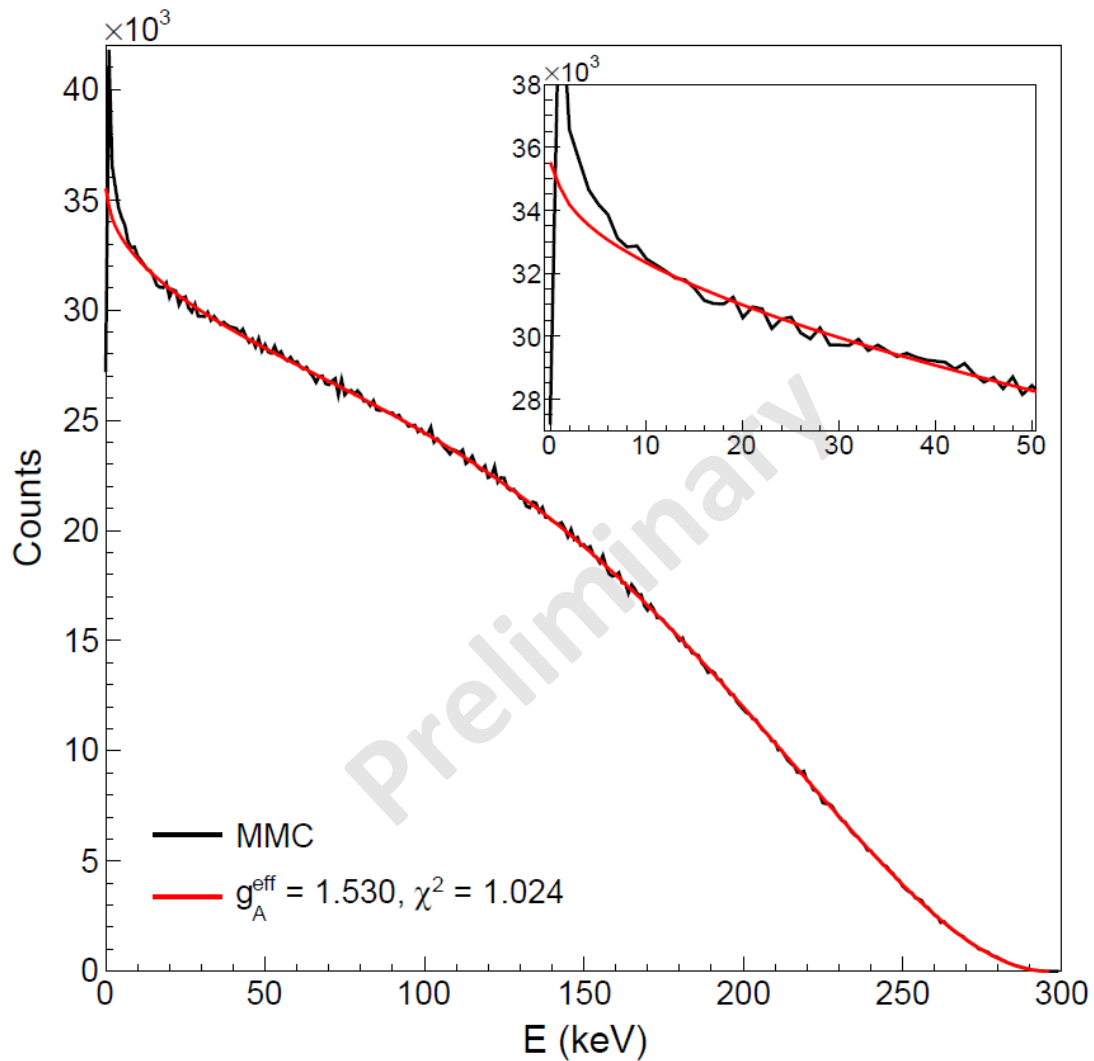
→ J. Suhonen proposed in a review [Front. Phys. 5, 55 (2017)] a formula that depends on a quenching factor in infinite nuclear matter and the free-nucleon value [PDG 2020]  $g_A^{\text{free}} = 1.2754(13)$ .

→ For  $^{99}\text{Tc}$ , one thus expects  $g_A^{\text{inf}} = 1.12$ .



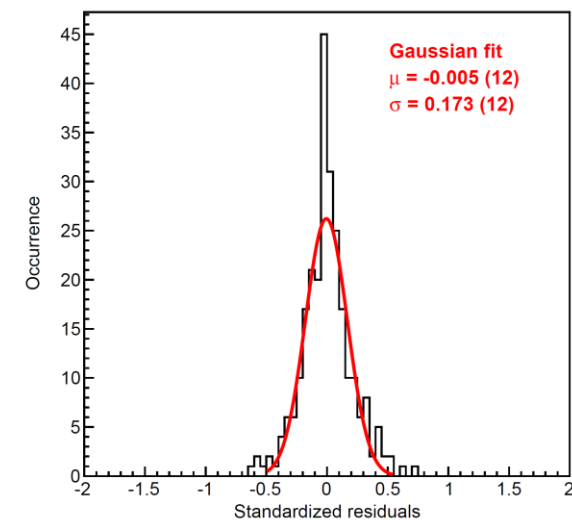
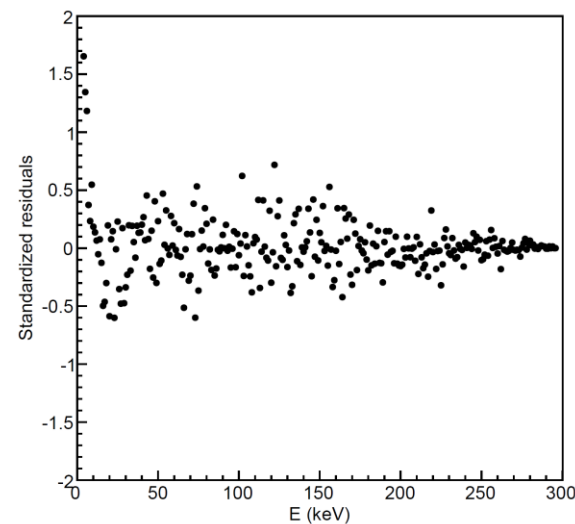
The value of  $g_A$  can be affected by several nuclear effects due to the necessary assumptions in nuclear models to deal with the many-body problem.

- ✓ High-precision measurements of  $^{99}\text{Tc}$  spectrum with Metallic Magnetic Calorimeters (MMC) at LNHB and PTB, and with Silicon detectors at LNHB.
- ✓ Excellent agreement of all the three spectra.
- ✓ New Q-value = 295.82 (16) keV not consistent with AME2020 value of 297.5 (9) keV.
- ✓ Confirmation of the spectrum shape sensitivity to  $g_A$ .

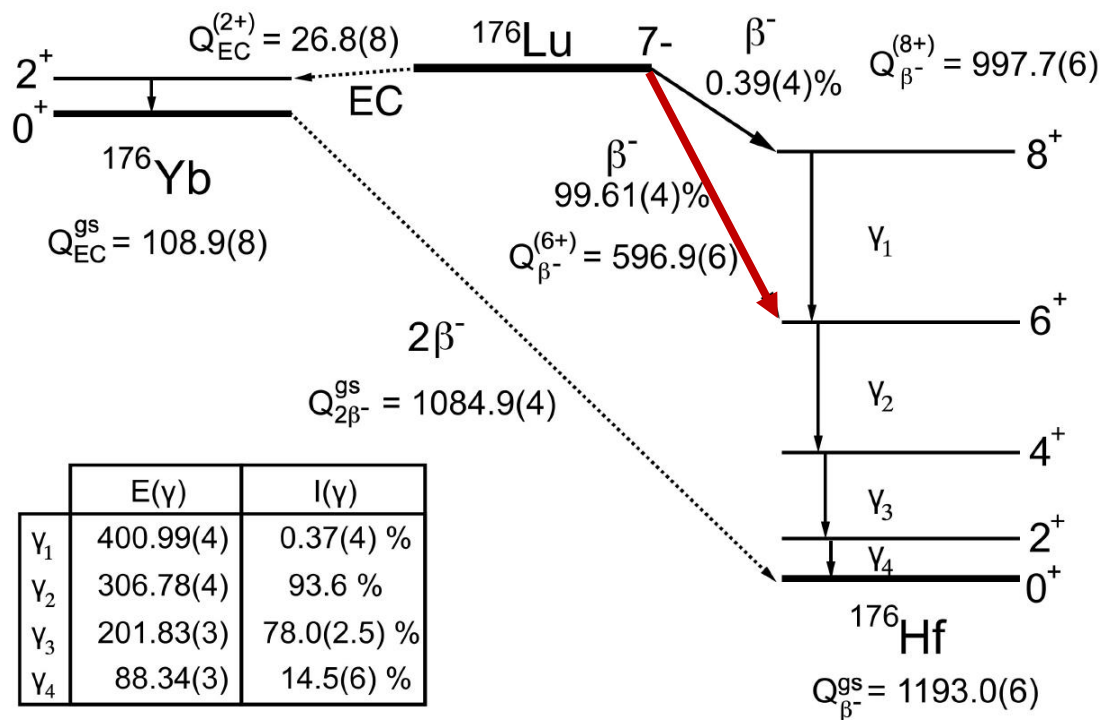


The value of  $g_A$  can be affected by several nuclear effects due to the necessary assumptions in nuclear models to deal with the many-body problem.

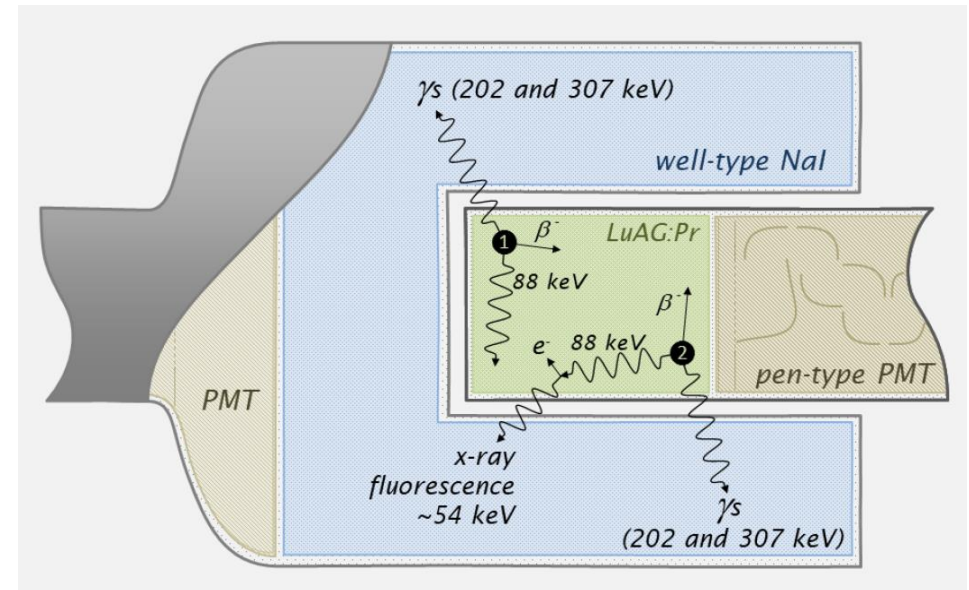
- ✓ Best adjustment gives  $g_A^{\text{eff}} = 1.53$  (8)
- !! Result far from  $g_A^{\text{inf}} = 1.12$ , which cannot give an accurate spectrum shape in any of the considered assumptions.
- ✓ Residuals without any trend down to 6 keV.

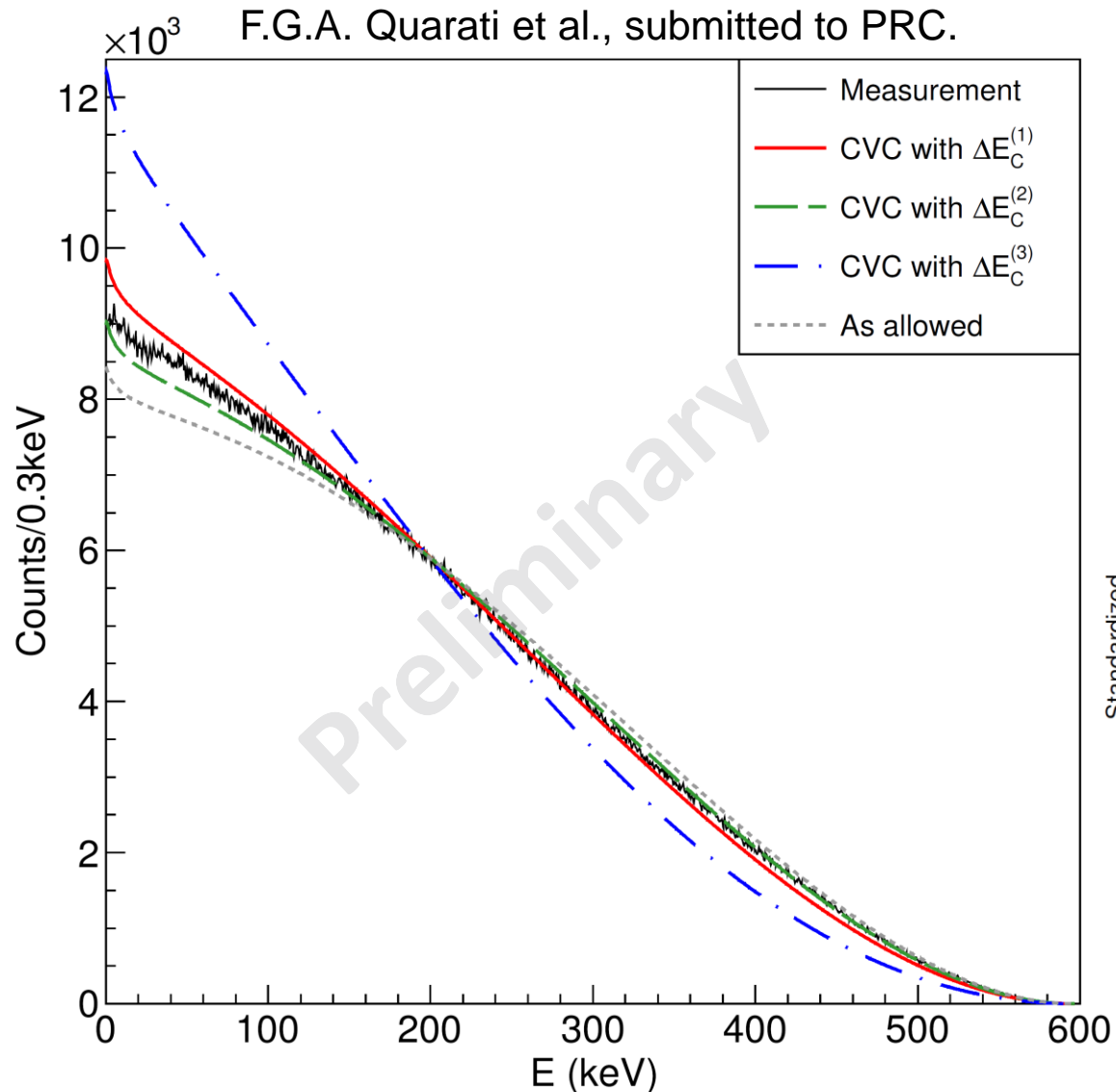


F.G.A. Quarati et al., submitted to PRC.

**First forbidden non-unique transition**

- ✓ First high-precision spectrum measurement from self-scintillation of a LuAG:Pr crystal.



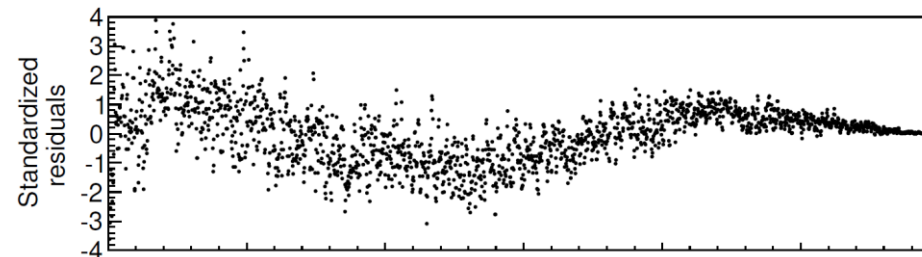


### First forbidden non-unique transition

- ✓ First high-precision spectrum measurement from self-scintillation of a LuAG:Pr crystal.
- Realistic shape only possible with CVC, found to be quite sensitive to the Coulomb displacement energy  $\Delta E_C$ .

Different methods to estimate  $\Delta E_C$ . Adjustments lead to similar residuals but very different  $g_A^{\text{eff}}$ .

→ **A non-linear trend remains.**

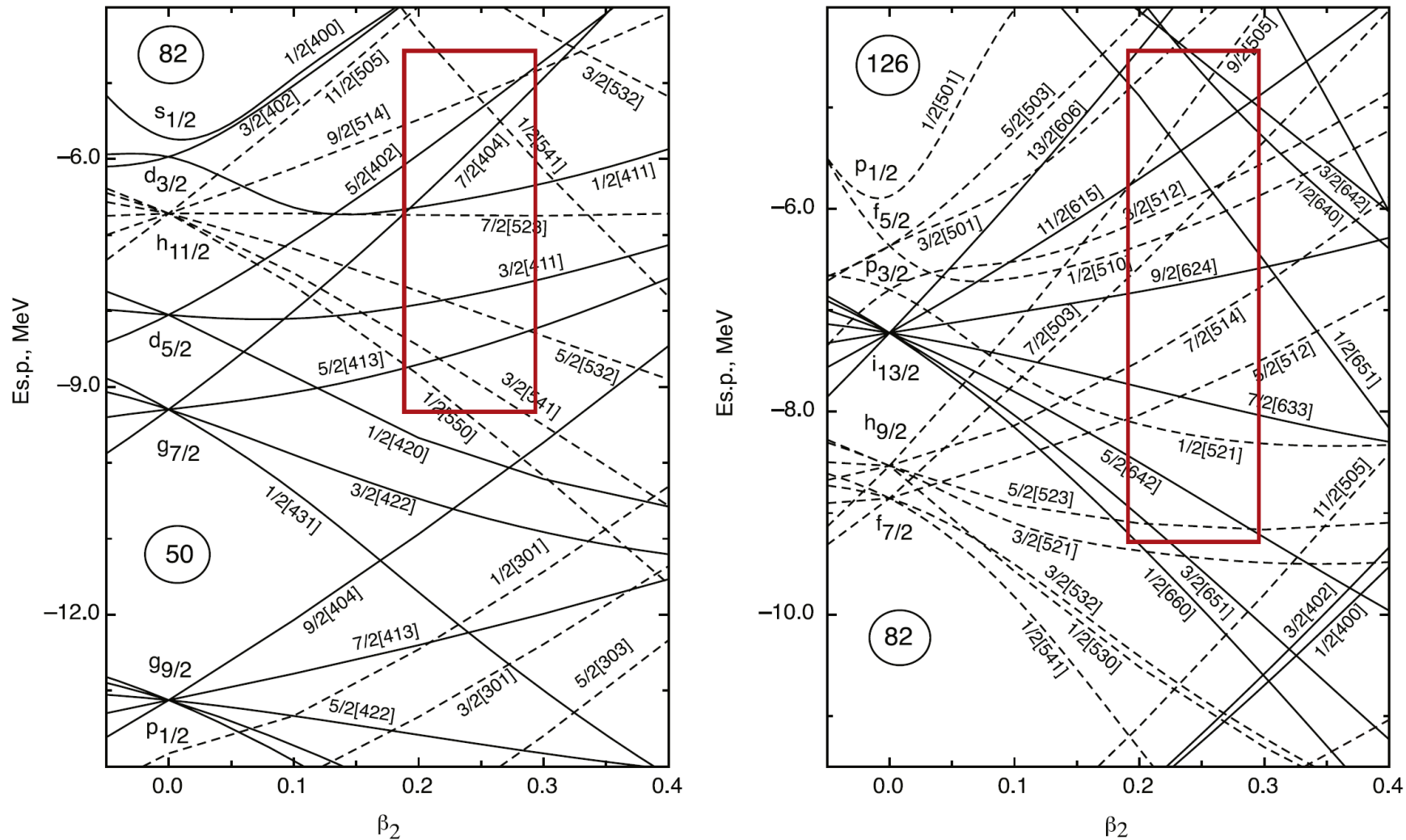


$\Delta E_C$ (MeV)	$g_A$
20.527(53)	$g_A^{\text{free}}$
$\Delta E_C^{(1)}$	1.057(5)
$\Delta E_C^{(2)}$	1.560(6)
$\Delta E_C^{(3)}$	0.834(4)

Nucleus deformation: hindered transition ( $\Delta K = 7$ )

!! Calculated half-life shorter by 13 orders of magnitude.

→ **Detailed analysis would require accurate modelling with nuclear deformation.**



Kondev, Dracoulis and  
Kibédi, ADNDT 103-  
104, 50-105 (2015)

**Fig. 2.** Nilsson levels for protons (left) and neutrons (right) in the  $A \sim 170-190$  region. Boxes indicate the main orbitals of interest.

## The BetaShape code

- Modelling and examples
- Developments
- Validation

The LogFT program is the reference code for B and EC properties in nuclear decay data evaluations, having been used for the last 50 years.

### Written in end of the 1960s, still used

- Handles B and EC transitions.
- Provides mean energies of B spectra, log-*ft* values, and a few B+ and EC probabilities.
- Propagates uncertainties from input parameters.
- Reads and writes ENSDF files (*Evaluated Nuclear Structure Data File*).

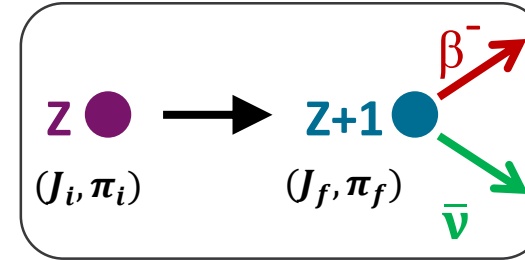
### However

- Too simple analytical models → lack of accuracy.
- Forbiddenness limitation (allowed, first- and second- forbidden unique).
- Users now require B spectra and correlated neutrino spectra.
- Users now require detailed information for many subshells in EC.



**Coulomb part  
(Fermi function)**

$$\text{Beta spectrum } \frac{dN}{dW} \propto \underbrace{p W q^2}_{\text{Phase space}} \underbrace{F_0 L_0}_{\text{Coulomb part (Fermi function)}} \underbrace{C(W)}_{\text{Shape factor}}$$



Nuclear current can be **factored out** for **allowed** and **forbidden unique** transitions

$$C(W) = (2L - 1)! \sum_{k=1}^L \lambda_k \frac{p^{2(k-1)} q^{2(L-k)}}{(2k - 1)! [2(L - k) + 1]!}$$

$$F_0 L_0 = \frac{\alpha_{-1}^2 + \alpha_1^2}{2p^2} \quad \lambda_k = \frac{\alpha_{-k}^2 + \alpha_k^2}{\alpha_{-1}^2 + \alpha_1^2}$$

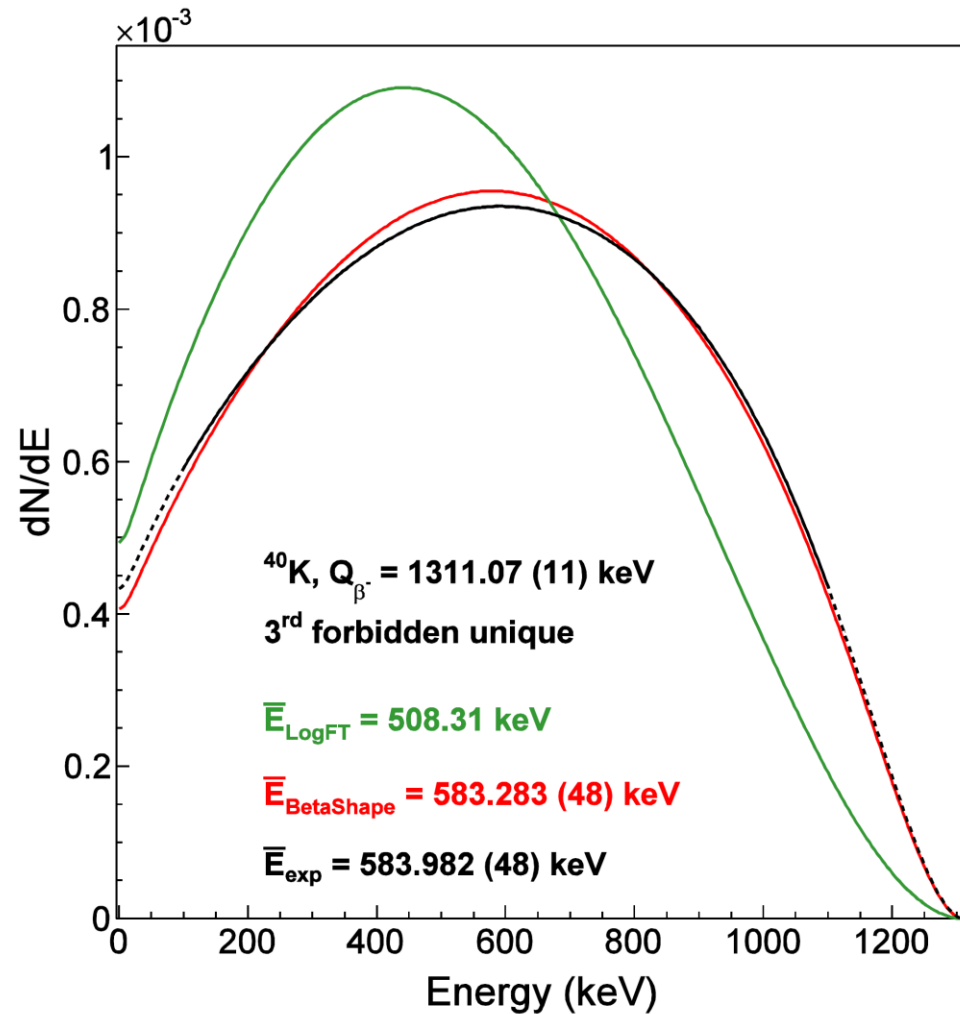
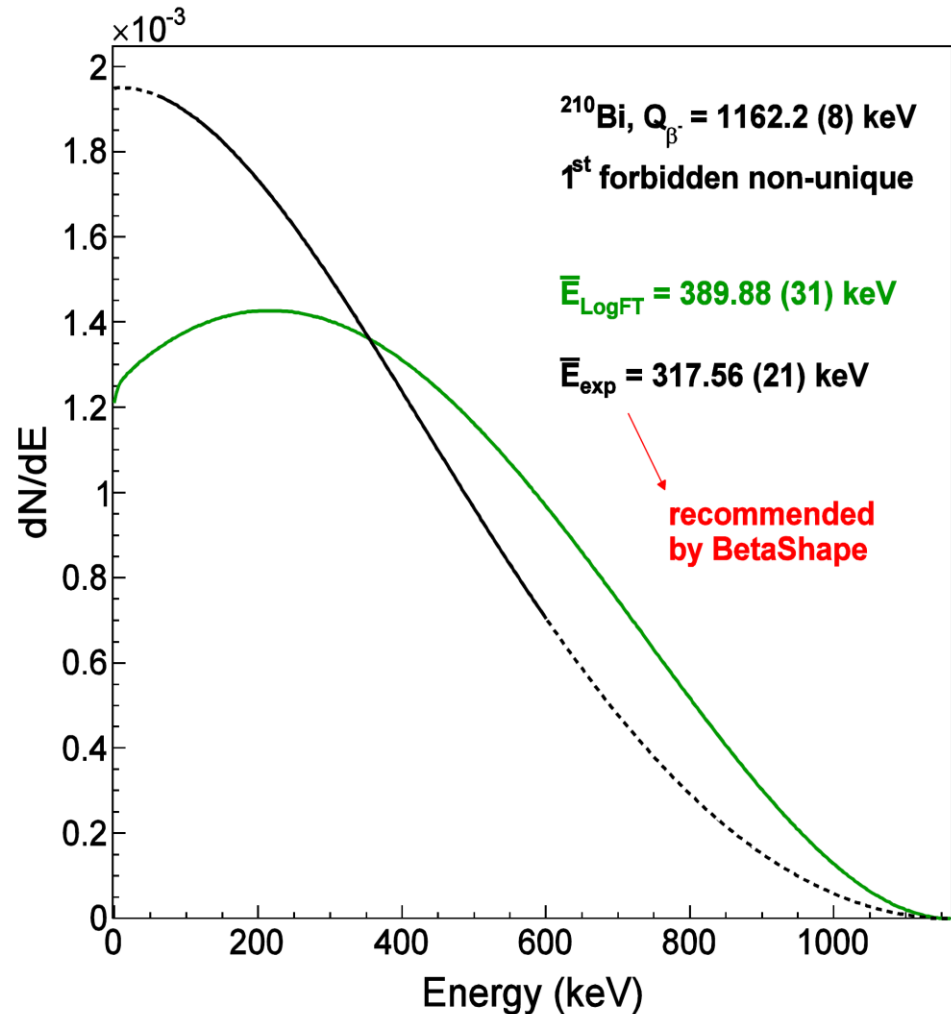
→ Numerical solving of Dirac equation for the leptons

X. Mougeot, Phys. Rev. C 91, 055504 (2015)

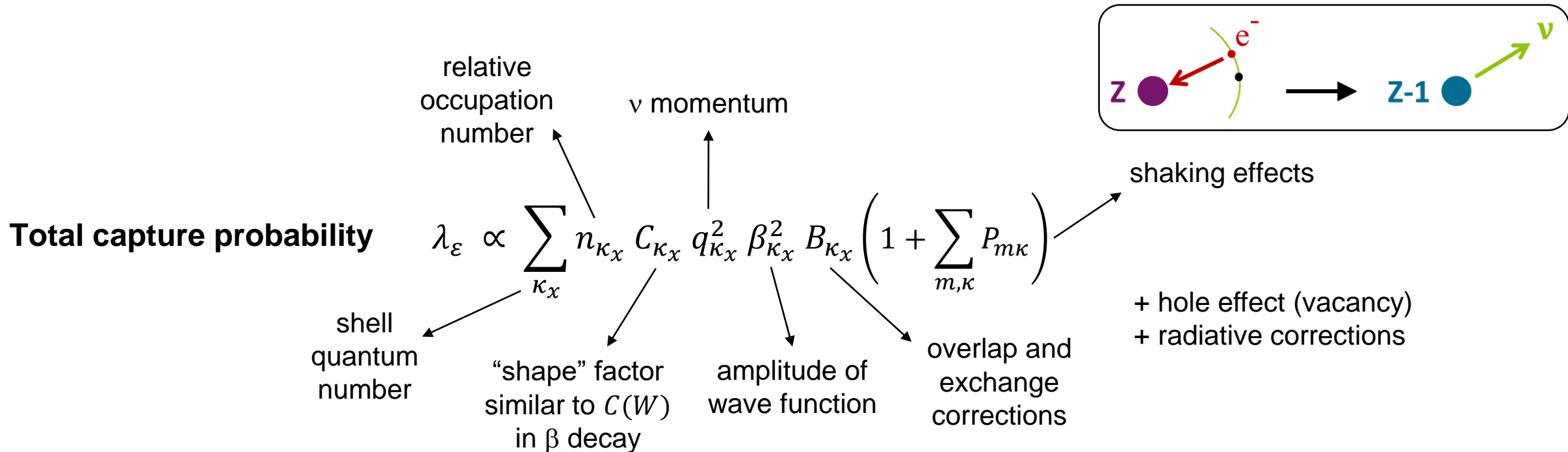
**Forbidden non-unique** transitions calculated according to the  **$\xi$ -approximation**

if  $2\xi = \alpha Z/R \gg W_0$   
 1<sup>st</sup> fnu → allowed  
 applied to 2<sup>nd</sup>, 3<sup>rd</sup>, etc.

- Analytical **screening correction** from Bühring, adapted to precise potentials
- **Radiative corrections** from high-precision study of superallowed decays
- **Database of 131 experimental shape factors**
- **Propagation of uncertainties**



These two transitions are calculated as allowed by the LogFT program, which does not provide any beta spectrum.



### Allowed and forbidden unique

→ no nuclear structure

If transition energy  $\geq 2m_e$

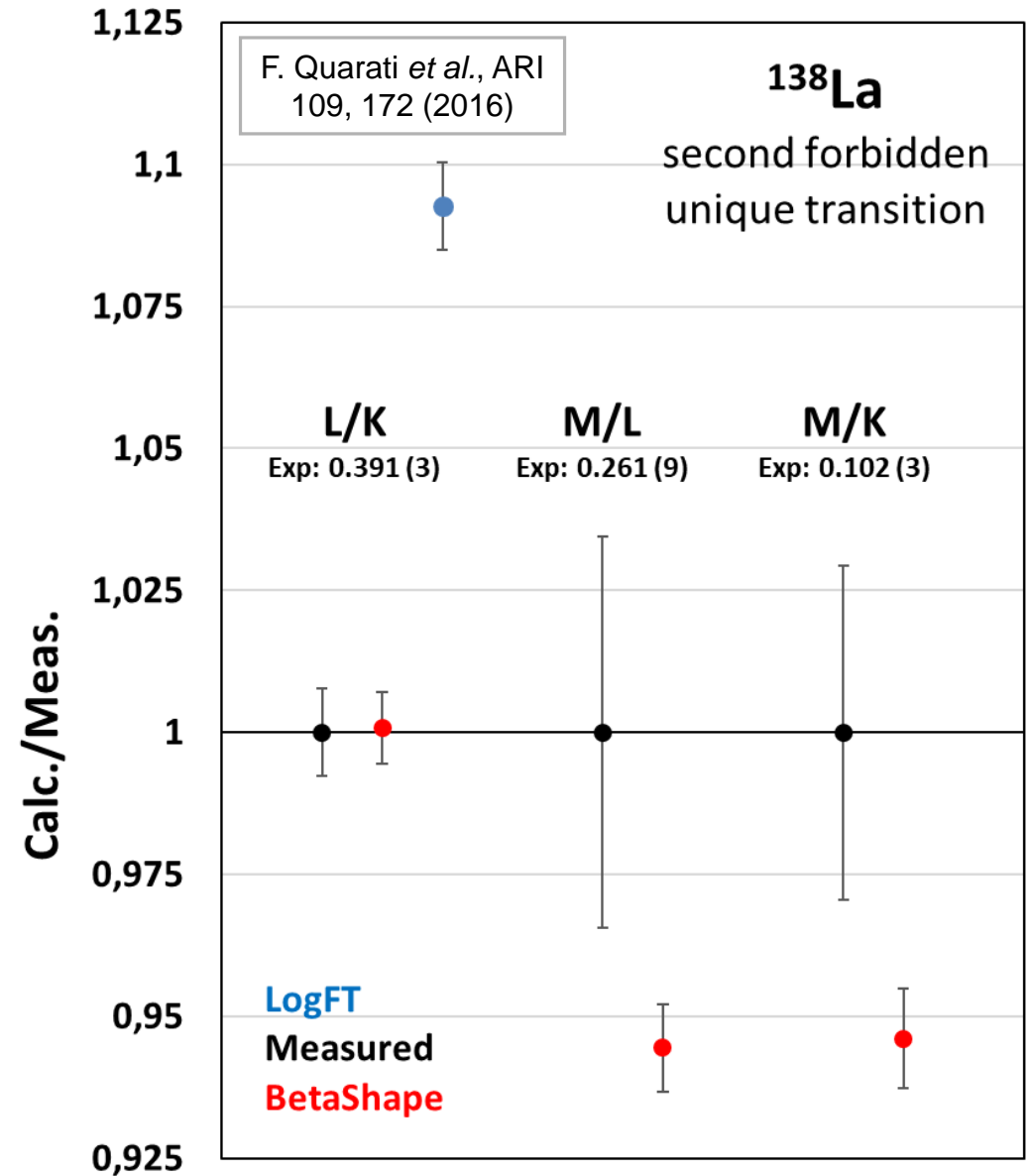
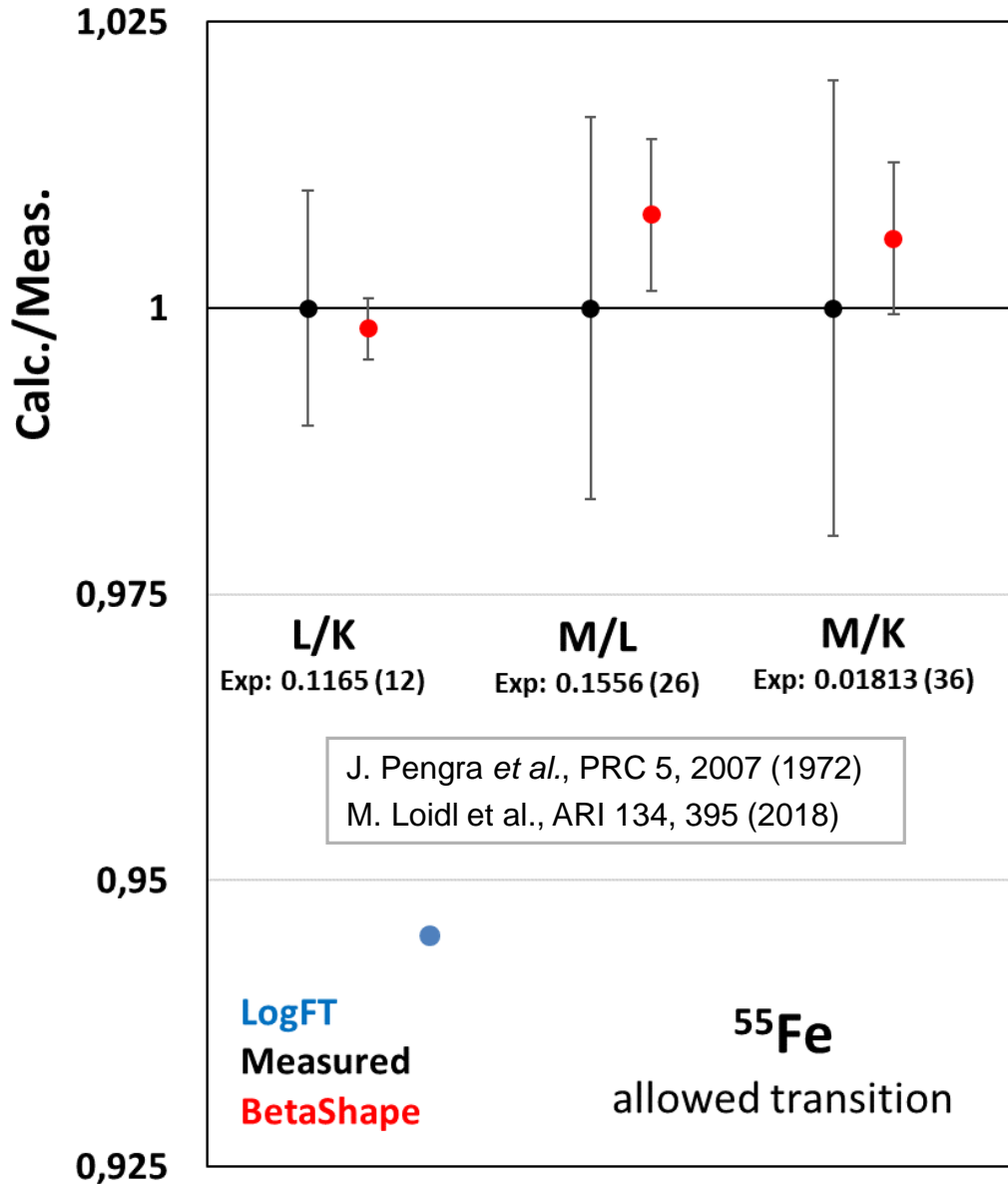
→ **competition with a  $\beta^+$  transition**

X. Mougeot, Appl. Radiat. Isot. 154, 108884 (2019)

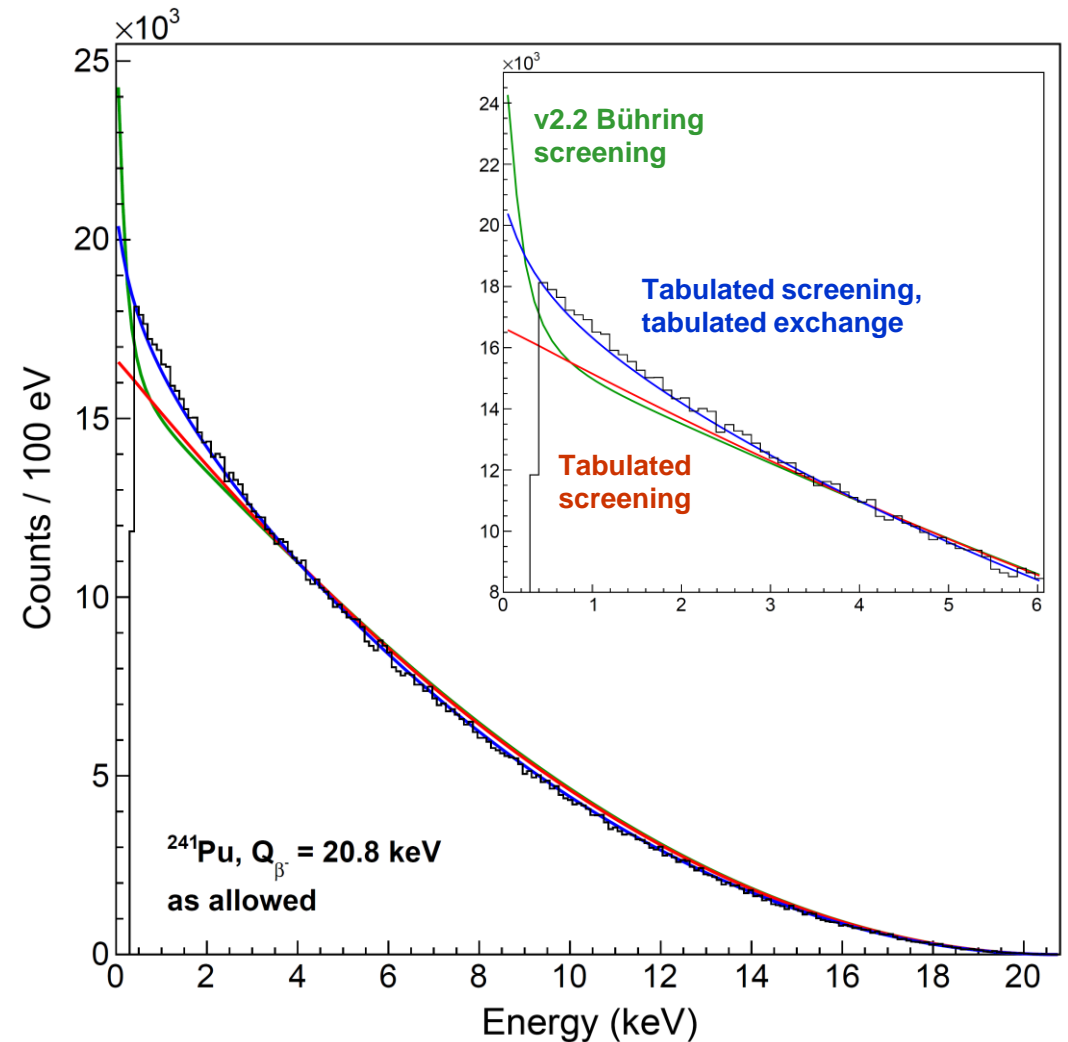
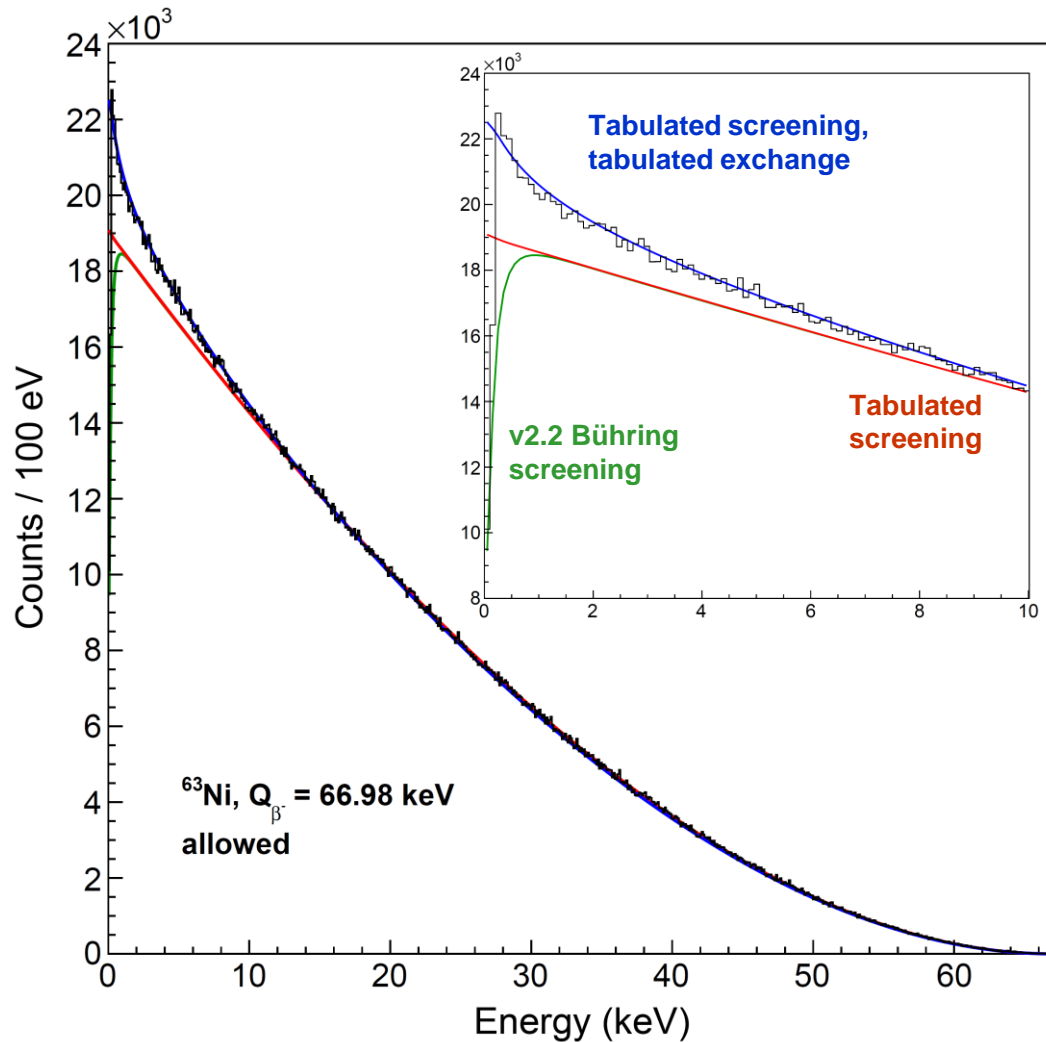
### Atomic wave functions

- Numerical solving of Dirac equation
- Forced convergence to relativistic DFT energies, with electron correlations

S. Kotochigova *et al.*, Phys. Rev. A 55, 191 (1997)



- ✓ Tabulation of atomic screening and exchange effects from full numerical calculations.
- ✓ Inclusion of the atomic overlap correction in beta decays. Negligible influence except close to the end-point energy, which can appear lower by hundreds of eV.
- ✓ A few bugs have been fixed in output format in very specific cases.
- ✓ Negative Q-values are now possible: decay of isomeric state with stable ground state ( $^{87m}\text{Sr}$ ).
- ✓ Some security checks have been added to deal with ENSDF files that are not following the format, making code crashing.
- ✓ Unknown uncertainties (AP, SY, GT, etc.) are treated as null. Implementation is ongoing to treat them correctly for intensities and log- $ft$  values.
- ✓  $^{129}\text{I}$  experimental shape factor has been updated. Waiting for the publication of  $^{176}\text{Lu}$  study to update this shape factor too.

Comparison with high-precision spectra from  $^{63}\text{Ni}$  and  $^{241}\text{Pu}$  decays

	LogFT	BetaShape
Range	B-, B+ and EC transitions Allowed, 1 <sup>st</sup> and 2 <sup>nd</sup> unique	B-, B+ and EC transitions Allowed, all unique, $\xi$ -approximation for non-unique
Calculated values	Mean energies, log- <i>ft</i> , a few EC/B+ intensities/probabilities.	Mean energies, log- <i>ft</i> , B and correlated (anti)neutrino spectra, total decay spectrum, EC/B+ intensities/probabilities for all subshells.
Input	ENSDF files	ENSDF files
Output	Report file, updated ENSDF file.	Report file, updated ENSDF file, text files with spectra and all details for each transition.
Structure	Fortran, 1 program, 78 functions, $\approx$ 6 800 lines.	C++, 7 interfaced programs, 9 classes, > 260 functions, > 35 500 lines.
Model improvements		Forbiddenness; Fermi function and $\lambda_k$ parameters; finite nucleus size; atomic overlap, screening and exchange effects; radiative corrections; experimental shape factors; shaking effect; hole effect.

**Preliminary benchmark** on 23 radionuclides that span over a large range of elements:  $^{11}\text{C}$ ,  $^{26}\text{Al}$ ,  $^{40}\text{K}$ ,  $^{52}\text{V}$ ,  $^{60}\text{Co}$ ,  $^{63}\text{Ni}$ ,  $^{68}\text{Ga}$ ,  $^{75}\text{Ge}$ ,  $^{85}\text{Kr}$ ,  $^{99}\text{Tc}$ ,  $^{103}\text{Ru}$ ,  $^{112}\text{In}$ ,  $^{137}\text{Cs}$ ,  $^{138}\text{La}$ ,  $^{143}\text{Sm}$ ,  $^{166}\text{Ho}$ ,  $^{185}\text{W}$ ,  $^{198}\text{Au}$ ,  $^{206}\text{Tl}$ ,  $^{210}\text{Bi}$ ,  $^{214}\text{Pb}$ ,  $^{231}\text{Th}$ ,  $^{241}\text{Pu}$ .

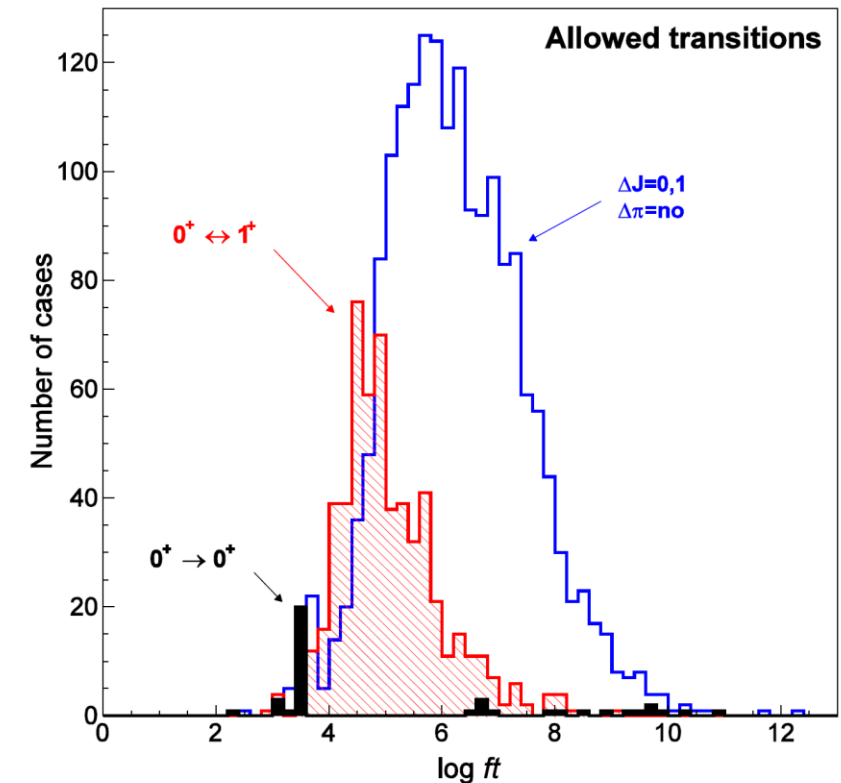
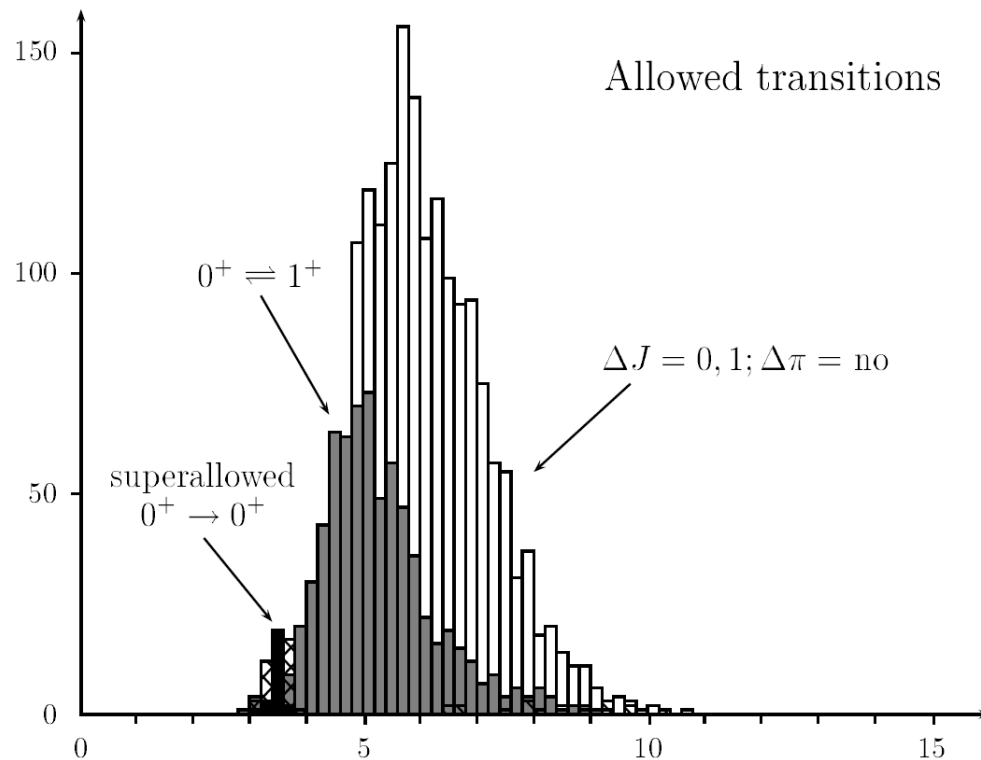
### Systematic study of DDEP decay data

→ 1 008 B transitions checked by hand in 144 radionuclides (218 in the database).

### Systematic comparison between LogFT and BetaShape over all ENSDF decay data

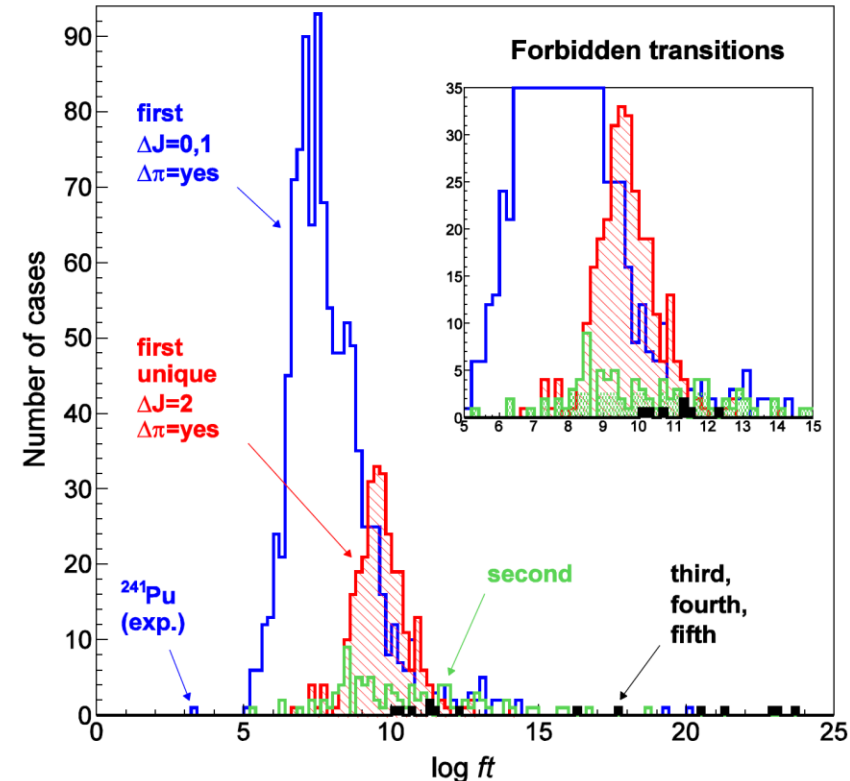
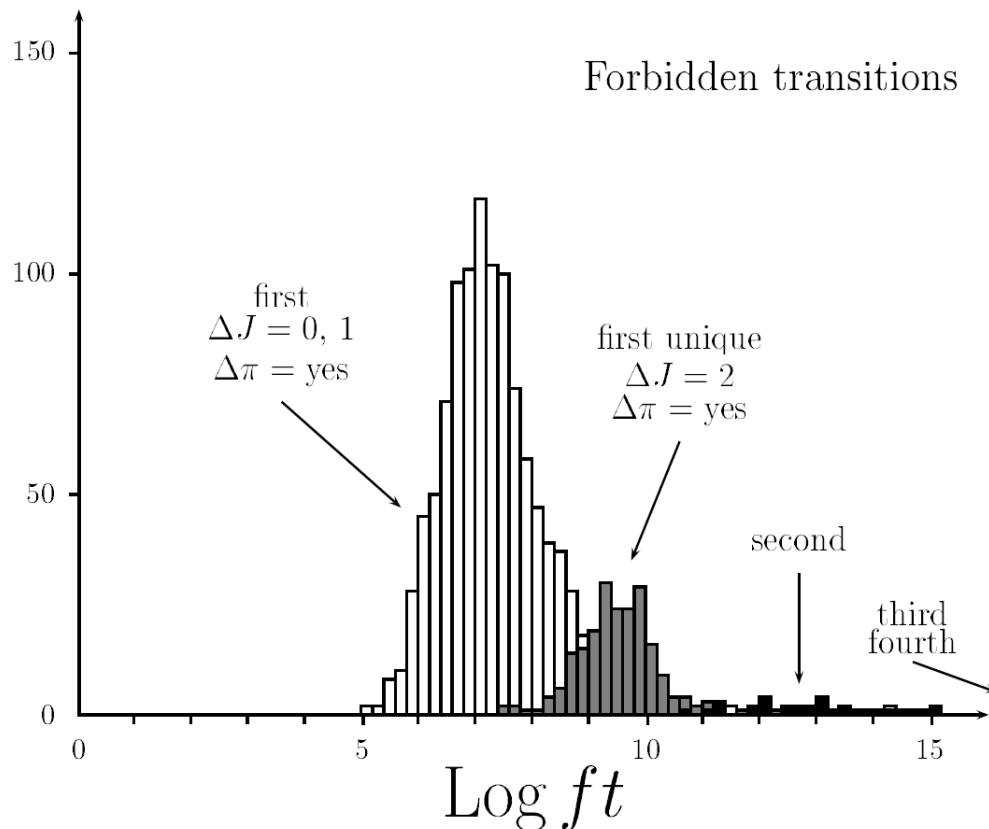
- Rare cases absent in DDEP evaluations (unplaced transitions, etc.).
- Problems and errors identified in 47 radionuclides (inconsistent Q-values, spins, parities, energies, intensities, uncertainties); corrected by hand.
- LogFT doesn't check the consistency between forbiddenness and spins/parities. Moreover, mean energies and log-*ft* values are sometimes not issued from LogFT. Thus, over all ENSDF decay data:
  - ✓ BetaShape was used for correcting the forbiddennesses according to the  $\xi$ -approximation.
  - ✓ LogFT was run.
  - ✓ BetaShape was run again to compare the results of both codes.

- ✓ Selection of well-defined transitions: spins, parities, Q-values, parent half-lives, energies, intensities, and the corresponding uncertainties.
- ✗ Rejection of ionized or excited atomic states, uncertain or questionable states and decays, and decays with more than one parent (mixed sources).



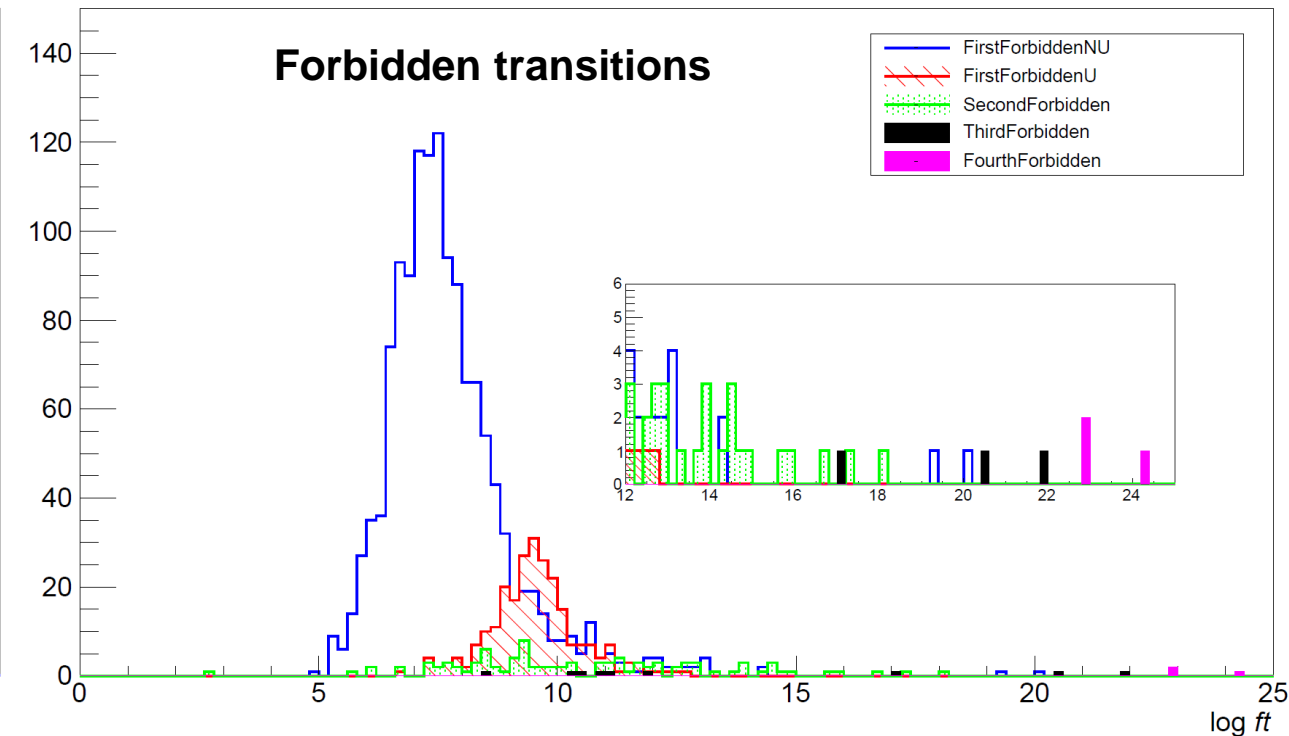
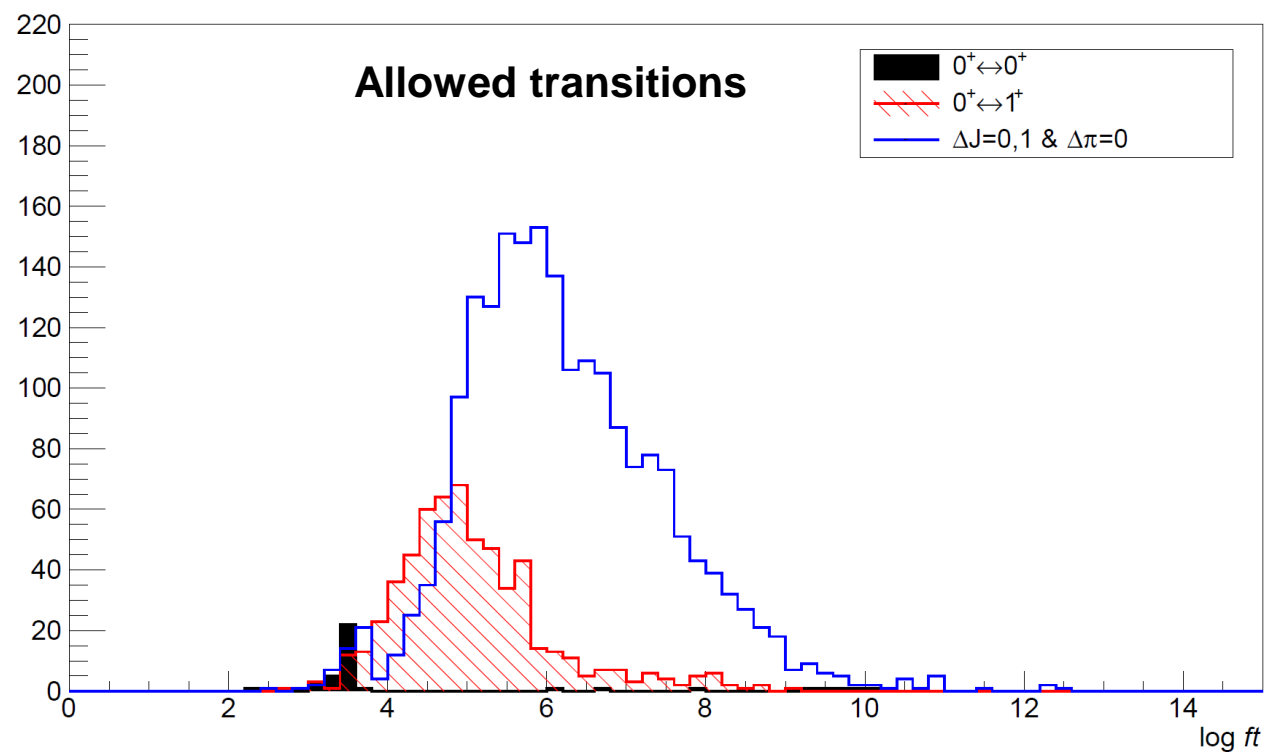
B. Singh, J.L. Rodriguez,  
S.S.M. Wong, J.K. Tuli,  
*Review Of Logft Values  
In  $\beta$  Decay*, Nuclear Data  
Sheets 84, 487 (1998)

- ✓ Selection of well-defined transitions: spins, parities, Q-values, parent half-lives, energies, intensities, and the corresponding uncertainties.
- ✗ Rejection of ionized or excited atomic states, uncertain or questionable states and decays, and decays with more than one parent (mixed sources).



Collaborative work: B. Singh (McMaster University), S. Turkat and K. Zuber (TU Dresden), X. Mougeot (CEA)

- ✓ Update of B and EC decays present in ENSDF database (as of September 2022).
- ✓ Use of BetaShape to calculate the log-ft values (including new developments since v2.2).
- Preliminary results:



# Conclusion

- Beta decays are of importance for nuclear decay data, but also for a wide range of scientific topics from fundamental physics to applications.
- **Allowed and forbidden unique transitions can be calculated** without any nuclear structure **with good accuracy**. Except in a few specific cases (“accidental cancellation of nuclear matrix elements”).
- If targeted accuracy better than 1-5%, detailed models are necessary. For some transitions, 0.1% is possible.
- **Forbidden non-unique transitions are sensitive to nuclear structure**. Some can be calculated accurately as allowed or forbidden unique.
- **Comparison with measurement is always preferable.**
- In nuclear decay data evaluations, **the BetaShape code** can replace the longstanding used LogFT code.
  - More precise mean energies, capture probabilities and log-ft values.
  - Additional useful information: energy spectra, subshell capture probability, etc.
  - Living code: modelling and output continuously improved.
  - Already officially adopted by the DDEP collaboration.



**Thank you for attention.**

